# Hydraulic Properties and Processes of Conifer Trees in the Inland Northwest Through Extended Seasonal Drought

A Dissertation

Presented in Partial Fulfillment of the Requirements for the

Degree of Doctor of Philosophy

with a

Major in Natural Resources

in the

College of Graduate Studies

University of Idaho

by

Kathryn V. Baker

Major Professors: Daniel Johnson, Ph.D.; Tara Hudiburg, Ph.D.

Committee Members: Timothy Link, Ph.D.; Janet Rachlow, Ph.D.; Charles Goebel, Ph.D.

Department Chair: Charles Goebel, Ph.D.

August 2019

# Authorization to Submit Dissertation

This dissertation of Kathryn Baker, submitted for the degree of Doctor of Philosophy with a Major in Natural Resources and titled "Hydraulic Properties and Processes of Conifer Trees in the Inland Northwest Through Extended Seasonal Drought," has been reviewed in final form. Permission, as indicated by the signatures and dates below, is now granted to submit final copies to the College of Graduate Studies for approval.

Major Professors: _____ Date: _____

Daniel Johnson, Ph.D.

_____ Date: _____

Tara Hudiburg, Ph.D.

Committee Members: _____ Date: _____

Timothy Link, Ph.D.

_____ Date: _____

Janet Rachlow, Ph.D.

_____ Date: _____

Charles Goebel, Ph.D.

Department Chair: _____ Date: _____

Charles Goebel, Ph.D.

# Abstract

The overarching question of this dissertation is: how do conifer trees in Northern Idaho use water across long growing seasons with little precipitation? There are four chapters, an introductory chapter first followed by three research projects. All three projects took place on the University of Idaho Experimental Forest. As in the much of the region, the soils on the experimental forest can hold large amounts of water because of their depth and composition (more than a meter-deep silt loam). Paired with a climate that allows for very little summer precipitation, the soils facilitate a slow and consistent dry down. That allowed us to study trees' responses to drought and how they changed throughout growing seasons. The first research project described here was conducted in 2015 addresses the question: how do six of the most regionally important conifer species function from June to October of the worst drought on record? That study produced an interesting dataset that, in collaboration with Drs. Xiaonan Tai and Scott Mackay (now of University of Utah and SUNY-Buffalo, respectively), was incorporated into the TREES process-based tree physiology model. We can now model those species under different scenarios of climate and substrate. However, that project inspired a question: how do specific parameters, like whole-tree conductance, whole-tree water flux, organ conductivity, and leaf gas exchange interact through a growing season? Chapter three addresses that question by describing intensely measured water use of three individual mature *P. ponderosa* trees from June to October of 2017. The insights that chapter provided were then scaled up to the fourth chapter, which explores the influence that different densities of pre-commercial thinning treatments have on *P. ponderosa* tree hydraulic function within the same site in 2018. Each of these three research projects

produced some results that were expected and consistent with literature and also some novel findings that add new insights to our understanding of conifers in the inland Northwest.

# Acknowledgements

Funding for these projects were provided by the National Science Foundation (#IOS-1146746), the National Institute of Food and Agriculture, U.S. Department of Agriculture, McIntire Stennis project under 1004149, and awards from the University of Idaho College of Natural Resources. Baker was supported by fellowships from the Northwest Climate Science Center and the Stillinger Foundation.

We would like to think the visiting researchers and field technicians who helped collect data: Laurie Bel, Dario Caminha Paiva, Jason Schlaffman, Laura Young, Forrest Sherman, Erika Berglund, Karl Meyer, and Ben Doty.

# Dedication

Thank you to the family, friends, and dogs who have helped me with fieldwork, coding, and coping.

# Table of Contents

# List of Figures

# List of Tables

# List of Abbreviations

| | |
|---|---|
| $A$ | Carbon assimilation |
| $A_L$ | Leaf area |
| $A_S$ | Sapwood area |
| $\Psi$ | Water potential |
| $\Psi_B$ | Branch water potential |
| $\Psi_L$ | Leaf water potential |
| $\Psi_{MD}$ | Midday leaf water potential |
| $\Psi_{MIN}$ | Most negative leaf water potential |
| $\Psi_{P50}$ | Water potential where conductivity has decreased by 50% |
| $\Psi_{PD}$ | Predawn leaf water potential |
| $\Psi_S$ | Soil water potential |
| $\Psi_{TLP}$ | Water potential at turgor loss point |
| $E_C$ | Predicted transpiration |
| $E_{CRIT}$ | Transpiration that would incur hydraulic failure |
| DBH | Diameter at breast height |
| HR | Hydraulic redistribution |
| $g_S$ | Stomatal conductance |
| $g_{S\text{-}MAX}$ | Maximum stomatal conductance |
| $g_{S\text{-}NOC}$ | Nighttime stomatal conductance |
| $k_H$ | Whole-tree hydraulic conductance |
| $k_L$ | Leaf hydraulic conductance |
| $k_{L\text{-}MAX}$ | Maximum leaf hydraulic conductance |
| $K_{MAX}$ | Maximum specific hydraulic conductivity |
| $K_S$ | Specific hydraulic conductivity |
| $K_{S\text{-}MAX}$ | Maximum specific hydraulic conductivity |
| $P_{50}$ | Water potential where conductivity has decreased by 50% |
| $P_{g12}$ | Water potential at which $g_S$ has decreased to 12% of $g_{S\text{-}MAX}$ |
| PAR | Photosynthetically active radiation |
| PCT | Precommercial thin |
| $Q_L$ | Flux per unit leaf area |
| VPD | Vapor pressure deficit |
| VWC | Volumetric water content |

# Statement of Contribution

Coauthors for Chapter 2, which is currently pending revision approval in the Annals of Botany Plants, are Xiaonan Tai, Megan L. Miller, and Daniel M. Johnson. The questions, methods, and analysis were planned by my advisor, Daniel M. Johnson, and me, Kathryn V. Baker. I conducted all field work, lab work, and data analysis with the help of technicians and friends, who are mentioned in the Acknowledgements. I wrote the initial draft of all chapters, with help from Daniel M. Johnson. Xiaonan Tai incorporated my data into the TREES model, the results of which are presented in Chapter 2. Xiaonan Tai and Megan L. Miller reviewed and edited Chapter 2. Funding for these projects was obtained by Daniel M. Johnson and me.

# Chapter 1: Fundamental concepts and background of tree hydraulic function in the inland northwest, USA

## 1.1.0 Context for the research

### 1.1.1 Importance of forests

Forests are a crucial part of global and atmospheric fluxes, particularly the carbon and water cycles. Covering 30% of land surface, they store 45% of terrestrially-stored carbon and annually sequester around 33% of human-emitted carbon dioxide ($CO_2$; Bonan 2008). Forested ecosystems in the inland northwest (eastern Washington, northern Idaho, and western Montana) are important economically, for recreation, for conservation, and for ecosystem services. In Idaho, over 40% of the total land is forested, and over 13,000 people are employed by the forest products industry (Oswalt *et al.* 2014, Pokharel *et al.* 2018). The health of forest ecosystems impacts the state's recreation industry as well. Activities such as river sports, skiing, and hunting support 5,600 jobs, contributing $4.6 billion to the state's economy according to Idaho's Department of Commerce (2018).

### 1.1.2 Basics of tree physiology

Tree leaves are the site of gas exchange between the tree and the atmosphere. Carbon dioxide from the atmosphere enters the trees' leaves through their stomata. The $CO_2$ is synthesized into sugars that are then used to power cells and form more complex compounds to grow the plant. As $CO_2$ enters the leaf water molecules also exit through the same stomata (Lorimer *et al.* 2010). Throughout plant evolution, the trade-off between carbon gain and water loss has driven many adaptations, such as waxy cuticles and wood. The manner by

which trees now move water from the soil through the leaves (transpiration) is mechanically impressive (Sperry 2003).

While humans require positive pressure to move water upwards or across lateral distances, trees use a type of suction, or negative pressure to draw water from the soil up into their leaves (Zimmermann 1983). This tension is initiated inside the leaf, where water evaporates from the surface of mesophyll cells into the interstitial spaces, from which it exits the stomata. As the water molecules evaporate, it induces more tension on the molecules behind it; and so on down a kind of column of water, strengthened by the liquid's hydrogen bonds, that continues through the branches, bole, and roots, into the soil. As soil water is depleted, the suction, or negative water potential, has to become greater to continue drawing water upwards.

This becomes dangerous when the tensions within the xylem (dead conductive cells within wood or leaves) become so great that embolism occurs (Tyree & Zimmerman 2002). Embolisms can have different sources: air seeding from a neighboring embolized cell or injury can induce them (Cosgrove & Holbrook 2010), as can freezing and thawing of xylem sap (Pittermann and Sperry 2006). There is also some evidence that dissolved air within the sap itself can come out of solution at negative water potentials, allowing "nanobubbles" to expand to fill the xylem conduit (Schenk *et al.* 2015, 2017). As emboli form, the cell that has become air-filled can no longer be used to conduct water and is isolated from its neighbors. Then, according to Darcy's Law, the water potential gradient (more negative moving from soil to leaf) must become greater to maintain the flow of sap.

So, as continuing to allow $CO_2$ into the leaf to fuel photosynthesis also creates greater tension via transpiration, maintaining open stomata in times of water stress can be dangerous

for a tree. Allowing embolism to occur throughout the sapwood decreases and can ultimately halt sap flow altogether. An option for the trees, then, is to close their stomata, halt transpiration and relieve the water potential gradient that it induces. However, while transpiration is arrested, so is photosynthesis. And, because all living cells require sugars to stay alive, the tree has to resort to stored carbon to fuel respiration. A traditional outlook on tree mortality relies on using those two strategies as examples of two potential mechanisms of tree death. In times of a soil water shortage, failure to close stomata and relieve the tension can lead to runaway embolism and hydraulic failure. On the other hand, a tree that dutifully closes its stomata and prevents very negative water potentials within itself is prone to die of carbon starvation under prolonged drought (McDowell *et al.* 2008). This is an important if overly simplified generalization of how trees deal with water stress.

Generally and intuitively speaking, trees exist in places where their physiological strategies allow them to persist. Slow natural adaptation rates and the incremental quality of their migration leaves forests particularly vulnerable to the rapidity of climate change. Large-scale forest mortality has become more common globally, but our ability to predict where, when, and how those events will occur remains poor (Allen *et al.* 2010, Jiang *et al.* 2013, Adams *et al.* 2017). In some instances, populations will shift or disappear due to mortality from pests, pathogens, wildfires, and drought. Even when water stress is not the only driver, most other mechanisms of forest mortality are exacerbated by droughts, which have increased in occurrence and intensity in the West (Clark et al. 2016). Prolonged droughts are widely predicted to continue increasing over the next century, resulting in increased forest mortality (Adams *et al.* 2009, van Mantgem *et al.* 2009, Williams *et al.* 2012, Anderegg *et al.* 2013, IPCC 2014). Because the urgency of improving predictions for forest mortality will

only intensify with time, it is important to build our understanding of how trees function under drought conditions (Hartmann *et al.* 2018).

### 1.1.3 Conifers in the northwest

Tree ecophysiological research related to hydraulics and drought has flourished in the Pacific Northwest since the late 1970's (Waring & Running 1978, Waring *et al.* 1982, Brooks *et al.* 2002, McCulloh *et al.* 2014). The mechanisms by which conifer trees, largely *Pinus ponderosa* and *Pseudotsuga menziesii* use water were systematically explored on either side of the Cascades by researchers from Oregon State University, the US Forest Service, and the Environmental Protection Agency. By comparing species and populations, they teased out how different parameters determine how trees function hydraulically in situ. *P. ponderosa* was generally the more vulnerable to embolism of the two species but employed other strategies to maintain functionality including tighter stomatal regulation of leaf water potentials and greater sapwood depth (e.g. Barnard *et al.* 2011). The trees avoid drought impacts, rather than tolerate them, through tight stomatal control, large water storage within the tree (capacitance), deep root systems, and allometric adjustments such as shedding needles to decrease water sink (Delucia *et al.* 2000, Maherali *et al.* 2000, Kerr *et al.* 2015).

However, relatively little is known about the hydraulic strategies of conifer trees in the inland northwest (but see Bond and Kavanagh 1999, Kavanagh et al. 2007, Pangle *et al.* 2015, Piñol and Sala 2000, Stout and Sala 2003). In the Missoula, MT area, Piñol and Sala reported a negative relationship between sapwood conductivity to water and branch resistance to cavitation in *P. ponderosa, P. menziesii, Larix occidentalis, Pinus contorta, Pinus albicaulis,* and *Abies lasiocarpa* (2000). Similar to the Oregon studies, they also saw

that *P. ponderosa* had less embolism-resistant sapwood and greater stomatal regulation of water loss than *P. menziesii* at the xeric sites. Stout and Sala further compared the strategies of *P. ponderosa* and *P. menziesii* in three months of the summer at two sites, xeric and mesic, in the same area of Montana. In that study, neither species had very different vulnerability to cavitation between sites, but *P. ponderosa* showed greater plasticity in its gas exchange, with much higher stomatal conductance ($g_s$) in June when soil water was more available contrasting with much lower values in July and August. Meanwhile, the gas exchange values for *Pseudotsuga* were not significantly different between the three months.

The current edict for the field of tree ecophysiology is to identify and broadly document metrics that can be used to model drought responses for various species (Choat *et al.* 2012, Fu & Meinzer 2018, Hartmann *et al.* 2018). An historically popular metric is branch $\Psi_{P50}$. It is determined in a lab by measuring the specific hydraulic conductivity ($K_S$) of an excised branch at different pressures (negative or the positive equivalent) to simulate the change in conductivity if the sample were to be drying out in situ. The $\Psi_{P50}$ is the water potential at which the $K_S$ has declined by 50%. While that parameter is convenient, not least because it has been published for hundreds of species, it is not a reliable estimate of whole-tree vulnerability to embolism, as the branches are rarely the most vulnerable organ (Willson et al. 2008, McCulloh et al. 2014, Johnson *et al.* 2016, 2018). Leaves and roots are more commonly limiting organs to water flow in trees. Leaf hydraulic parameters can be determined in the lab. Vulnerability curves can be constructed by measuring a leaf's ability to conduct water at different water potentials, and leaf pressure-volume curves show the relationship between the water potential of a leaf and its water content. From these, we can calculate, among other things, the turgor loss point ($\Psi_{TLP}$). As the name indicates, the $\Psi_{TLP}$ is

the water potential where the leaf loses turgor, which can result in reductions in water transport (e.g. Brodribb *et al.* 2003) and photosynthesis (Lawlor and Tezara, 2009; Tezara, et al. 1999). This, though not a new method/parameter, is emerging as a promising proxy for much more time-intensive methods (Fu *et al.* 2018). Root $K_S$ parameters are determined similarly to those in branches and speak to underground hydraulic dynamics, which can be more difficult to assess.

### 1.1.4 Focus of this dissertation

This dissertation, building on previous projects conducted in the American West, is comprised of three datasets that are particularly useful to understand how conifers function through different degrees of drought stress. The depth and composition of soils on the University of Idaho Experimental Forest, where the projects took place, allow for a large amount of water storage. This stored soil water enables forests to persist despite months of little to no precipitation in the summer. As the decline in soil water was slow, we were able to document systematically the strategies involved in tree growth and maintenance through several long growing seasons. The scale of our questions between the three research chapters goes from 1) broad, looking at the comparative physiology of six conifer species, to 2) specific, looking in-depth at water transport in mature *P. ponderosa* trees, to 3) more applied, looking at *P. ponderosa* water use after different thinning treatments.

### 1.2.0 References

Allen CD, Macalady AK, Chenchouni H, Bachelet D, McDowell N, Vennetier M, … Cobb N (2010) A global overview of drought and heat-induced tree mortality reveals emerging climate change risks for forests. Forest Ecology and Management, 259(4): 660–684.

Bonan GB (2008) Forests and climate change: forcings, feedbacks, and the climate benefits of forests. Science, 320: 1444-1449.

Bond BJ & Kavanagh KL (1999) Stomatal behavior of four woody species in relation to leaf-specific hydraulic conductance and threshold water potential. Tree Physiology, 19(8): 503–510.

Brodribb, T. J., N. M. Holbrook, E. J. Edwards, and M. V. Gutiérrez. 2003. Relations between stomatal closure, leaf turgor and xylem vulnerability in eight tropical dry forest trees. Plant, Cell and Environment 26:443–450.

Brooks JR, Meinzer FC, Coulombe R, & Gregg J (2002) Hydraulic redistribution of soil water during summer drought in two contrasting Pacific Northwest coniferous forests. Tree Physiology, 22: 1107–1117.

Choat, B., S. Jansen, T. J. Brodribb, H. Cochard, S. Delzon, R. Bhaskar, S. J. Bucci, T. S. Feild, S. M. Gleason, U. G. Hacke, A. L. Jacobsen, F. Lens, H. Maherali, J. Martínez-Vilalta, S. Mayr, M. Mencuccini, P. J. Mitchell, A. Nardini, J. Pittermann, R. B. Pratt, J. S. Sperry, M. Westoby, I. J. Wright, and A. E. Zanne. 2012. Global convergence in the vulnerability of forests to drought. Nature 491:752–755.

Clark JS, Iverson L, Woodall CW, Allen CD, Bell DM, Bragg DC, … Zimmermann NE (2016) The impacts of increasing drought on forest dynamics, structure, and biodiversity in the United States. Global Change Biology, 22(7): 2329–2352.

Cosgrove D & Holbrook M (2010). Water balance of plants. In Li. Taiz & E. Zeiger (Eds.), Plant Physiology (5th ed., pp. 85–105).

Fu X & Meinzer FC (2018) Metrics and proxies for stringency of regulation of plant water status (iso/anisohydry): A global data set reveals coordination and trade-offs among water transport traits. Tree Physiology, 39(1): 122–134.

Hartmann H, Moura CF, Anderegg WRL, Ruehr NK, Salmon Y, Allen CD, … O'Brien M (2018). Research frontiers for improving our understanding of drought-induced tree and forest mortality. New Phytologist, 218(1): 15–28.

Idaho Department of Commerce (2018) Annual Report. Boise, ID.

Kavanagh KL, Pangle, R., & Schotzko, A. D. (2007) Nocturnal transpiration causing disequilibrium between soil and stem predawn water potential in mixed conifer forests of Idaho. Tree Physiology, 27(4): 621–629.

Lawlor DW & Tezara W (2009) Causes of decreased photosynthetic rate and metabolic capacity in water-deficient leaf cells: A critical evaluation of mechanisms and integration of processes. Annals of Botany, 103(4): 561–579.

Lorimer GH, Buchanan BB, & Wolosiuk RA (2010) Photosynthesis: The carbon reactions. In L. Taiz & E. Zeiger (Eds.), Plant Physiology (5th ed., pp. 199–242).

Maherali H & DeLucia EH (2000) Xylem conductivity and vulnerability to cavitation of ponderosa pine growing in contrasting climates. Tree Physiology, 20(13): 859–867.

McDowell, N., W. T. Pockman, C. D. Allen, D. D. Breshears, N. Cobb, T. Kolb, J. Plaut, J. Sperry, A. West, D. G. Williams, A. Enrico, D. David, D. G. Williams, and E. A. Yepez. 2008. Mechanisms of plant survival and mortality during drought: Why do some plants survive while others succumb plants drought? New Phytologist 178:719–739.

McDowell, N., W. T. Pockman, C. D. Allen, D. D. Breshears, N. Cobb, T. Kolb, J. Plaut, J. Sperry, A. West, D. G. Williams, and E. A. Yepez. 2008. Mechanisms of plant survival and mortality during drought: Why do some plants survive while others succumb plants drought? New Phytologist 178:719–739.

Oswalt SN, Smith WB, Miles PD, Pugh SA (2014) Forest Resources of the United States, 2012: a technical document supporting the Forest Service 2015 update of the RPA Assessment. Gen. Tech. Rep. WO-91. Washington, DC: U.S. Department of Agriculture, Forest Service, Washington Office. 218 p.

Pan Y, Birdsey RA, Fang J, Houghton R, Kauppi PE, Kurz WA, Phillips OL, Shvidenko A, Lewis SL, Canadell JG et al. 2011. A large and persistent carbon sink in the world's forests. Science, 333: 988–993.

Pangle R, Kavanagh K, & Duursma R (2015). Decline in canopy gas exchange with increasing tree height, atmospheric evaporative demand, and seasonal drought in co-occurring inland Pacific Northwest conifer species. Canadian Journal of Forest Research, 45(8):1086–1101.

Piñol J & Sala A (2000). Ecological implications of xylem cavitation for several Pinaceae in the Pacific Northern USA. Functional Ecology, 14(5): 538–545.

Pittermann J, Sperry JS (2006) Analysis of freeze-thaw embolism in conifers. The interaction between cavitation pressure and tracheid size. Plant Physiology, 140: 374-382.

Pokharel R, Latta G, Alward G, Cook PS, Becker DR (2019) Idaho's Forest Products Industry 2018. 1–4.

Schenk HJ, Espino S, Romo DM, Nima N, Do AYT, Michaud JM, … Jansen S (2017) Xylem Surfactants Introduce a New Element to the Cohesion-Tension Theory. Plant Physiology, 173(2): 1177–1196.

Schenk HJ, Steppe K, Jansen S (2015) Nanobubbles: a new paradigm for air-seeding in xylem. Trends in Plant Science, 20(4): 199-205.

Sperry, J. S. 2003. Evolution of Water Transport and Xylem Structure. International Journal of Plant Sciences 164:S115–S127.

Stout DL & Sala A (2003) Xylem vulnerability to cavitation in Pseudotsuga menziesii and Pinus ponderosa from contrasting habitats. Tree Physiology, 23(1): 43–50.

Tezara W, Mitchell VJ, Driscoll SD, & Lawlor DW (1999) Water stress inhibits plant photosynthesis by decreasing coupling factor and ATP. Nature, 401(6756): 914–917.

Tyree MT & Zimmermann, MH (2002) *Xylem Structure and the Ascent of Sap*. Springer Berlin Heidelberg.

Van Mantgem JP, Stephenson NL, Byrne JC, Daniels LD, Franklin JF, … Veblen TT (2009) Widespread Increase of Tree Mortality Rates in the Western United States. Science, 323(5913): 521–524.

Waring RH & Running SW (1978) Sapwood water storage: its contribution to transpiration and effect upon water conductance through the stems of old-growth Douglas-fir. Plant, Cell & Environment, 1(2), 131–140.

Waring R, Schroeder P, & Oren R (1982) Application of the pipe model theory to predict canopy leaf area. Journal of Forest Research, 12: 556–560.

Williams AP, Allen CD, Macalady AK, Griffin D, Woodhouse CA, Meko DM, … McDowell, NG (2013) Temperature as a potent driver of regional forest drought stress and tree mortality. Nature Climate Change, 3(3): 292–297.

Willson CJ, Manos PS, & Jackson RB (2008) Hydraulic traits are influenced by phylogenetic history in the drought-resistant, invasive genus Juniperus (Cupressaceae). American Journal of Botany, 95(3): 299–3

# Chapter 2: Six co-occurring conifer species in northern Idaho exhibit a continuum of hydraulic strategies during an extreme drought year

## 2.0.0 Abstract

As growing seasons in the northwestern USA lengthen, on track with climate predictions, the mixed conifer forests that dominate this region will experience extended seasonal drought conditions. The year of 2015, which had the most extreme drought for the area on record, offered a potential analog of future conditions. During this period, we measured the daily courses of water potential and gas exchange as well as the hydraulic conductivity and vulnerability to embolism of six dominant native conifer species, *Abies grandis*, *Larix occidentalis*, *Pinus ponderosa*, *Pinus monticola*, *Pseudotsuga menziesii*, and *Thuja occidentalis*, to determine their responses to 5 months of record low precipitation. The deep ash-capped soils of the region allowed gas exchange to continue without significant evidence of water stress for almost two months after the last rainfall event. Midday water potentials never fell below -2.2 MPa in the evergreen species and -2.7 MPa in the one deciduous species. Branch xylem was resistant to embolism, with $P_{50}$ values ranging from -3.3 to -7.0 MPa. Root xylem, however, was more vulnerable, with $P_{50}$ values from -1.3 to -4.6 MPa. This range resulted in roots from the two *Pinus* species to experience predicted declines in hydraulic conductivity. Stomatal conductance of all six species was significantly responsive to vapor pressure only in the dry months (August-October), with no response evident in the wet months (June-July). While there were similarities among species, they exhibited a continuum of isohydry and safety margins. Despite the severity of this drought, all species were able to continue photosynthesis until mid-October, likely due to the

mediating effects of the meter-deep, ash-capped silty-loam soils with large water storage capacity. Areas with these soil types, which are characteristic of much of the Northwest USA, could serve as refugia under drier and warmer future conditions.

### 2.1.0 Introduction

Conifers inhabit some of the most extreme habitats on earth that are capable of supporting tree life forms (Farjon 2008; Brodribb *et al.* 2012). As climate change extends growing seasons, many of these forests will likely experience drought stress earlier, longer, and at greater severities. Effects of climate change have been evident in the Pacific Northwest, USA for more than a decade, with rising temperatures and drier summers (Abatzoglou *et al*. 2014). These changes are predicted to continue, with precipitation regimes shifting to greater ratios of rain to snow and temperatures potentially increasing by 4 °C within the 21$^{st}$ century (Mote and Salathé 2010). Increased temperatures will cause the reduced snowpack to melt earlier, creating a positive feedback loop that will further exacerbate extended, xeric growing seasons (Luce and Holden 2009: Klos *et al*. 2014;). Characterized by dry summers, the mixed-conifer forests of northern Idaho largely depend on soil water storage recharged by snowmelt and springtime precipitation to sustain transpiration throughout the growing season (Baker 1981). Widespread ash-capped soil deposits in the northwestern United States provide high water storage capacity, due to their high porosity and water infiltration, facilitating highly productive forest ecosystems (Kimsey *et al.* 2005). In this region, the deep, ash-capped soils provide mixed conifer forests with adequate soil moisture during the long (3-5 months) dry portion of the growing season (Page-Dumroese *et al*. 2005).

While traditional comparisons of tree species in the region are based on plants' survival and growth during drought (Daubenmire 1968a and 1968b; Minore 1979), another type of framework, degree of isohydry, has been used more recently to describe a continuum of trees' response to drought (Tardieu and Simonneau 1998; Fu *et al*. 2019; Li et al 2019). Although there have been different definitions, more isohydric species generally control their leaf water potentials ($\Psi_L$) by decreasing their stomatal conductance when $\Psi_L$ approaches the "set point" values (Meinzer *et al.* 2016, Martínez-Vilalta and Garcia-Forner 2017). These set points can be related to the xylem vulnerability to embolism to characterize the safety margins that the plants allow (Meinzer *et al.* 2009, Choat *et al.* 2012, Skelton *et al.* 2015). Alternatively, relatively anisohydric species allow gas exchange and photosynthesis to continue as their $\Psi_L$ values decline (McDowell et al. 2008, Fu and Meinzer 2018). Stomatal sensitivity to vapor pressure deficit (VPD), with stomatal conductance ($g_S$) declining in response to greater VPDs, has also been related to drought performance (Domec *et al.* 2009, Anderegg *et al.* 2014). However, which parameters are most appropriate for evaluating drought response strategies remains unclear (Hartmann *et al.* 2018).

As climate regimes change and historical species' distribution areas become potentially unfavorable for continued survival, it is important to address the questions of which tree populations will be prone to mortality and what conditions can facilitate survival (Millar *et al.* 2007, Hartmann *et al.* 2015, McDowell *et al.* 2016, Mathys *et al.* 2017). Local climate plays a large role in driving population success, but other abiotic site characteristics such as favorable soil type and depth can mediate drought conditions (Wei *et al.* 2018). Because few comparisons of hydraulic strategies across regionally dominant conifer species exist (but see Bond and Kavanagh 1999, Piñol and Sala 2000, and Pangle *et al.* 2015), our

original goal was a general comparative study of several regionally-dominant conifer species: *Abies grandis*, *Larix occidentalis*, *Pinus monticola*, *Pinus ponderosa*, *Pseudotsuga menziesii*, and *Thuja plicata*. However, as 2015 proved to be an unusually hot and dry year (Marlier 2017), we took advantage of the unprecedented drought to understand how mixed conifer forests in northern Idaho will fare under future extended seasonal drought conditions. Because this area experiences growing seasons marked by little or no rainfall and high evaporative demand, we expected that these species would exhibit drought-resistant traits such as stomata that are sensitive to VPD, embolism-resistant xylem, and positive hydraulic safety margins. In the 1960's, Daubenmire established a wet to dry continuum, characterizing the sites where different tree species are found. For our species, the order on that continuum was: *P. ponderosa* (driest)*, P. menziesii, L. occidentalis, A. grandis, P. monticola,* and *T. plicata* (Daubenmire 1966, 1968, also see Rehfeldt *et al*. 2006 and Franklin and Dyrness 1973).

We hypothesized, based on the positions that these species occupy on Daubenmire's dry to wet continuum, that they would exhibit a continuum of drought-resistant traits where the species considered most drought tolerant would exhibit 1) the greatest stomatal sensitivity, with $g_S$ decreasing with higher VPDs and more negative $\Psi_L$, and 2) the most embolism resistant xylem and the largest xylem hydraulic safety margins. Post hoc, we further employed a plant physiological model, the Terrestrial Regional Ecosystem Exchange Simulator (TREES) model (Mackay *et al*., 2015), to evaluate the influence of alternative soil types in mediating species' response to drought. We hypothesized that 3) the deep silty loam soils of the region are important for buffering drought impacts in addition to hydraulic strategies.

## 2.2.0 Methods

### 2.2.1 Site description and plant materials

This study took place in the (redacted) section of the (redacted) Forest, near Princeton, ID USA (46°50'/116°43') (Fig. 2-1). The area is 0.8 hectares NNE facing with an average slope of 8.5°. The climate is maritime/continental, which is characterized by snowy winters, wet springs, and dry summers. The soils are Reggear-Santa complex, an ash cap silty loam that extends ~1 m in depth (Soil Survey Staff, NRCS). For the years 1980-2015, mean annual precipitation was 875 mm; mean annual maximum temperature was 13.5 °C; mean annual minimum temperature was 1.8 °C (Thornton *et al.*, 2016).

Eight conifer species exist on this single-aged stand, established through a combination of planting and natural regeneration after the site was cleared and burned in 2000. The average spacing between trees was approximately 3 m. Six of the eight were selected as study species due to their relative abundance: *A. grandis*, *L. occidentalis*, *P. monticola*, *P. ponderosa*, *P. menziesii*, and *T. plicata*. As Figure 2-1 illustrates, these species comprise a large portion of the forests in the northwestern United States. These six species can co-occur naturally but also span a range of topographical and micro-climatic environments. Ten trees per species were then selected for the study, based on their apparent health, access to sunlight, consistent intra-specific size, and range across the site in an effort to keep variation in soil water as similar as possible among species. The trees were between 1.5 and 4 meters in height, with diameter at breast height of 5-10 cm and leaves that were easily accessible from the ground. In several cases, individual study trees showed signs of pathogens (i.e. *Cronartium ribicola*, blister rust, in *P. monticola* and *Rhabdocline spp.* fungus in *P. menziesii*) later in the season; in these cases, alternate healthy trees were chosen as

replacements. Measurements were performed two to three days per month from June to October 2015; for each day (Fig. 2-2), three to four individuals per species were randomly selected from the original ten for gas exchange and water potential measurements, and no individuals were measured more than once within a month so that six to ten trees per species were studied each month.

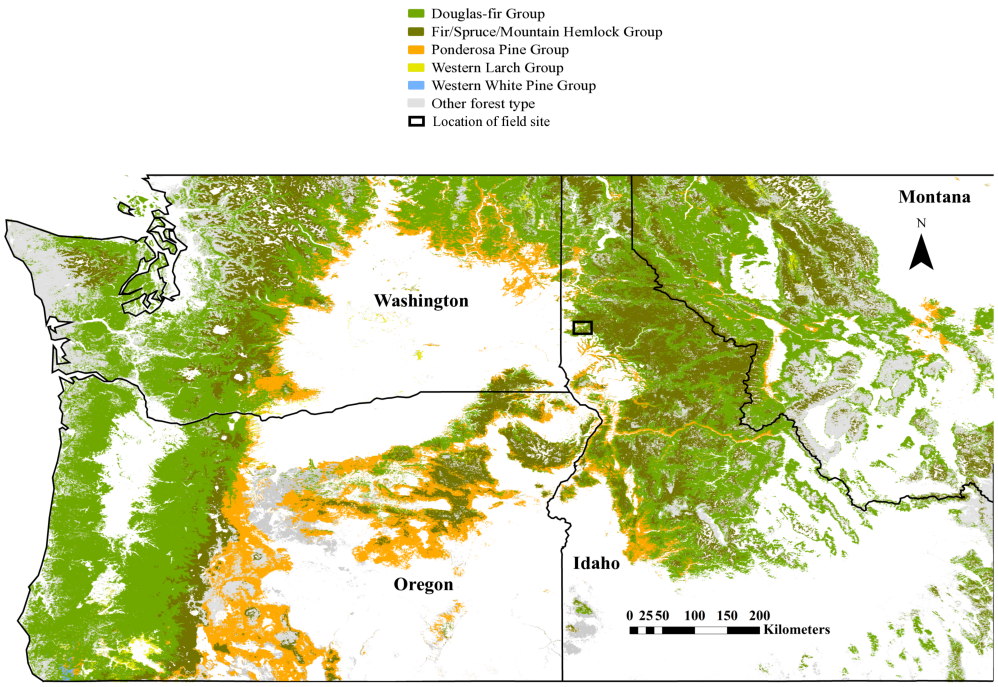


Figure 2-1. Non-grey highlighted sections represent mixed conifer forests that contain one or more of the study species. The field site is located within the black rectangle in northern Idaho. Forest-type map layer was developed by USDA Forest Service Forest Inventory and Analysis Program and Remote Sensing Applications Center.

### 2.2.2 Meteorological station

Volumetric soil water content and soil water potential (VWC and $\Psi_S$, GS-1 and MPS-6 sensors respectively, Decagon Devices, Inc., Pullman, WA) were continuously measured at

30 cm and 80 cm depths in two soil pits on the site, one in a more densely treed part of the stand and one in a less dense area (pits 2 and 1, respectively, in Fig. 2-3). Temperature and relative humidity were measured every five minutes and averaged over 30 minutes (CS-215, Campbell Scientific, Logan, UT), and precipitation was recorded every 30 minutes using a tipping bucket rain gauge (TE-525, Campbell Scientific). All meteorological sensors were attached to dataloggers (CR-1000T, Campbell Scientific).

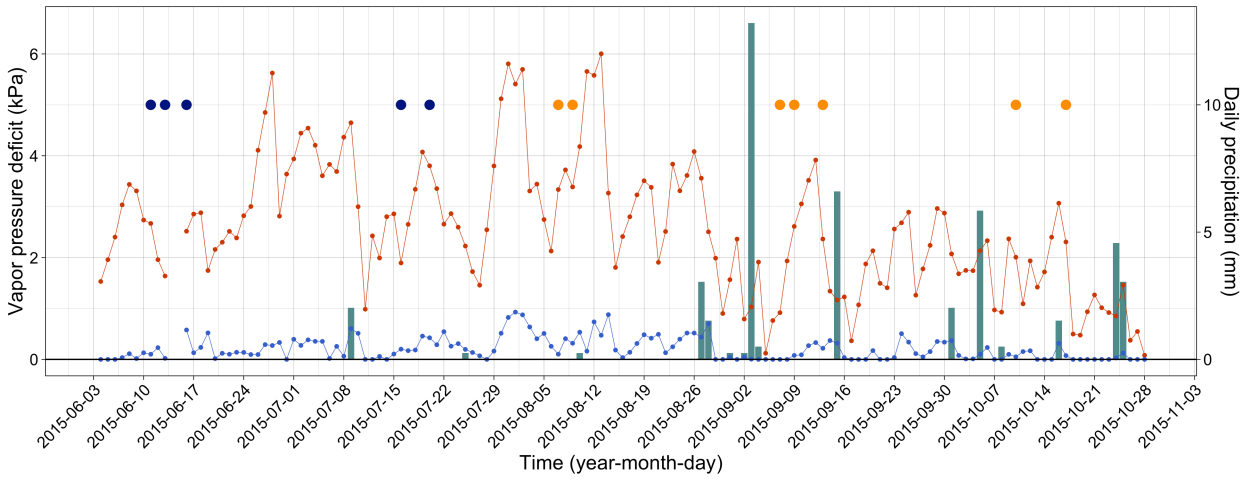


Figure 2-2. Minimum (blue) and maximum (red) daily VPDs on primary y-axis and wet (navy) and dry (orange) sub-season field days with precipitation (bars) on the secondary y-axis.

### 2.2.3 Gas exchange

Gas exchange was measured with a LI-6400 (LI-COR Biosciences Lincoln, NE) on 3-4 individuals per species per day (6-10 individuals per species per month) every two hours, beginning at 06:00 or 08:00, depending on time of sunrise, and was repeated every two hours until 16:00. For the five species with needle-like leaves, a set number of needles were removed from the tree (five needles for *A. grandis*, *L. occidentalis*, and *P. menziesii*, and one

fascicle bundle for *P. monticola* and *P. ponderosa*) and placed in the sample chamber, with at least one leaf touching the leaf thermocouple. Previous studies have shown that conifer gas exchange is not affected by removing leaves from the tree in this timeframe (Dang *et al.* 1997; Woodruff *et al.* 2009). Leaves from *T. plicata* were not removed from the tree prior to measurements. The $CO_2$ concentration inside the leaf chamber was set to 400 μmol $CO_2$ $mol^{-1}$, and flow rate was set to 500 μmol $s^{-1}$; PAR was set to 1500 μmol $m^{-2}$ $s^{-1}$, and ambient temperatures were maintained. To determine leaf area, leaves of six individuals of each species were brought back to the lab each month, trimmed to the LICOR chamber area, and measured on the LI-3100C Area Meter. All leaf areas were expressed on a silhouette area basis. The mean of those six samples per species was calculated and used as leaf area for all measurements that month.

### 2.2.4 Water Potential Measurements

Leaf water potential was measured using a pressure chamber (Scholander *et al.* 1965; PMS, Albany OR) beginning well before sunrise, at either 04:00 or 06:00, and was repeated every two hours until 16:00. Samples of the youngest hardened needle or branchlet from fully exposed, south-facing branches were clipped and immediately sealed in a bag. Prior to sealing, the air in the bag was humidified by breathing into the bag. The samples were then measured in the pressure chamber within an hour.

In August and September, six total intact branches of each species were covered with plastic bags and aluminum wrap the evening before diurnal measurements. They were sealed to be light- and air-tight to allow their $\Psi_L$ to equilibrate with branch water potential (Bucci *et*

*al*. 2003). The next afternoon, samples were removed from inside the bags, and their $\Psi_L$ were recorded for branch $\Psi_{MIN}$.

### 2.2.5 Vulnerability Curves

Six root and branch samples were taken of each study species, from trees that were not used for other measurements. Roots were excised from the shallowest available portion of the root system, which was between 20 and 40 cm deep. The root samples were 18-20 cm long when excised with 0.45 – 1.76 cm diameters after bark was removed. Branches were clipped from the trees, at least 5 cm proximal from the segment to be measured. Their diameters after bark removal were 0.54 – 1.78 cm. Root and branch samples were immediately placed into black plastic bags with wet paper towels, stored in a cooler, and transported to the lab. Samples were cut to 14 cm lengths under water, stripped of their bark, and placed in a 20 mM KCl solution (pH = 2) under a partial vacuum overnight. Maximum hydraulic conductivity ($K_{S\text{-}MAX}$) was determined after overnight vacuuming.

The flow rates of the samples were measured using a plastic tubing manifold with a hydrostatic pressure head of 2.4-6.2 kPa (Sperry *et al.* 1988). After recording the maximum flow rates, negative water potentials were induced in the samples using a centrifuge with submerged sample tips, as described in Alder *et al*. (1997). Care was taken to maintain a balanced centrifuge, adding water into cups, which were 7 mm deep, symmetrically with a pipette to avoid a pressure gradient that would induce pit aspiration (Beikircher *et al.* 2010, Bouche *et al.* 2015). It should be noted that there have been recent debates about the artefacts when measuring vulnerability to embolism (Cochard *et al.* 2010, Sperry *et al.* 2012), however these artefacts have been predominantly found in long-vesseled angiosperms and

not in conifers (Li *et al.* 2008, Cochard *et al.* 2013, Choat *et al.* 2016, Torres-Ruiz *et al.* 2017). Hydraulic conductivity was calculated by multiplying the flow by the length and dividing by the cross-sectional area of the sample to get specific conductivity ($K_S$). This process was repeated with progressively more negative water potentials until the flow was < 10% of its maximum value. Measurements were completed within a week of sampling. Branch and root $K_S$ curves were fit using 3-parameter sigmoidal curves, except *P. monticola* branch $K_S$, which was fit with a 4-parameter sigmoidal curve because of its greater adjusted $R^2$ value. $P_{50}$ values were subsequently determined from the curves as the estimated water potential at 0.5 $K_{S\text{-}MAX}$.

### 2.2.6 Data analysis

Gas exchange and water potential data were separated into two "sub-seasons", i.e. wet, June-July, and dry, August-October. The sub-seasons were partitioned not based on precipitation but rather on shallow soil $\Psi_S$ (Fig. 2-2). Soil water potentials, measured at 30 cm in two soil pits, remained less negative as volumetric water content declined until late July.

The reported numbers for $g_S$ and $\Psi_L$ are the mean hourly values within that month or sub-season. To determine whether species' stomatal responses to VPD or $\Psi_L$ were significantly different between sub-seasons, we used linear ANOVA models with sub-season as an interaction term and post-hoc Tukey's HSD analyses in R (R Development Core Team, 2016) with sub-season as an interaction term ($\alpha = 0.05$). VPD was natural log transformed to compare linear regression parameters (Oren *et al*. 1999). Regression models, curve fits, and confidence intervals were calculated using either R or Sigma Plot 12.5 for Windows (1999,

Jandel Scientific Software, San Rafael, CA). Simple and multiple linear regressions were performed in R (R Development Core team, 2015, 2017, and 2018) to address the variables potentially affect $g_S$, $\Psi_L$, $\Psi_{PD}$, and VPD. Stomatal conductance and VPD were transformed using a natural log to satisfy normality assumptions.

### 2.2.7 TREES Model

To compare the influence of different soil types on the study species' ability to continue transpiring through extended drought, we incorporated our observed physiological traits into the TREES model (Mackay *et al.* 2015). TREES explicitly solves soil-plant hydraulic status following the approach described in Sperry *et al.* (1998), based on half-hourly meteorological forcing data that include air temperature, wind speed, radiation, vapor pressure deficit, and soil temperature. It integrates the hydraulic properties of both soil and plant to predict actual transpiration ($E_C$) and transpiration potential ($E_{CRIT}$).

TREES was parameterized for each species based on measured vulnerability to embolism, gas exchange, and predawn and midday leaf water potential observations ($\Psi_{PD}$ and $\Psi_{MD}$). Leaf area index was assumed to be 2 $m^2$ $m^{-2}$. Rooting zone was assumed to be 1 m deep and discretized into three layers. Site-specific soil texture data was used to parameterize the soil hydraulic properties (geometric mean particle diameter and geometric standard deviation of particle size), following methods in Campbell (1985). Modeled $\Psi_{PD}$ and $\Psi_{MD}$ values were compared with observations to assess the ability of TREES in capturing the seasonal dynamics of six conifer species (Supp. Fig. 2-1).

We imposed TREES to different soil types while keeping all other conditions the same and calculated relative hydraulic safety envelopes following the approach described in

Johnson *et al.* (2018). For every species and soil type, we calculated the difference between $E_{CRIT}$ and $E_C$, which is the hydraulic safety envelope. The relative safety envelopes were then determined by normalizing the seasonal mean values by the seasonal maximum. This metric has been used to represent plant vascular health status (Johnson *et al.* 2018; Tai *et al.* 2017).

## 2.3.0 Results

### 2.3.1 Climate

The temperature, humidity, and precipitation of 2015 was compared to the previous 14 years based on data from a nearby SNOTEL site (snow telemetry, Natural Resource Conservation Service; Site Number 989, 1433m a.s.l.) and to the previous 100 years using National Oceanic and Atmospheric Administration's (NOAA) Global Historical Climatology Network data for Potlatch, ID (46°54'/116°51'), located 16 km from the field site. Compared to the previous 14 years, the 2015 date of peak snow water equivalent was 43 days earlier than the mean day of March 25$^{th}$. The ablation date, when the snow is completely melted, was 31 days earlier than the mean of May 10$^{th}$. VPDs at the field site ranged from 0.0 to 6.3 kPa. Comparing the dates of our study period (June 5$^{th}$ to October 17$^{th}$) with a 106-year record, 2015 was the third driest year (49.5 mm of rain) with the two drier years being significantly cooler in both mean minimum and maximum temperatures ($\alpha = 0.01$, Supp. Fig. 2-2).

Our field site received even less precipitation than the weather station, with only 27 mm of rain during the study period, and soil water potential measurements from soil sensors showed clear depth-based differences in temporal soil desiccation during the growing season. Water potentials at a depth of 30 cm began to decline at a much greater rate in late July,

reaching ca. -8.0 MPa (which is the lower operational limit of these sensors; Decagon, personal comm.) by mid-August to early-September. The water potentials at 80 cm, however, maintained relatively non-negative values during the study period (Fig. 2-3).

### 2.3.2 Gas exchange

Stomatal conductance was higher in the wet sub-season compared to the dry sub-season; this comparison was significant for *L. occidentalis*, *P. monticola*, *P. ponderosa*, and *P. menziesii* ($p < 0.05$) and was not significant for *A. grandis* and *T. plicata* ($p = 0.065$ and 0.051, respectively). There was greater variation in $g_s$ as a function of VPD during the wet sub-season, while the dry sub-season $g_s$ became more consistent throughout the day with less variation (Fig. 2-4 and 2-5, data points included in Supp. Fig. 2-3). Comparing $g_s$ to VPD, *L. occidentalis*, *P. monticola*, and *P. ponderosa* had significantly different slopes between the two sub-seasons, whereas *A. grandis*, *P. menziesii*, and *T. plicata*, did not. There was a trend across species of stomata being more sensitive to VPD in the dry sub-season as indicated by the more negative slopes (Fig. 2-5). In fact, none of the wet sub-season linear regressions of the log of $g_S$ and the log of VPD (transformed to satisfy normality assumptions) were significant, while all of the same comparison for the dry sub-season were (Table 2-1). Analyzing $g_S$ as a function of $\Psi_L$, with sub-season as an interaction term, illustrated that only *L. occidentalis* and *P. monticola* had significantly different slopes between sub-seasons, while the dry season again showed generally greater stomatal sensitivity (Supp. Fig. 2-4).

There was no significant effect of either $\Psi_L$ or VPD on $g_S$ during the wet sub-season. In the dry sub-season, however, the same simple linear regressions for both $\Psi_L$ and the natural log of VPD were both significant for each species. In all cases, lower $g_S$ was

associated with greater VPD and more negative $\Psi_L$. The results of the multiple linear regressions were more varied, with the incorporation of $\Psi_{PD}$ improving the models in the wet sub-season. Increasing variables generally improved adjusted $R^2$ values, but coefficients were not necessarily significant (Supp. Table 2-1).

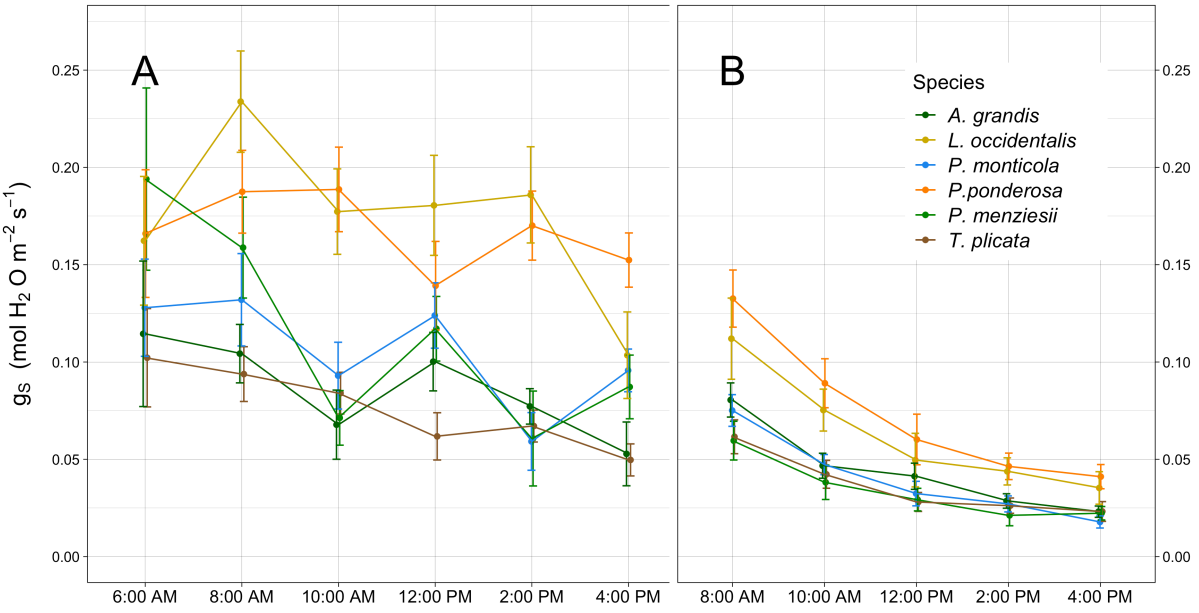


Figure 2-4. Stomatal conductance, $g_S$, of each species throughout the day in the a) wet vs. b) dry months. Error bars are standard error.

### 2.3.3 Water potentials

For all species, $\Psi_{PD}$ values were significantly more negative in the dry sub-season than in the wet sub-season (Table 2-2). Only *L. occidentalis* and *P. ponderosa* had significantly distinguishable $\Psi_{MIN}$ between the two sub-seasons ($\alpha = 0.05$). *L. occidentalis* had a more negative $\Psi_{MIN}$ in the wet sub-season than in the dry, and *P. ponderosa* had a more negative value in the dry sub-season than in the wet. *L. occidentalis* were not measured in October due to its deciduousity and an early loss of leaves in mid-September.

Previous research in northern Idaho has shown that $\Psi_{PD}$ equilibrate with $\Psi_S$ on nights with VPDs less than 0.12 kPa (Kavanagh 2007). Despite consistently large midday VPDs (Fig. 2-2), the predawn VPDs were low enough to allow the soil and the leaves to equilibrate for half of the field days. Within each week, there were nights with VPDs either above or below the 0.12 kPa threshold. There was not a significant difference in the $\Psi_{PD}$ measurements between those days (P-values ranging from 0.29 in *A. grandis* to 0.97 in *P. ponderosa*). Therefore, we considered $\Psi_{PD}$ to be equal to the average $\Psi_S$ where the roots are active for this study. An exception to this occurred in September, when the $\Psi_{PD}$ for three species, L. *occidentalis*, *P. ponderosa*, and *P. menziesii* increased to values comparable to those in July (Fig. 2-3). The September field days occurred just after a 14 mm rainfall event (Fig. 2-2), which did not affect the $\Psi_S$ measured in soil pits and did not appear to infiltrate past the litter layer above the soil (pers. obs.). The increase in $\Psi_{PD}$ may have been due to foliar water uptake (Limm *et al.* 2009, Berry and Smith 2013), but that phenomenon was not addressed in this study.

| | | $\ln(g_S) = a + b * \ln(VPD)$ | | $\ln(g_S) = a + b * \lvert \Psi_L \rvert$ | |
|---|---|---|---|---|---|
| | | b | Adjusted $R^2$ | b | Adjusted $R^2$ |
| Wet sub-season | *A. grandis* | | -0.05 | | 0.17 |
| | *L. occidentalis* | | 0.04 | | 0.02 |
| | *P. monticola* | | -0.04 | | -0.06 |
| | *P. ponderosa* | | 0.02 | | -0.02 |
| | *P. menziesii* | | 0.00 | | 0.01 |
| | *T. plicata* | | 0.12 | | 0.15 |
| Dry sub-season | *A. grandis* | -1.09 | 0.64 | -0.93 | 0.39 |
| | *L. occidentalis* | -1.28 | 0.63 | -1.05 | 0.28 |
| | *P. monticola* | -1.10 | 0.45 | -0.95 | 0.20 |
| | *P. ponderosa* | -1.10 | 0.70 | -0.95 | 0.23 |
| | *P. menziesii* | -0.93 | 0.46 | -0.95 | 0.49 |
| | *T. plicata* | -0.64 | 0.27 | -0.99 | 0.35 |

Table 2-1. Linear regressions relating stomatal conductance to vapor pressure deficit and leaf water potential for the six species in the two sub-seasons. Coefficient b was included when p-value was less than 0.05. Vapor pressure deficit and $g_S$ were transformed to satisfy normality.

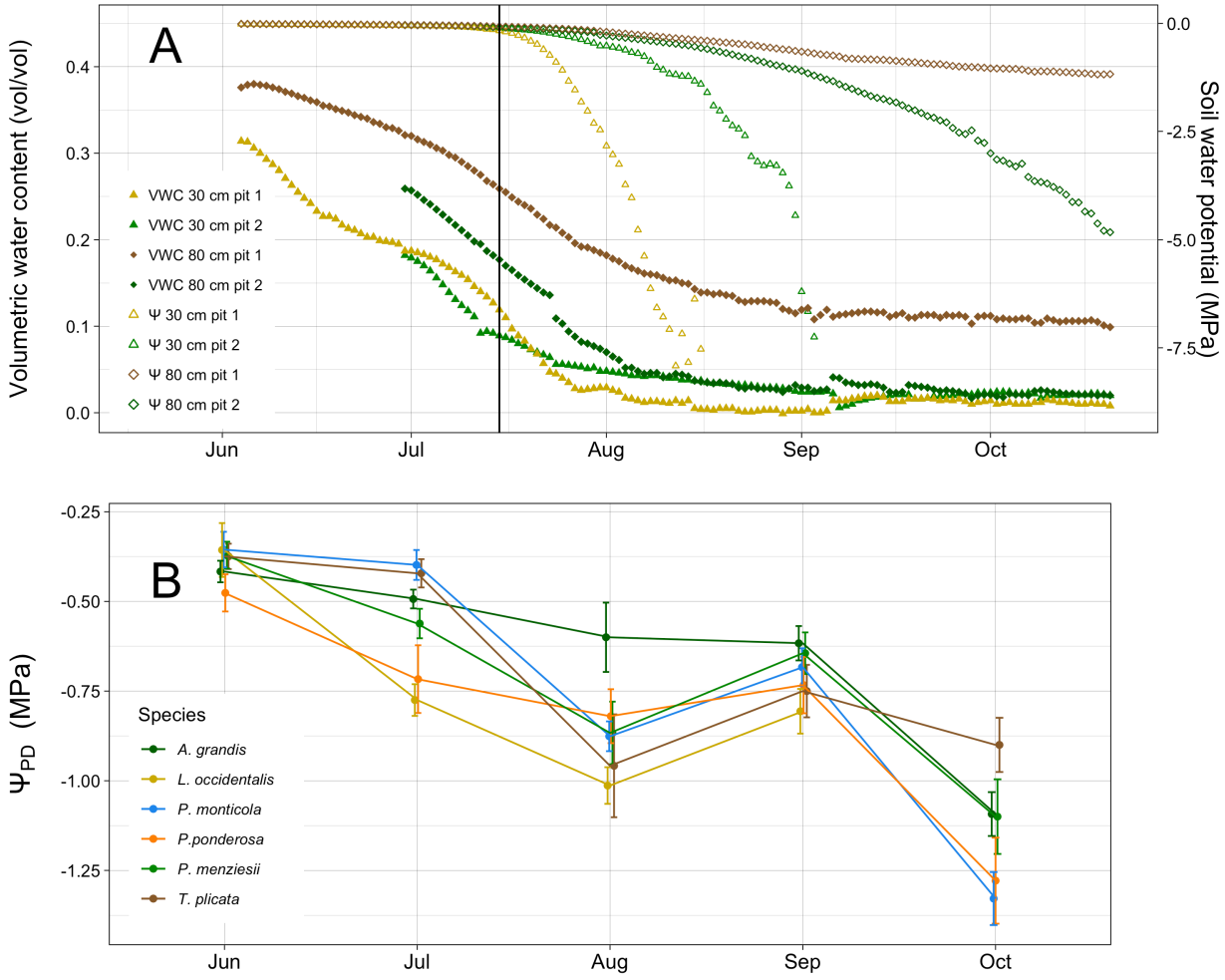


Figure 2-3. Water potentials of the soil where roots were active declined after more than 1.5 months without precipitation. (a) Soil water potential and volumetric water content from two positions within field site, with a vertical line positioned one day after final July field day to show the partitioning of wet and dry sub-seasons. (b) predawn water potentials of the six species, averaged within each month. Error bars show standard error.

| | Sub-season | $\Psi_{PD}$ | $\Psi_{MIN}$ | Branch $\Psi_{MD}$ |
|---|---|---|---|---|
| *A. grandis* | wet | -0.45 (0.03) | -1.93 (0.22) | -1.27 (0.21) |
| | dry | -0.78 (0.11) | -1.98 (0.10) | |
| *L. occidentalis* | wet | -0.52 (0.13) | -2.71 (0.13) | -1.84 (0.19) |
| | dry | -0.95 (0.04) | -2.12 (0.12) | |
| *P. monticola* | wet | -0.37 (0.05) | -1.98 (0.21) | -1.47 (0.06) |
| | dry | -0.96 (0.12) | -1.82 (0.09) | |
| *P. ponderosa* | wet | -0.61 (0.09) | -1.39 (0.18) | -1.47 (0.25) |
| | dry | -0.98 (0.11) | -1.95 (0.08) | |
| *P. menziesii* | wet | -0.45 (0.06) | -2.21 (0.21) | -1.55 (0.09) |
| | dry | -0.90 (0.07) | -2.07 (0.06) | |
| *T. plicata* | wet | -0.39 (0.03) | -1.63 (0.05) | -1.35 (0.07) |
| | dry | -0.82 (0.08) | -1.72 (0.04) | |

Table 2-2. $\Psi_{PD}$ and $\Psi_{MIN}$ for sub-seasons (in MPa; SE in parentheses). Emphasis indicates significant differences for term between sub-seasons. Branch $\Psi_{MD}$ was only recorded in August and September.

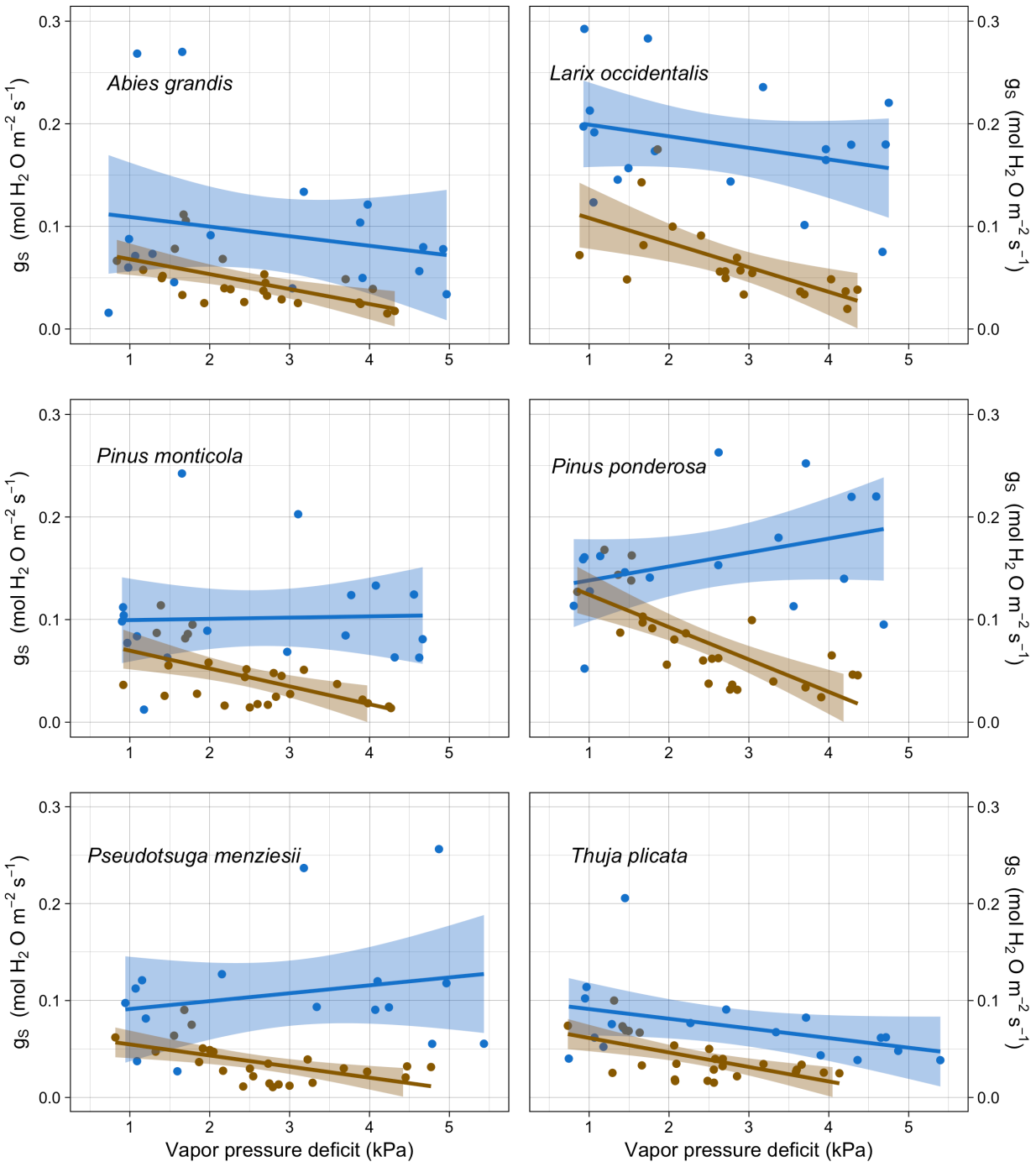


Figure 2-5. Blue lines and points represent wet sub-season data, and brown lines and points are dry sub-season data. *L. occidentalis*, *P. monticola*, and *P. ponderosa* have significantly different slopes between the dry and wet seasons. *A. grandis*, *P. menziesii*, and *T. plicata* have slopes that are not significantly different from each other.

### 2.3.4 Vulnerability curves, isohydry, safety margins, and TREES model

Vulnerability curves and estimated $P_{50}$ values for branches and roots (Fig. 2-6, Table 2-3) indicated generally large safety margins in those two organs. For all species, branch water potentials remained above the threshold for embolism-induced loss in hydraulic conductivity over the entire study period. For roots, the results were more varied. *A. grandis, L. occidentalis*, *P. menziesii, and T. plicata,* were predicted to lose less than 6% of their $K_S$. The two pines, *P. ponderosa* and *P. monticola*, however, experienced soil water potentials that were predicted to reduce their $K_S$ by 19% and 56% respectively. Using TREES to simulate relative hydraulic safety envelopes in different soil types, silt-loam soil provided the greatest buffer against hydraulic failure for all species. This supported our hypothesis that suitable soil types mediate drought stress.

| | Branch $P_{50}$ | Root $P_{50}$ |
|---|---|---|
| *A. grandis* | -7.00 (-7.78, -6.34) | -2.81 (-3.34, -2.25) |
| *L. occidentalis* | -5.88 (-6.00, -5.53) | -2.87 (-3.24, -2.48) |
| *P. monticola* | -5.25 (-6.00, -4.73) | -1.30 (-1.49, -0.81) |
| *P. ponderosa* | -3.32 (-3.59, -3.16) | -1.59 (-2.11, -1.09) |
| *P. menziesii* | -4.78 (-5.27, -4.34) | -4.59 (-5.44, -3.75) |
| *T. plicata* | -5.49 (-6.15, -4.84) | -3.00 (-3.28, -2.71) |

Table 2-3. Branch and root $P_{50}$ values (MPa; confidence intervals in parentheses).

Using a framework relating $g_s$ to $P_{50}$ and safety margins, all species exhibited isohydric behavior but to different degrees (Supp. Fig. 2-5). We determined each species' $P_{g12}$ and $g_{S\text{-}MAX}$ using a linear model between dry sub-season $g_S$ and $\Psi_L$ measurements. The linear models had negative slopes, with $g_{S\text{-}MAX}$ considered the predicted $g_S$ at the least

negative mean $\Psi_L$ and $P_{g12}$ being the $\Psi_L$ associated with a $g_S$ 88% lower than the $g_{S\text{-}MAX}$ (Skelton *et al.* 2015). There was a strong positive correlation between degree of isohydry and safety margins across all species ($p = 0.001$; $R^2=0.986$). *A. grandis* exhibited the largest safety margin along with the highest degree of isohydry while *P. ponderosa* exhibited the lowest safety margin and degree of isohydry. All other species exhibited characteristics between the two extremes. However, using another framework that compared $\Psi_{MIN}$ to $\Psi_{PD}$, only four species, *A. grandis*, *P. monticola*, *P. menziesii*, and *T. plicata*, could be categorized as strictly isohydric. Meanwhile, *P. ponderosa* appeared to be partially isohydric, and *L. occidentalis* falls outside the parameters for categorization (Supp. Fig. 2-6, Martínez-Vilalta *et al.*, 2014).

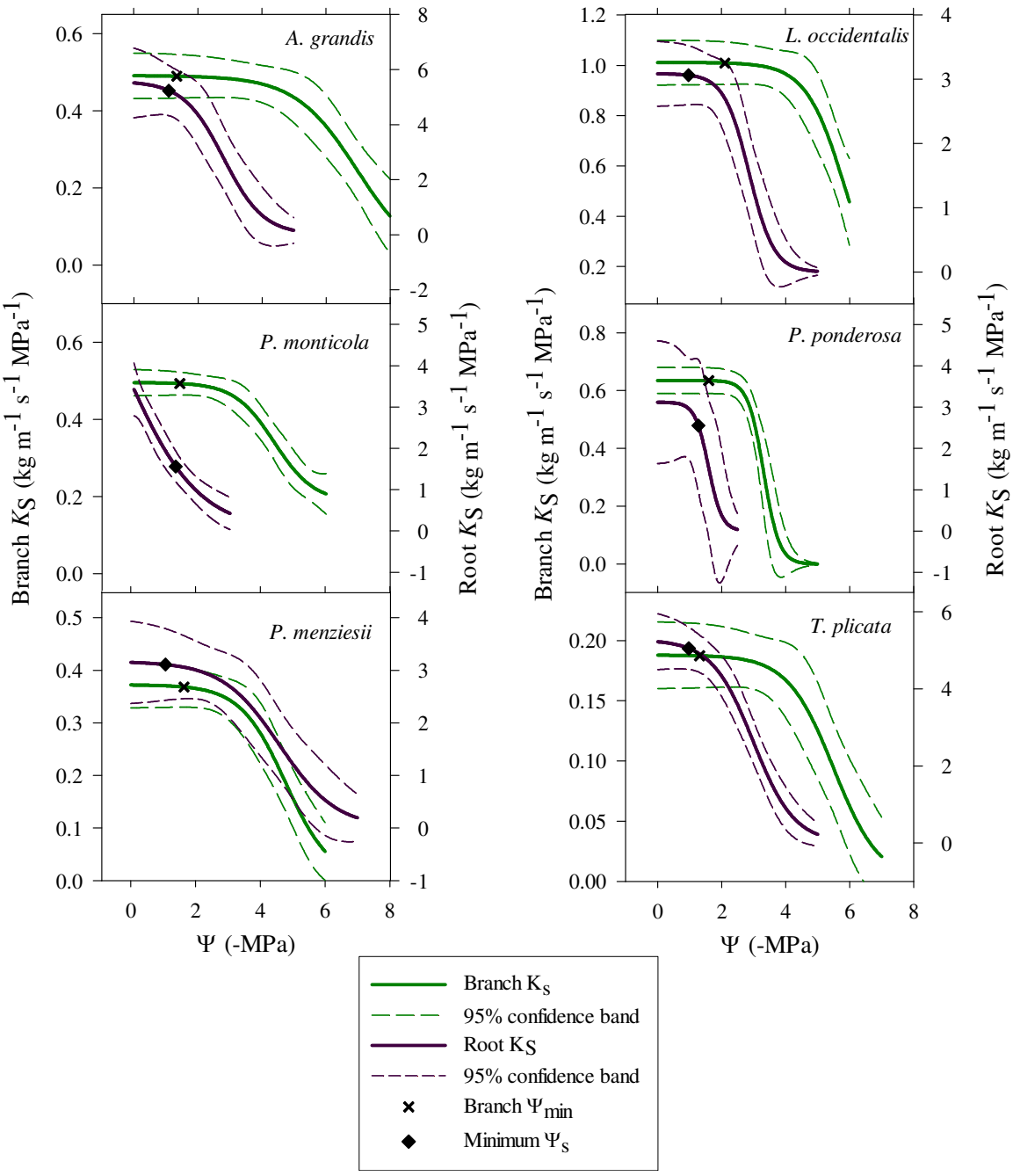


Figure 2-6. Branch $K_S$ (solid green lines) and Root $K_S$ (solid purple lines) for the six study species. Thick lines show the regression curve, and dashed lines represent the 95% confidence interval. Black x's indicate branch $\Psi_{MIN}$, and black diamonds show minimum $\Psi_S$, which is the most negative predawn water potential by month.

## 2.4.0 Discussion

### 2.4.1 Water potentials and stomatal conductance

Predawn water potential for the six species became more negative as the season progressed, as would be expected during an extended summer drought; however, only *L. occidentalis* and *P. ponderosa* had significantly different $\Psi_{MIN}$ between the two sub-seasons. Interestingly, *L. occidentalis* exhibited more negative $\Psi_{MIN}$ during the wet sub-season. Subsequent data from June of 2016 indicated that, for *L. occidentalis*, this may have been due to the morphology of the samples taken (Baker, unpubl. data, elaboration in Supplemental Text 1). Leaf water potentials did not decline to values that were measured in the soil at 30 and 80 cm, suggesting that these species likely have access to deeper pools of water.

Our first hypothesis, that all species would have stomatal responses sensitive to VPD, was conditionally supported. In relation to VPD, time of day, and $\Psi_L$, $g_S$ was more tightly regulated during the dry sub-season than when soil water was more readily available. During the dry sub-season, $g_s$ decreased to less than 20% of $g_{S\text{-}MAX}$ for all species for most of the day. In the face of extended seasonal drought, this isohydric strategy may lead to decreased carbon stores for these species (e.g. McDowell *et al*. 2008). This trend of having more sensitive stomata in the dry season, which was significantly different from the wet sub-season in *L. occidentalis*, *P. monticola*, and *P. ponderosa*, is not entirely explained by the data here. One reason could be the more negative soil water potentials during the dry sub-season; as soil water decreases and becomes more difficult to extract, the plants may adjust their stomatal sensitivity to prevent declines in upstream hydraulic conductivity. This could also be due to changes in leaf turgor during the dry season and/or upregulation of ABA

production which could prime stomata to be more sensitive to dry soils (e.g., Mitchell *et al.* 2016).

The shift in stomatal conductance between wet and dry seasons could also be due to hydraulic capacitance, wherein stored water in the sapwood relieves water stress through the day (e.g. Scholz *et al.* 2011). For this to occur daily, the stored water must be recharged overnight. Mildly negative soil water potentials in the early season may allow the tree to replenish water storage at night, while the dry soil later in the season could prevent recharge (Waring and Running 1978, Meinzer *et al*. 2006, 2009). For the multiple linear regressions in Supplemental Table 2-1, adding $\Psi_{PD}$ to the wet sub-season models made the other variables' coefficients more likely to be significant. This may indicate that capacitive recharge, with greater influence at less negative $\Psi_{PD}$, influenced the trees' response to other parameters. Continued investigation of capacitive storage in these species is required to determine whether it contributes to dynamic stomatal responses.

### 2.4.2 Vulnerability curves, safety margins, and TREES model

Many conifer species, including the ones in this study, are on the more isohydric end of the iso/anisohydric continuum (Fu and Meinzer 2018). This can be a successful mechanism for maintaining functionality through a dry period, but it can become harmful during extended drought. Because photosynthetic assimilation ceases after continued stomatal closure, this could eventually lead to carbon reserve depletion (e.g., McDowell *et al.* 2008, Sala *et al.* 2012). Our hypothesis that all six species would fall along a spectrum of isohydry in order of site preference aridity was not supported. There was a strong positive linear correlation between the degree of isohydry and the hydraulic safety margin, which was

mainly driven by the species' very negative $P_{50}$ values and the similarity of their $P_{g12}$ and $\Psi_{MIN}$ values across species (Supp. Fig. 2-5). A similar relationship between stomatal regulation and xylem vulnerability has been seen across 16 species in three California ecosystems where species with more negative minimum leaf water potentials had more resistant xylem (Pivovaroff *et al.* 2018).

Our data is consistent with prior studies describing large hydraulic safety margins in conifers (Choat *et al*. 2012, Johnson *et al*. 2012, 2016). Most of the species in the current study do not have published vulnerability curves for both branches and roots, but those that do, *P. ponderosa* and *P. menziesii*, have similar differences between the organs, with roots being more vulnerable than branches (Domec et al. 2006, Koepke & Kolb 2012, Johnson *et al.* 2012; McCulloh *et al*. 2014). As predicted, all species' xylem had positive safety margins with the exception of the two *Pinus* species' roots, which were predicted to lose some hydraulic conductivity. All species maintained branch water potentials much less negative than their respective $P_{50}$ values (Table 2-2). This safety margin was greatest in *A. grandis* and least in *P. ponderosa*, contradicting our hypothesis that the species most traditionally accepted as drought tolerant would also have the greatest safety margins. *P. ponderosa*, which is well-established as a xeric species (Minore 1979), is the least isohydric of the six species according to Skelton *et al.*'s (2015) metrics for calculating isohydry and degree of safety. Meanwhile *A. grandis*, a mesic species, was the most isohydric and most conservative in terms of branch and root xylem safety margins, which is consistent with another study in the region (Piñol and Sala 2000). It is worth noting that many other plant physiological parameters including allometry (Lines *et al*. 2012), rooting depth (Padilla & Pugnaire 2007), and hydraulic capacitance (Barnard *et al*. 2011) may be responsible for species drought

tolerances and by looking only at xylem vulnerability curves, we may be missing part of the picture.

Based on TREES simulations, each species exhibited higher relative hydraulic safety envelopes in silt-loam compared to alternative soil types (Fig. 2-7). This indicates that the soils at our site provided a buffer against the severe atmospheric drought and also helps to explain the observed delay in drought stress responses, such as tighter stomatal regulation. This is consistent with earlier suggestions that plant response to drought could be limited by both xylem traits and the rhizosphere (Sperry *et al.* 1998). Our species' limitations appear to be primarily underground: soil water being ultimately limiting for all species and root embolism starting to affect conductivity in the *Pinus* species.

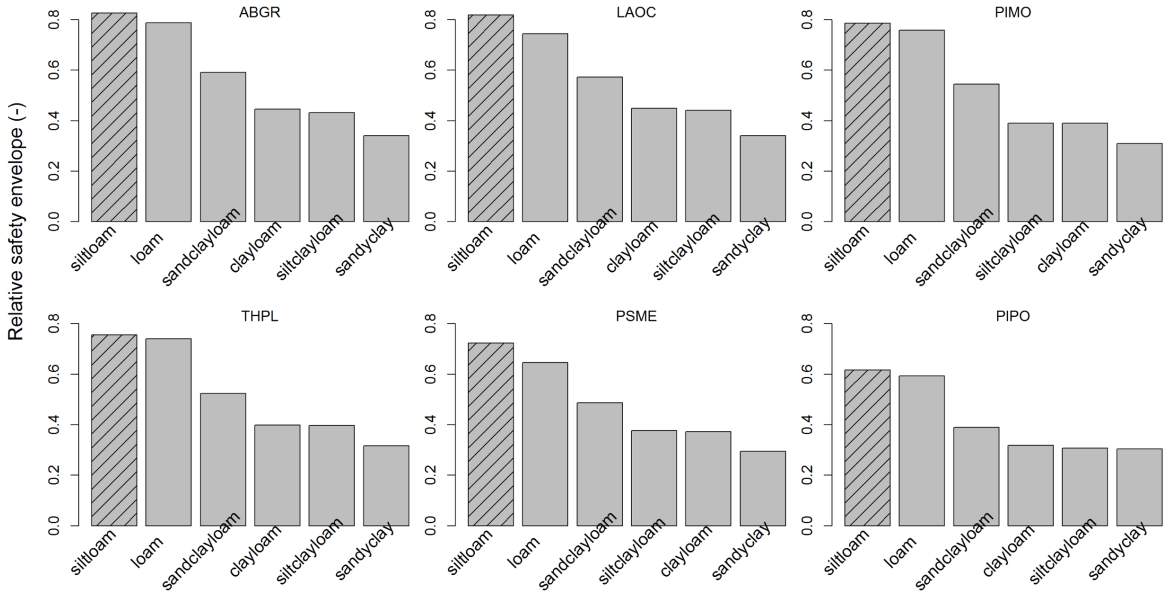


Figure 2-7. Relative safety envelope of six species throughout the 2015 growing season associated with different soil types. Bars with hatches were the soil type of the current study site.

### 2.4.3 Implications

The study period of 2015 was the most severe summer drought in the region on record with combined high temperatures and low precipitation. Our findings provide insights into these conifer species' resilience to extended seasonal droughts that are predicted for this region. Their high stomatal conductance in the early season allowed them to assimilate carbon when soil water was abundant, and their greater regulation during the dry sub-season prevented embolism in their branches and roots (with the exception of *Pinus* roots). If longer growing season droughts occur, these strategies may not be as successful, especially for the species that exhibited some degree of root embolism (*Pinus*). It is important that models predicting plant performance under future climate scenarios take roots into account for this reason. While the 2015 season was an extreme drought, there had been 122 mm of rainfall that recharged the soil over the three weeks directly preceding our study; this rain followed more than a month with negligible precipitation (total of 15 mm), with the last freeze occurring in mid-April (snow telemetry, Natural Resource Conservation Service; Site Number 989, 1433m a.s.l.). Without the rainfall in May, the 2015 drought would have been two months longer. While a drought of that magnitude would certainly cause more water stress, these trees have an advantage over most montane forests: a meter of silty loam soil that stores water long after precipitation ceases. The ash-capped soils of this region may allow the established forests to persist as their growing seasons become longer, warmer, and drier.

### 2.5.0 References

Abatzoglou JT, Rupp DE, Mote PW (2014) Seasonal climate variability and change in the pacific northwest of the united states. J Clim 27:2125–2142 (2014).

Alder NN, Pockman WT, Sperry JS, Nuismer S (1997) Use of centrifugal force in the study of xylem cavitation. J Exp Bot 48:665–674.

Anderegg WR, Anderegg LD, Berry JA, Field CB (2014) Loss of whole-tree hydraulic conductance during severe drought and multi-year forest die-off. Oecologia 175(1):11-23.

Baker RJ (1981) Soil survey of Latah County area, Idaho. United States Department of Agriculture Soil Conservation Service with University of Idaho Soil Conservation Commission, Moscow, ID.

Barnard DM, Meinzer FC, Lachenbruch B, McCulloh KA, Johnson DM, Woodruff DR (2011) Climate-related trends in sapwood biophysical properties in two conifers: avoidance of hydraulic dysfunction through coordinated adjustments in xylem efficiency, safety and capacitance. Plant Cell & Environ 34:643-654.

Beikircher B, Ameglio T, Cochard H, Mayr S (2010) Limitation of the Cavitron technique by conifer pit aspiration. J of Exp Bot 60(12)3385-3393.

Berry ZC and Smith WK (2013) Ecophysiological importance of cloud immersion in a relic spruce-fir forest at elevational limits, southern Appalachian Mountains, USA. Oecologia, 173(3):637-648.

Bond BJ and Kavanagh KL (1999) Stomatal behavior of four woody species in relation to leaf-specific hydraulic conductance and threshold water potential. Tree Phys 19:503–510.

Bouche PS, Jansen S, Cochard H, Burlett R, Capdeville G, Delzon S (2015) Embolism resistance of conifer roots can be accurately measured with the flow-centrifuge method. J of Plant Hyd 2(2):1-9.

Bouche PS, Delzon S, Choat B, Badel E, Brodribb, Burlett R, Cochard H, Charra-Vaskou K, Lavigne B, Li S, Mayr S, Morris H, Torres-Ruiz JM, Zuffrey V, Jansen S (2016) Are needles of Pinus pinaster more vulnerable to xylem embolism than branches? New insights from X-ray computed tomography. Plant Cell & Environ 39:860-870.

Brodribb TJ, Pittermann J, Coomes DA (2012) Elegance versus speed: examining the competition between conifer and angiosperm trees. Int J of Plant Sci, 173(6): 673-694.

Brodribb TJ, McAdam SAM, Jordan GJ, Martins SCV (2014) Conifer species adapt to low-rainfall climates by following one of two divergent pathways. PNAS 111: 14489–14493.

Bucci SJ, Scholz FG, Goldstein G, Meinzer FC, Sternberg L DA SL (2003) Dynamic changes in hydraulic conductivity in petioles of two savanna tree species: Factors and mechanisms contributing to the refilling of embolized vessels. Plant Cell & Environ 26:1633–1645.

Campbell GS. 1985. *Soil physics with BASIC: Transport models for soil-plant systems*, 1st edn. Amsterdam: Elsevier Science B.V.

Cochard H (2002) A technique for measuring xylem hydraulic conductance under high negative pressures. Plant Cell & Environ 25:815-819.

Cochard H, Herbette S, Barigah T, Badel E, Ennajeh M, Vilagrosa A (2010) Does sample length influence the shape of xylem embolism vulnerability curves? A test with the Cavitron spinning technique. Plant Cell & Environ , 33(9):1543-1552.

Cochard H, Badel E, Herbette S, Delzon S, Choat B, Jansen S (2013) Methods for measuring plant vulnerability to cavitation: A critical review. J of Exp Bot 64: 4779–4791.

Choat B, Jansen S, Brodribb TJ, Cochard H, Delzon S, Bhaskar R, Bucci SJ, Feild TS, Gleason SM, Hacke UG, Jacobsen AL, Lens F, Maherali H, Martínez-Vilalta J, Mayr S, Mencuccini M, Mitchell PJ, Nardini A, Pittermann J, Pratt RB, Sperry JS, Westoby M, Wright IJ, Zanne AE (2012) Global convergence in vulnerability of forests to drought. Nature 491:752-756.

Choat B, Badel E, Burlett R, Delzon S, Cochard H, Jansen S (2016) Noninvasive measurement of vulnerability to drought-induced embolism by X-ray microtomography. Plant Phys. 170(1):273-282.

Dang Q-L, Margolis HA, Coyea MR, Sy M, Collatz GJ (1997) Regulation of branch-level gas exchange of boreal trees: roles of shoot water potential and vapor pressure difference. Tree Phys. 17:521-535.

Daubenmire RF (1966) Vegetation: identification of typal communities. Science 151:291-298.

Daubenmire RF (1968a) Soil Moisture in Relation to Vegetation Distribution in the Mountains of Northern Idaho. Ecol Soc of America 49:431–438.

Daubenmire RF, Daubenmire J (1968b) Forest Vegetation of Eastern Washington and Northern Idaho. Technical Bulletin 60. Washington Agricultural Experiment Station, Pullman, WA.

Delucia EH, Maherali H, Carey EV (2000) Climate-driven changes in biomass allocation in pines. Global Change Bio 6:587-593.

Domec J-C, Gartner BL (2003) Relationship between growth rates and xylem hydraulic characteristics in young, mature and old-growth ponderosa pine trees. Plant Cell & Environ 26:471–483.

Domec JC, Lachenbruch B, Meinzer FC (2006) Bordered pit structure and function determine spatial patterns of air-seeding thresholds in xylem of Douglas-fir (Pseudotsuga menziesii; Pinaceae) trees. Am J of Bot 93(11): 1588-1600.

Domec J-C, Noormets AK, King JS, Sun GE, McNulty SG, Gavazzi MJ, Boggs JL, Treasure EA (2009) Decoupling the influence of leaf and root hydraulic conductances on stomatal conductance and its sensitivity to vapour pressure deficit as soil dries in a drained loblolly pine plantation. Plant Cell & Environ 32(8):980-991

Farjon A (2008) A natural history of conifers. Timber Press, Portland, OR.

Franklin JF, Dyrness CT (1973) Natural vegetation of Washington and Oregon. USDA Forest Service General Technical Report PNW-GTR-8. Pacific Northwest Research Station, Portland, OR.

Fu X and Meinzer FC (2018) Metrics and proxies for stringency of regulation of plant water status (iso/anisohydry): a global data set reveals coordination and trade-offs among water transport traits. Tree Phys 39:122-134.

Fu X, Meinzer FC, Woodruff DR, Liu YY, Smith DD, McCulloh KA, Howard AR (2019) Coordination and trade-offs between leaf and stem hydraulic traits and stomatal regulation along a spectrum of isohydry to anisohydry. Plant Cell & Environ 1:1-14.

Gleason SM, Westoby M, Jansen S, Choat B, Hacke UG, Pratt RB, Bhaskar R, Brodribb TJ, Bucci SJ, Cao KF, Cochard H, Delzon S, Domec JC, Fan ZX, Feild TS, Jacobsen AL, Johnson DM, Lens HM, Martínez-Vilalta J, Mayr S, McCulloh KA, Mencuccini M, Mitchell PJ, Morris H, Nardini A, Pittermann J, Plavcová L, Schreiber SG, Sperry JS, Wright IJ, Zanne AE (2015) Weak tradeoff between xylem safety and xylem- specific hydraulic efficiency across the world's woody plant species. New Phytol 209:123–136.

Hartmann H, Moura CF, Anderegg WRL, Ruehr NK, Salmon Y, Allen CD, Arndt SK, Breshears DD, Davi H, Galbraith D, Ruthrof KX, Wunder J, Adams HD, Bloemen J, Cailleret M, Cobb R, Gessler A, Grams TEE, Jansen S, Kautz M, Lloret F, and O'Brien M (2018) Research frontiers for improving our understanding of drought-induced tree and forest mortality. New Phytol 218:15–28.

Johnson DM, McCulloh KA, Woodruff DR, Meinzer FC (2012) Hydraulic safety margins and embolism reversal in stems and leaves: Why are conifers and angiosperms so different? Plant Sci 195:48-53.

Johnson DM, Wortemann R, McCulloh KA, Jordan-Meille L, Ward E, Warren JF, Palmroth S, Domec JC (2016) A test of the hydraulic vulnerability segmentation hypothesis in angiosperm and conifer tree species. Tree Phys 36:989–993.

Johnson DM, Domec J-C, Berry ZC, Schwantes AM, Woodruff DR, McCulloh KA, Polley HW, Wortemann R, Swenson JJ, Mackay DS, McDowell NG, Jackson RB (2018) Co-occurring woody species have diverse hydraulic strategies and mortality rates during an extreme drought. Plant Cell and Environ 41:576-588.

Kavanagh KL, Pangle R, Schotzko AD (2007) Nocturnal transpiration causing disequilibrium between soil and stem predawn water potential in mixed conifer forests of Idaho. Tree Phys 27:621–629.

Kimsey M, Gardner B, Busacca A (2005) Ecological and topographic features of volcanic ash-influenced forest soils. November 2005; Coeur d'Alene, ID. Proceedings RMRS-P-44; Fort Collins, CO: U.S. Department of Agriculture, Forest Service, Rocky Mountain Research Station. 220 p.

Klos PZ, Link TE, Abatzoglou JT (2014) Extent of the rain-snow transition zone in the western U.S. under historic and projected climate. Geophysical Research Letters. AGU Publ 41:4560–4568.

Koepke DF and Kolb TE (2012) Species variation in water relations and xylem vulnerability to cavitation at a forest-woodland ecotone. Forest Sci 59(5):524-535.

Li Y, Sperry JS, Taneda H, Bush SE, Hacke UG (2008) Evaluation of centrifugal methods for measuring xylem cavitation in conifers, diffuse- and ring-porous angiosperms. New Phyt 177: 558–568.

Limm EB, Simonin KA, Bothman AG, and Dawson TE (2009) Foliar water uptake: a common water acquisition strategy for plants of the redwood forest. Oecologia, 161(3):449-459.

Lines ER, Zavala MA, Purves DW, Coomes DA (2012) Predictable changes in aboveground allometry of trees along gradients of temperature, aridity and competition. Global Ecology and Biogeography 21:1017-1028.

Luce CH, Holden ZA (2009) Declining annual streamflow distributions in the Pacific Northwest United States, 1948-2006. Geophys Res Lett 36:1–6.

Mackay DS, Roberts DE, Ewers BE, Sperry JS, NG McDowell NG, and Pockman WT (2015) Interdependence of chronic hydraulic dysfunction and canopy processes can improve integrated models of tree response to drought. J of the Am Water Res Assoc 51: 6156–6176.

Marlier EM, Xiao M, Engel R, Livneh B, Abatzoglou JT, Lettenmaier DP (2017) The 2015 drought in Washington State: a harbinger of things to come? Environ Res Lett 12:1-8.

Martínez-Vilalta J, Poyatos R, Aguadé D, Retana J, and Mencuccini M (2014) A new look at water transport regulation in plants. New Phyt 204(1):105-115.

Martínez-Vilalta J and Garcia-Forner N (2017) Water potential regulation, stomatal behavior and hydraulic transport under drought: deconstructing the iso/anisohydric concept. Plant Cell & Environ 40:962-976.

Mathys AS, Coops NC, and Waring RH (2017) An ecoregion assessment of projected tree species vulnerabilities in western North America through the 21st century. Global Change Biology 23:920–932.

McDowell N, Pockman WT, Allen CD, Breshears DD, Cobb N, Kolb T, Plaut J, Sperry J, West A, Williams DG, Yepez EA (2008) Mechanisms of plant survival and mortality during drought: why do some plants survive while others succumb to drought? New Phyt 178:719-739.

McDowell NG, Williams AP , Xu C, Pockman WT, Dickman LT, Sevanto S, Pangle R, Limousin J, Plaut J, Mackay DS, Ogee J, Domec J-C, Allen CD, Fisher RA, Jiang X, Muss JD, Breshears DD, Rauscher SA, and Koven C (2016) Multi-scale predictions of massive conifer mortality due to chronic temperature rise. Nature Clim Change 6:295–300.

McCulloh KA, Johnson DM, Meinzer FC and DR Woodruff (2014) The dynamic pipeline: Hydraulic capacitance and xylem hydraulic safety in four tall conifer species. Plant Cell & Environ 37:1171-1183.

Meinzer FC, Brooks JR, Domec J-C, Garner BL, Warren JM, Woodruff DR, Bible K, Shaw DC (2006) Dynamics of water transport and storage in conifers studied with deuterium and heat tracing techniques. Plant Cell & Environ 29:105-114.

Meinzer FC, Johnson DM, Lachenbruch B, McCulloh KA, Woodruff DR (2009) Xylem hydraulic safety margins in woody plants: coordination of stomatal control of xylem tension with hydraulic capacitance. Functional Ecology 23:922-930.

Meinzer FC, McCulloh KA, Lachenbruch B, Woodruff DR, Johnson DM (2010) The blind men and the elephant: the impact of context and scale in evaluating conflicts between plant hydraulic safety and efficiency. Oecologia 164:287-296.

Meinzer FC, Woodruff DR, Marias DE, Smith DD, McCulloh KA, Howard AR, Magedman AL (2016) Mapping 'hydroscapes' along the iso-to anisohydric continuum of stomatal regulation of plant water status. Ecology Lett 19, 1343-1352.

Millar CI, Stephenson NL, Stephens SL (2007) Climate change and forests of the future: Managing in the face of uncertainty. Ecological Applications 17:2145–2151.

Miller ML, Johnson DM (2017) Vascular development in very young conifer seedlings: Theoretical hydraulic capacities and potential resistance to embolism. Am J of Bot 104(7):979-992.

Minore D (1979) Comparative autecological characteristics of northwestern tree species---a literature review. Gen Tech Rep PNW-GTR-087.

Mitchell PJ, McAdam SA, Pinkard EA, Brodribb TJ (2016) Significant contribution from foliage-derived ABA in regulating gas exchange in Pinus radiata. Tree Phys 37: 236-245.

Mote PW, Salathé EP (2010) Future climate in the Pacific Northwest. Clim Change 102:29–50.

Oren R, Sperry JS, Katul GG, Pataki DE, Ewers BE, Phillips N, Schäfer KVR (1999) Survey and synthesis of intra- and interspecific variation in stomatal sensitivity to vapour pressure deficit. Plant Cell & Environ 22:1515-1526.

Page-Dumroese D, Miller R, Mital J, McDaniel P, Miller D (tech eds) 2005. Volcanic-Ash-Derived Forest Soils of the Inland Northwest: Properties and Implications for Management and Restoration. 9-10 November 2005; Coeur d'Alene, ID. Proceedings RMRS-P-44; Fort Collins, CO: U.S. Department of Agriculture, Forest Service, Rocky Mountain Research Station. 220 p.

Padilla FM, Pugnaire FI (2007) Rooting depth and soil moisture control Mediterranean woody seedling survival during drought. Functional Ecology 21:489-495.

Pangle R, Kavanagh K, Duursma R (2015) Decline in canopy gas exchange with increasing tree height, atmospheric evaporative demand, and seasonal drought in co-occurring inland Pacific Northwest conifer species. Can J of For Res 45: 1086–1101.

Piñol J, Sala A (2000) Ecological implications of xylem cavitation for several Pinaceae in the Pacific Northern USA. Fun Ecol 14:538-545.

Pivovaroff AL, VMW Cook, LS Santiago (2018) Stomatal behaviour and stem xylem traits are coordinated for woody plant species under exceptional drought conditions. Plant Cell & Environ 41:2617-2626

R Development Core Team (2016) R: A language and environment for statistical computing. R Foundation for Statistical Computing, Vienna, Australia http://www.r-project.org.

Rehfeldt GE, Crookston NL, Warwell MV, Evans JS (2006) Empirical Analyses of Plant-Climate Relationships for the Western United States. Int J Plant Sci 167:1123–1150.

Sala A, Woodruff DR, Meinzer FC (2012). Carbon dynamics in trees: feast or famine?. Tree Phys, 32(6), pp.764-775.

Scholander P, Hammel H, Bradstreet E, Hemmingsen E (1965) Sap Pressure in Vascular Plants. Sci AAAS 148:339-346.

Scholz FG, Phillips NG, Bucci SJ, Meinzer FC, Goldstein G, 2011. Hydraulic capacitance: biophysics and functional significance of internal water sources in relation to tree size. In Size-and age-related changes in tree structure and function (pp. 341-361). Springer Netherlands.

Skelton RP, West AG, Dawson TE (2015) Predicting plant vulnerability to drought in biodiverse regions using functional traits. PNAS USA 112:5744-9.

Sperry J S, Adler FR, Campbell GS, Comstock JP (1998) Limitation of plant water use by rhizosphere and xylem conductance: Results from a model. Plant Cell and Environ 21:347–359.

Sperry JS, Donnelly JR, Tyree MT (1988) A method for measuring hydraulic conductivity and embolism in xylem. Plant Cell & Environ 11:35-40.

Sperry JS (2000) Hydraulic constraints on plant gas exchange. Agric For Meteorol 104:13-23.

Sperry JS, Christman MA, Torres-Ruiz JM, Taneda H, and Smith DD (2012) Vulnerability curves by centrifugation: is there an open vessel artefact, and are ‘r’ shaped curves necessarily invalid? Plant Cell & Environ. 35(3):601-610.

Tai X, Mackay DS, Anderegg WRL, Sperry JS, Brooks PD (2017) Plant hydraulics improves and topography mediates prediction of aspen mortality in southwestern USA. New Phyt 213:113-127.

Tardieu F, Davies WJ (1993) Integration of hydraulic and chemical signaling in the control of stomatal conductance and water status of droughted plants. Plant Cell & Environ 16:341-349.

Tardieu F, Simonneau T (1998) Variability among species of stomatal control under fluctuating soil water status and evaporative demand: modelling isohydric and anisohydric behaviours. J of Exp Bot 49(Special Issue):419-432.

Thornton PE, Thornton MM, Mayer BW, Wei Y, Devarakonda R, Vose RS, Cook RB (2016) Daymet: Daily Surface Weather Data on a 1-km Grid for North America; Version 3. ORNL DAAC, Oak Ridge, Tennessee, USA.

Torres-Ruiz JM, H Cochard, B Choat, S Jansen, R López, I Tomášková, CM Padilla-Díaz, E Badel, R Burlett, A King, and N Lenoir (2017) Xylem resistance to embolism: presenting a simple diagnostic test for the open vessel artefact. New Phyt 215(1):489-499.

Tyree MT, Zimmerman M (1987) Xylem structure and the ascent of sap (2nd ed). Springer Verleg Heidelberg, New York, 1983.Waring RH, Running SW (1978) Sapwood water storage: its contribution to transpiration and effect upon water conductance through the stems of old-growth Douglas-fir. Plant Cell & Environ 1:131-140.

Sperry JS, Adler FR, Campbell GS, Comstock JP (1998) Limitation of plant water use by rhizosphere and xylem conductance: Results from a model. Plant Cell and Environ 21:347–359.

Wei L, Zhou H, Link TE, Kavanagh KL, Hubbart JA, Du E, Hudak AT, and Marshall JD (2018) Forest productivity varies with soil moisture more than temperature in a small montane watershed. Ag and For Met 259:211–221.

Woodruff DR, Meinzer FC, Lachenbruch B, Johnson DM (2009) Coordination of leaf structure and gas exchange along a height gradient in a tall conifer. Tree Phys 29:261-272.

# Chapter 3: Hydraulic function of three Pinus ponderosa trees through a seasonal drought

## 3.0.0 Abstract

The range of *Pinus ponderosa* trees spans much of the North American West, from northern Mexico to southern British Columbia, occupying xeric sites and surviving prolonged drought. In this chapter, we documented the hydraulic strategies used by three individual *P. ponderosa* trees in northern Idaho through more than four months with very little rainfall. Early in the season, before predawn water potentials declined, the trees allowed nighttime transpiration at the leaf level ($\Psi_{PD}$ = -0.8 MPa). This type transpiration was not observed later in the season, when the predawn water potentials had dropped to below published turgor loss points for the species ($\Psi_{PD}$ = -1.6 MPa). Capacitive water storage was smaller in volume but greater in its importance to the total transpired water when the soil was drier. By the end of the season, the whole-tree hydraulic conductance declined to 83-98% of its starting value, meaning that the trees' resistance to water flow increased to a point of nearly ceasing transpiration by September.

## 3.1.0 Introduction

### 3.1.1 Background and purpose

We generally think about tree water following a direct path from soil to atmosphere, a tidy column of water that moves upward during daylight hours and halts in the dark. The reality of water movement in trees is more complicated and circuitous than that. One complicating aspect is that sap is not always moving towards the leaves. Water does move

upward in trees but can also flow backwards and horizontally, transitioning in and out of capacitive storage. Deuterated water took between 2.5 and 21 days to reach the crown after being injected directly into bole sapwood of *Pseudotsuga menziesii* and *Tsuga heterophylla* trees (Meinzer *et al.* 2006). Labeled water also moved via hydraulic redistribution, which is water moving out of the roots to drier soil, to understory plants as far as 5 m away from the injected trees (Brooks *et al.* 2006). The degree to which trees move water through hydraulic redistribution changes situationally, with more mature trees showing a greater tendency to do it, likely due to their more developed root system (Domec *et al.* 2004).

Capacitive water storage also makes the xylem water pathway more complex. Wood can store water in multiple places: capillary water (Tyree and Yang 1990, Tyree and Zimmermann 2002, Jupa *et al*. 2016), living parenchyma in the xylem (Holbrook 1995, Meinzer *et al*. 2008), xylem conduits that later embolize (Domec and Gartner 2002, Höltta *et al*. 2009, Vergeynst *et al.* 2015), or other tissues such as pith (e.g., Goldstein *et al*. 1984) and phloem cells (Nardini *et al*. 2011, Pfautsch *et al*. 2015). During the day, the increased tension on the water column can pull water out of storage to contribute to the total transpired water (Phillips *et al.* 2003, Scholz *et al.* 2011). As water storage is restored at night, the water content in the tree increases and the water potential gradient is relieved. This type of water storage is common in *P. ponderosa*, but trees' reliance on it varies depending on the water potentials in the system. This relationship can be explained by the following equation:

Equation 3-1:

$$C = \frac{\Delta VWC}{\Delta \Psi}$$

Wherein capacitance is represented by C; VWC is volumetric water content of the sample, and Ψ is the water potential of the sample (Meinzer *et al.* 2003).

Capacitance in wood is greater at less negative water potentials, meaning that at less negative water potentials more water can be removed with a small change in water potential (see Fig. 3-1). Then, as water potentials become more negative with increasing water stress, a much smaller amount of water can be removed from the wood with a decreasing water potential. Examples of this relationship can be seen in Fig. 3-1, where the steeper sections of the curve represent greater capacitance. Capacitance is generally greater in boles than in small or large branches, and boles are the locus of large amounts of stored water during times of low water stress (McCulloh *et al.* 2014). Most studies looking at capacitance have taken place during these times of low water stress, and as such the degree to which it is important during times of drought is less established (but see Richards *et al.* 2014 and Salomón *et al.* 2017).

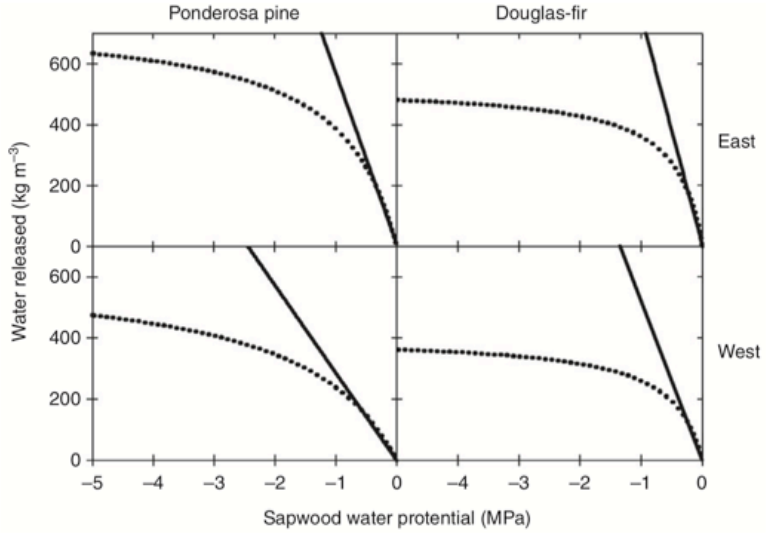


**Figure 2.** Representative graphs of capacitance show the relationship between the cumulative amount of water released (kg m$^{-3}$) and water potential in east-side and west-side populations of Douglas-fir and ponderosa pine. Capacitance values are calculated as the slope of the initial, nearly linear portion of the curve.

Figure 3-1. Published in Barnard *et al.* (2011) water release curves from the boles of four tree populations: *P. ponderosa* and *P. menziesii*, from east and west of the Cascades in Oregon, USA. Dots indicate a representative relationship between water released from a sample and the corresponding water potential value. The solid lines are approximations of the part of the curve where capacitance is greatest.

Hydraulic conductivity, flow per difference in pressure and sample length, can be measured in the lab and by inducing negative water potentials inside these samples and reassessing conductivity, we are able to assess the organ's vulnerability to embolism. The way the different organs' conductivity relates to each other has been the subject of lively discussion within the plant hydraulics community (Zimmerman & Brown 1971, McCulloh *et al.* 2014). For conifers, though, it is generally agreed that the differences in conductivity between organs is valid and that roots are often the most vulnerable organ to embolism (Johnson *et al.* 2016). It is common for distal organs, roots and leaves, to be the most vulnerable organs. These more easily replaced organs could serve as a kind of fuse that, in failing, protect the bole, which represents a greater investment of resources.

Whole tree hydraulic conductance ($k_H$), flow per difference in pressure, can be calculated from field observations of sap flux and water potentials (for specific differences between conductance and conductivity, see Tyree and Zimmerman 2002). It is generally reduced passively due to embolism in the water transport pathway or actively in response to low soil water and/or high VPD (Ryan *et al.* 2000, Sperry 2000, Bell *et al.* 2015, Sperry & Love 2015). As it declines, the amount and ratio of water going to other sources changes; for instance, it can reduce hydraulic redistribution (Warren *et al.* 2006). Also, as $k_H$ declines, carbon assimilation (A) does as well (Hubbard *et al.* 1999, 2001, Barnard and Bauerle 2013). At times of low water stress, trees are able to maximize A by maintaining high conductances, both of which decline in times of greater water stress (Anderegg *et al.* 2018).

Whether there is a similar relationship between water stress and nighttime transpiration ($E_n$) has not been established for trees in general. One study did observe a reduction in $E_n$ for two *Acer* species as soil dried (Dawson *et al.* 2007), but little is known about $E_n$ in conifer trees. Kavanagh *et al.* (2007) showed that it does occur in this region during times of high vapor pressure deficit (VPD) but did not include observations from times of drought stress ($\Psi_{PD}$ > -0.9 MPa). Additionally, Fisher *et al.* (2007) did see nighttime sap flow in a California population of *P. ponderosa* increase during nights with higher VPD but did not report $\Psi_{PD}$ to relate the fluxes to drought stress.

The goal of this project was to assess the hydraulic strategies used by three individual *P. ponderosa* trees across a growing season, from a time of high water availability through a progressive dry-down until they were experiencing water stress. We had four hypotheses: 1) Nighttime gas exchange occurs throughout the season, with $g_{S\text{-}NOC}$ ~33% of midmorning $g_S$ (as in Kavanagh *et al.* 2007). 2) Capacitively stored water is a greater contributor to

transpiration in the early season than in the drier later season. 3) Roots are the most vulnerable woody organ; resistance to embolism increases downstream, with small branches being the most resistant organ. 4) Whole-tree conductance will decrease to a level commensurate with the reduction in conductivity predicted in the roots.

## 3.2.0 Methods

### 3.2.1 Field site description

This study took place in a *P. ponderosa* plantation in the Flat Creek section of the University of Idaho Experimental Forest in May – September of 2017. The three trees selected for this study were 23-27m in height, 25-32 cm in diameter at breast height (DBH), and 35 years old at DBH. The three study trees were located on the edge of a dense (3.7 m mean spacing) single-aged *P. ponderosa* stand. A clearing to the southeast allowed for nearly full sun exposure in the morning, and the continuous canopy to the northwest cast shade on the study trees in the afternoon. Mixed in with the *P. ponderosa* trees were occasional conifers, *Pseudotsuga menziesii* and *Abies grandis*, and angiosperm shrubs: *Physocarpus malvaceus*, *Acer glabrum*, *Holodiscus discolor*, and *Symphoricarpos albus*. The soil at the site is a deep (>1m) sandy loam.

### 3.2.2 Meteorological station and soil water

A meteorological station was installed in a clearing in an adjacent stand of 15-year-old *P. ponderosa, Pinus monticola,* and *Larix occidentalis*. Temperature, relative humidity, and precipitation, mounted at 1.5 m, were recorded every 15-minutes (CS-215, Campbell

Scientific, Logan, UT; TE-525 Campbell Scientific) on a CR-1000T datalogger (Campbell Scientific).

### 3.2.3 Sap flux

Heat ratio method sap flux sensors (Burgess *et al*. 2001) were constructed in various lengths (2.5 cm, 3.8 cm, 5.1 cm, and 7.6 cm) for installation in different organs within the tree. Each sensor included two thermocouple probes 0.6 cm above and below a heater probe. Each thermocouple probe measured temperatures at three depths to incorporate the heat pulse velocity throughout the active xylem. Sensors were installed in roots, in the bole at breast height and just below the lowest living branch, in the lowest healthy branch (determined visually), and in the highest accessible branch (7 – 10 m). In two of the three trees, sap flux sensors were installed in what appeared to be tap roots. The root system in the third tree did not allow for a successful installation in a tap root; all three trees had sap flux sensors installed in lateral roots. For installation and maintenance, the canopy was accessed by stackable ladder segments strapped to the tree and climbing safety gear.

Sap flux sensors, which each had 10 m communication cables, were connected to three Campbell CR-1000 data loggers with AM 16/32B multiplexers. Every five minutes, initial temperatures were recorded, heat pulses sent through the center probe, and temperatures were recorded again after 40-80 seconds. The temperature differences were used to calculate sap flux velocity as in Burgess *et al.* with a wounding coefficient of 0.17 (2001).

### 3.2.4 Water potentials and gas exchange

Leaf water potentials ($\Psi_L$) were measured using a Scholander-style pressure chamber (Scholander *et al.* 1965; PMS, Albany, OR) before dawn ($\Psi_{PD}$; 04:00-06:00, depending on time of year) and at midday ($\Psi_{MD}$; 12:00-13:00) every 1 – 3 weeks from May 23rd to September 28th to track seasonal changes. Two 24-hour diurnal measurements of both $\Psi_L$ and gas exchange were also conducted during periods of high and low available soil moisture (see Fig. 3-4; July 13th-14th and September 10-11th). The canopy was accessed every two hours using a boom lift. Several needle bundles were removed from the six branches in which sap flux sensors were installed, and the bundles were immediately placed in a plastic bag that was humidified by breathing into it. The samples were brought down to the ground, away from the boom lift's generator, to have gas exchange recorded by a LI-COR 6400 (LI-COR Biosciences, Lincoln, NE, USA). The pressure chamber was again used to determine $\Psi_L$ from bundles not used for gas exchange.

Gas exchange protocol was adjusted between daytime and nighttime (Table 3-1). Chamber flow rate was decreased at nighttime to allow more time for the small amount of water potentially being released from the leaf to accrue to measurable levels before returning to the infrared gas analyzer (Howard *et al.* 2009). All artificial light sources (i.e. headlamps and boom lift controls) were covered with green filter film and tested with the LI-COR photosynthetically active radiation (PAR) sensor to assure that the needles were not inadvertently exposed to light that could initiate stomatal opening. The youngest needles that had hardened were used. In July, that was a second-year cohort, and in September the first-year cohort of needles were used. During the midnight measurements in September, gas exchange of both first- and second-year needles were recorded to check for a difference.

| LI-COR control variables | daytime | nighttime |
|---|---|---|
| flow rate (μmol $s^{-1}$) | 500 | 300 |
| CO2 concentration (μmol $s^{-1}$) | 400 | 400 |
| Chamber PAR (μmol $m^{-2}$ $s^{-1}$) | 1500 | Off |
| Number of three-needle bundles used | 2 | 3 |

Table 3-1

### 3.2.5 Xylem conductivity

In mid-October to early-November of 2017, five organs from the three trees were excised to construct vulnerability curves. Large branch segments were removed distal to sap flux sensors in all six branches where sap flux was recorded. Small branch segments were removed from more distal portions of the same branches. Their diameters after removing bark were 0.5 – 1.7 cm. Lateral root segments were used, some of which were already small enough to fit into the centrifuge rotor without altering their diameter. After felling the trees, rounds from the upper and lower bole, each proximal to the sap flux sensors, were quartered and transported back to the lab. Sample lengths were about 50 cm prior to being processed in the lab. Large branches, some roots, and upper and lower bole segments were carved down to about 1.5 cm diameter using chisels as in Domec and Gartner (2001). Samples were placed in a vacuum chamber, submerged in 20 mM KCl acidic solution (HCl; pH = 2) solution in a refrigerator overnight to refill embolized cells and prevent mold growth (Sperry *et al.* 1988).

Each maximum conductivity ($K_{MAX}$) value was determined by connecting a tree segment to a tubing manifold with a small pressure head (20 – 60 cm) feeding into a cup of the HCl/KCl solution on a 4-decimal scale (Mettler Toledo, Columbus, OH; XS205**)** connected to a computer, using conductR (version 15 D.D. Smith). After 2-6 minutes, once the flow rates stabilized, that value was recorded. Conductivity could then be calculated from

the flow rate, length and diameter of the sample, the pressure head, and the temperature of the solution. Subsequent to maximum conductivity measurements, the samples were placed in a custom rotor and centrifuged with sample tips submerged (Alder *et al.* 1997). The water in each cup was measured using pipettes to prevent an unintended pressure gradient within the sample itself (Beikircher *et al.* 2010). Samples were kept in measurement solution when not being spun or measured. After spinning the samples at the appropriate RPM, they were attached to the to the tubing manifold within 5 – 15 minutes of being spun. The flow rates were then recorded for each centrifugally-induced water potential and conductivities calculated, producing vulnerability curves. Each curve was constructed from 5-6 samples, and the Duursma R package was used to fit sigmoidal curves and confidence intervals to the data (Duursma 2015).

### 3.3.0 Results

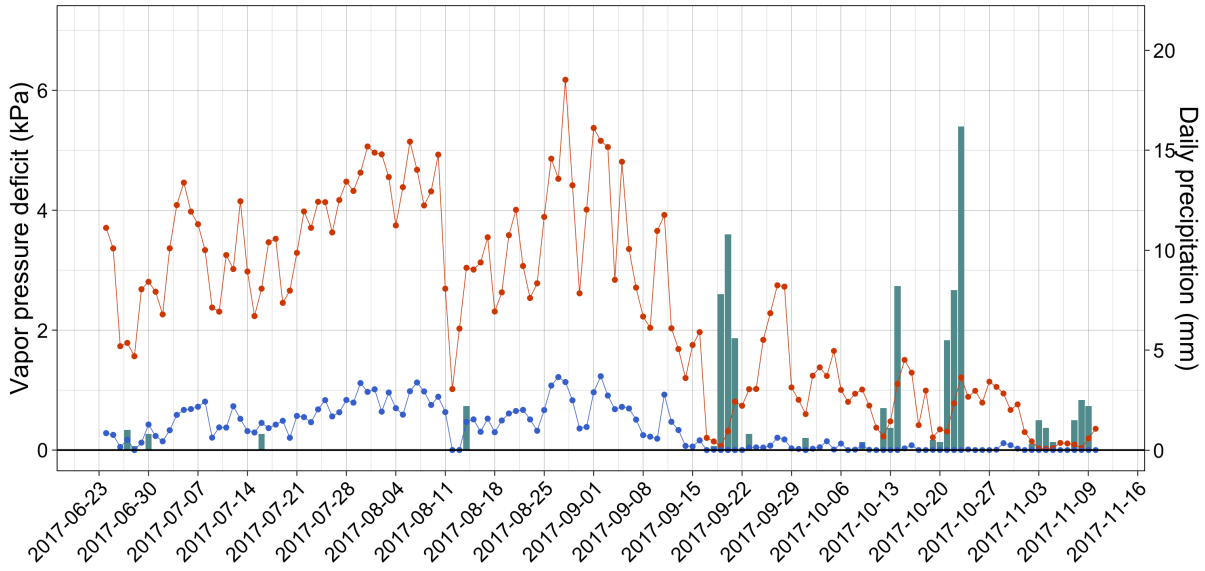


Figure 3-2. Minimum (blue) and maximum (orange) daily vapor pressure deficits and daily precipitation (bars) across the study period.

#### 3.3.1 Weather and leaf water potential

There was very little rainfall through most of the study period, with rain ceasing in mid-June and almost no precipitation falling until mid-September. Predawn water potentials were not significantly different between May and mid-July (~ -0.8 MPa) and then decreased into mid-September, reaching as low as -1.59 MPa (Fig. 3-2 and Table 3-2). After precipitation in mid-September, $\Psi_{PD}$ increased to -1.05 MPa. Midday water potentials, collected between 12:00 and 13:00, were fairly consistent throughout the study period.

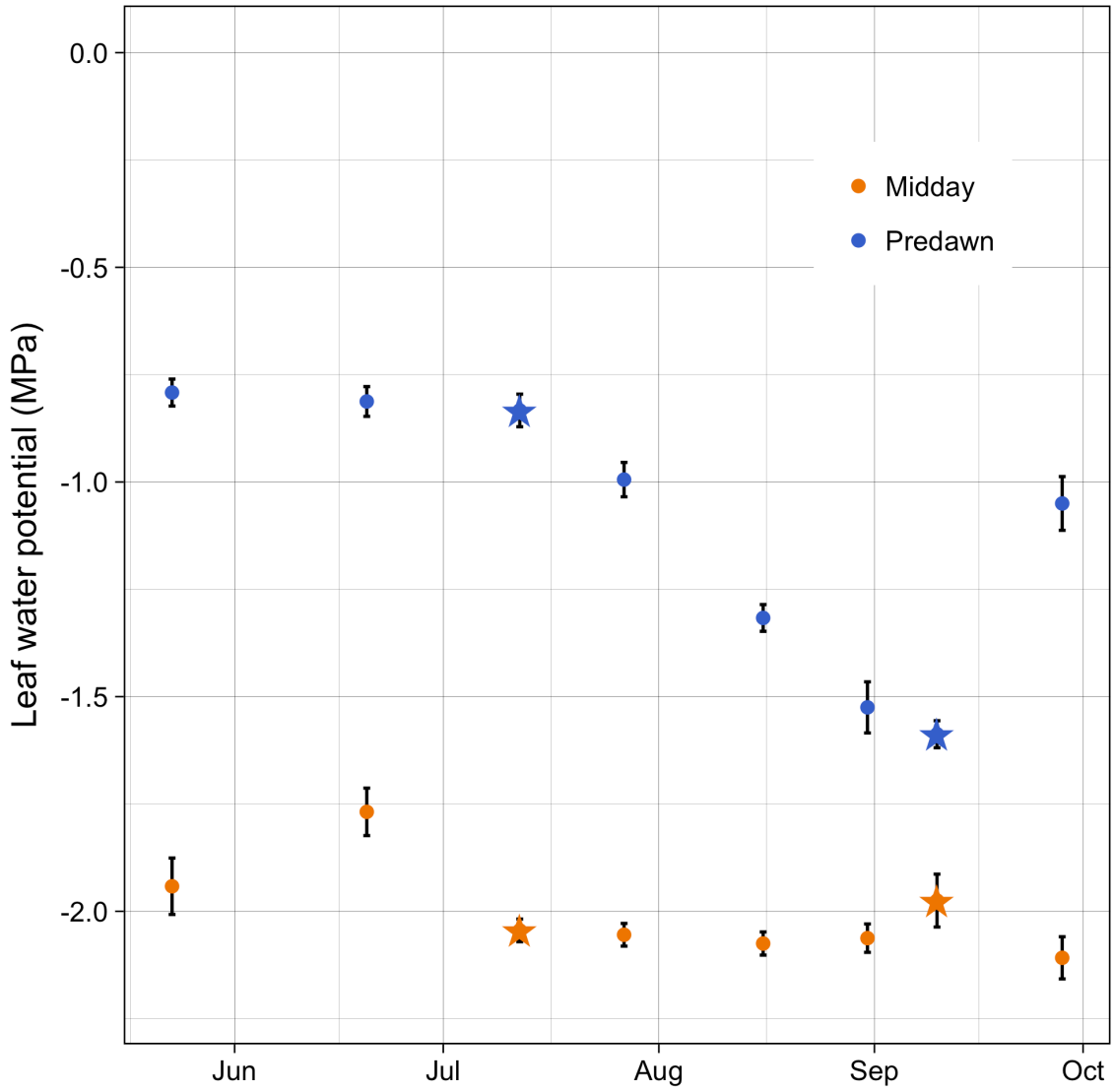


Figure 3-3. Predawn and midday leaf water potentials through the field season. The stars represent the two days when 24-hour gas exchange and water potential were measured.

| Date | $\Psi_{PD}$ | $\Psi_{PD}$ confidence range | $\Psi_{MD}$ | $\Psi_{MD}$ confidence range | $\Psi_{PD}$ - $\Psi_{MD}$ |
|---|---|---|---|---|---|
| 5/23/17 | -0.79 | (-0.76, -0.82) | -1.94 | (-1.88, -2.01) | 1.15 |
| 6/20/17 | -0.81 | (-0.78, -0.85) | -1.77 | (-1.71, -1.82) | 0.96 |
| **7/12/17** | **-0.83** | **(-0.80, -0.87)** | **-2.04** | **(-2.02, -2.07)** | **1.21** |
| 7/27/17 | -0.99 | (-0.95, -1.03) | -2.05 | (-2.03, -2.08) | 1.06 |
| 8/16/17 | -1.32 | (-1.29, -1.35) | -2.08 | (-2.05, -2.10) | 0.76 |
| 8/31/17 | -1.53 | (-1.47, -1.58) | -2.06 | (-2.03, -2.10) | 0.54 |
| **9/10/17** | **-1.59** | **(-1.56, -1.62)** | **-1.98** | **(-1.91, -2.04)** | **0.39** |
| 9/28/17 | -1.05 | (-0.99, -1.11) | -2.11 | (-2.06, -2.16) | 1.06 |

Table 3-2. All values are in MPa. Diurnal gas exchange and water potential field days are in bold. Confidence ranges use standard errors for n = 6.

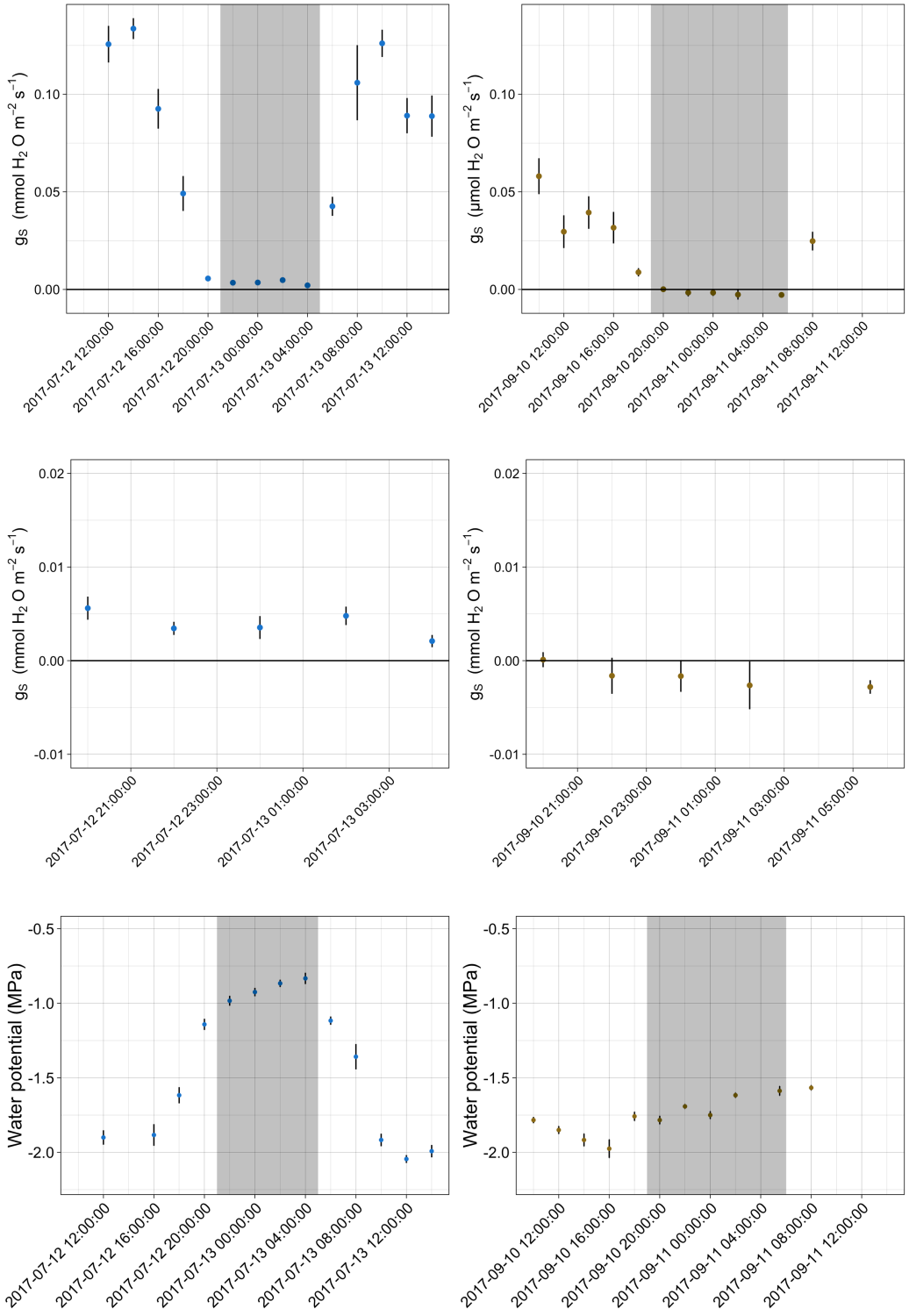


Figure 3-4. Diurnal a) $\Psi_L$ and b) $g_S$ for July 12-13 and September 10-11. Error bars represent standard error for n = 6. Time between sunset and sunrise is in grey.

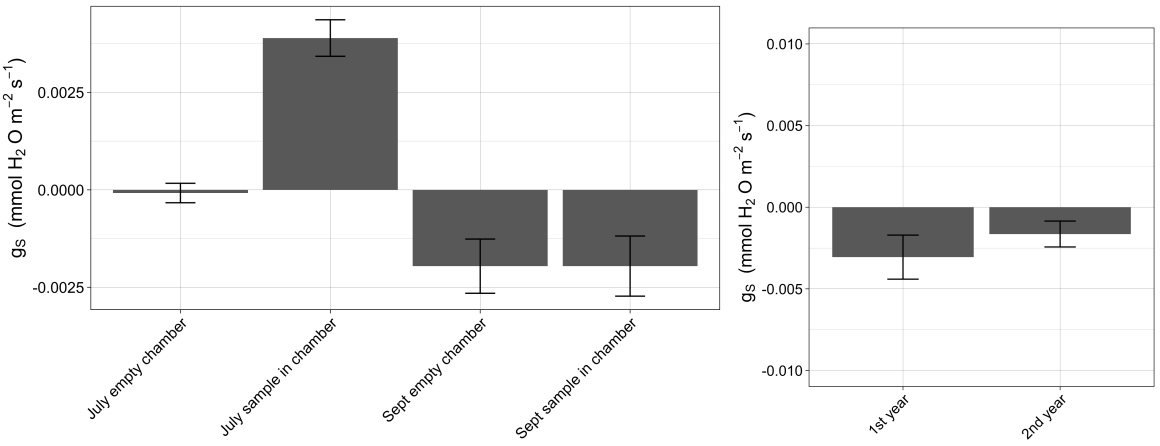


Figure 3-5. The left panel shows the difference between nighttime stomatal conductance values in chambers with samples in them and chambers with no samples. Stomatal conductance values from the midnight hour on September 11th, 2017, comparing the first-year cohort needles and the second-year cohort needles are in the right panel.

### 3.3.2 Gas exchange

Daytime leaf-level $g_s$ was significantly greater on the July date than the September date (Fig. 3-4). The greatest $g_S$ ($g_{S\text{-}MAX}$) in July was 29% of the September $g_{S\text{-}MAX}$. Nighttime stomatal conductances ($g_{S\text{-}NOC}$) were significantly greater than values recorded from an empty chamber in July but were not in September ($\alpha = 0.05$, Fig. 3-5).

### 3.3.3 Morning flux, compared to VPD

To consider seasonality of the relationships between VPD and sap flux within the different above-ground organs, simple linear regressions of morning sap flux and VPD with data were binned by month. Morning sap flux was used (09:00 to 11:45) to avoid interactions with reduced PAR in the afternoon from canopy shading and potential effects of $\Psi_L$ on transpiration. Adjusted $R^2$ values for the significant relationships are shown in Fig. 3-6. Overall, the branches had the highest correlations with VPD (adjusted $R^2$ as high as 0.9, $\alpha$= 0.05). Lagging the VPD by 15 minutes, to assess whether flux was responsive but delayed in

lower organs, did not improve the models. For branches, the strongest relationships were in the wetter months, June and October. The lower boles had the weakest correlations between sap flux and VPD, with July and August, the two driest months, having very little explanatory power.

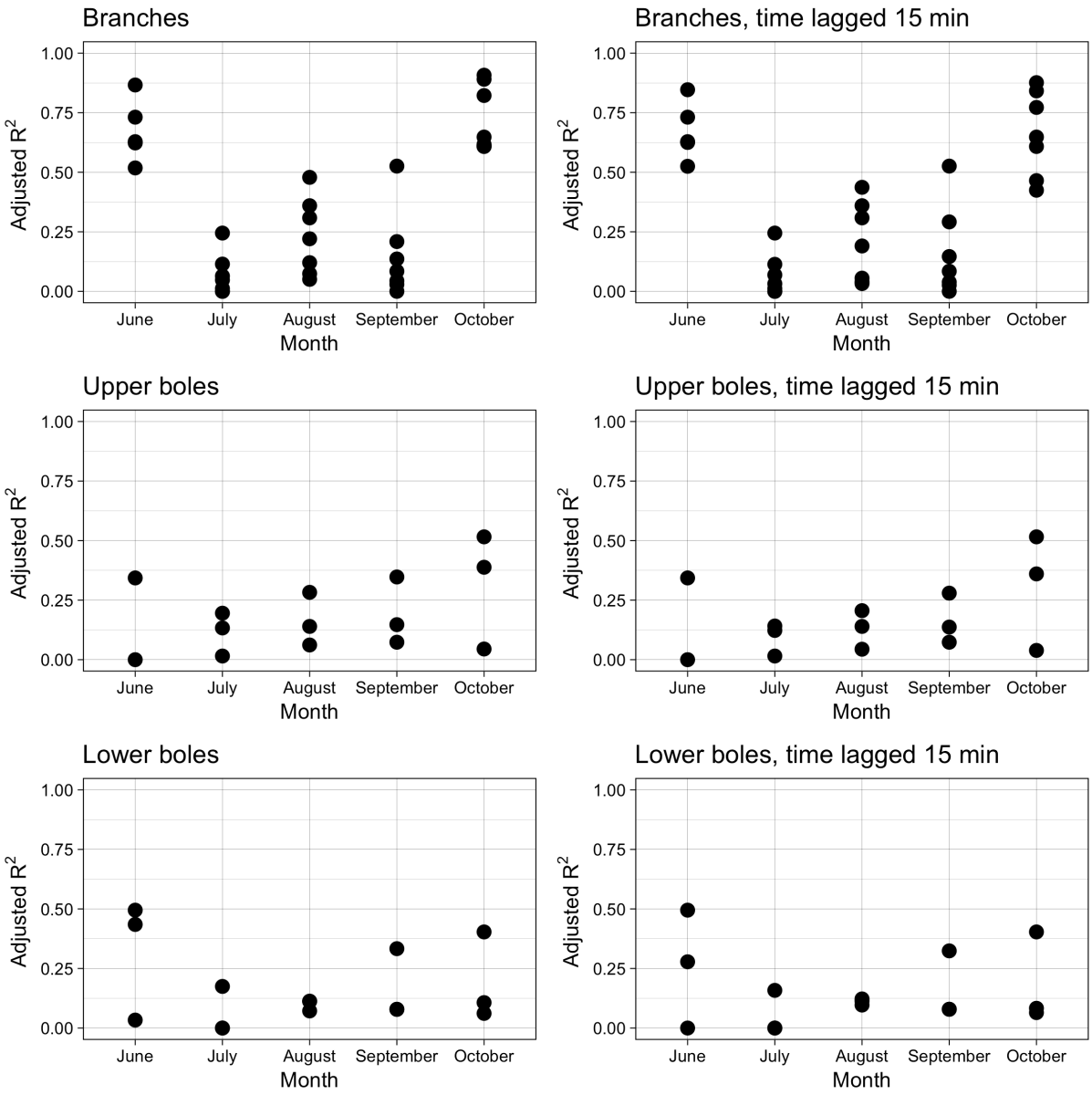


Figure 3-6. Adjusted $R^2$ values for simple linear regressions for morning (09:00 – 11:45) sap flux and VPD, binned by month.

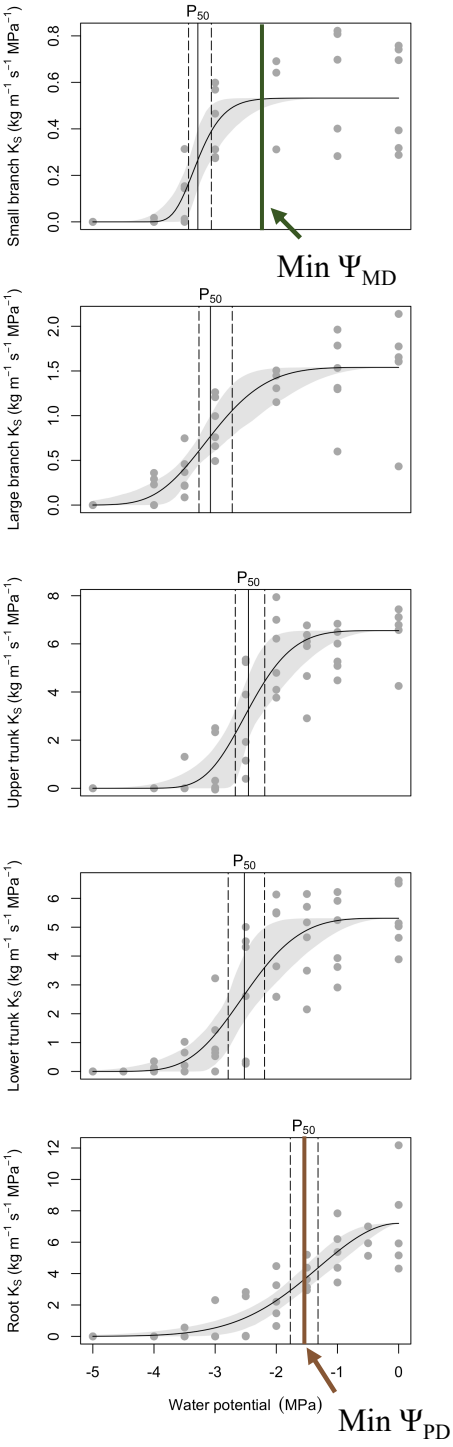


Figure 3-7. Vulnerability curves for the five organs with seasonal minimum $\Psi_{PD}$ and $\Psi_{MD}$ labeled.

### 3.3.4 Conductivity and conductance

Resistance to embolism was greater going up the tree. (Fig. 3-7, Table 3-3) The roots were the most vulnerable organ, and the small branches the least vulnerable. The difference between the $\Psi_{P50}$ of the most and least vulnerable organs was 1.6 MPa. Slopes of the vulnerability curves were also different with roots having a less steep slope (value).

| Organ | $\Psi_{P50}$ | Confidence range |
|---|---|---|
| Small branch | -3.29 a | (-3.16, -3.40) |
| Large branch | -3.03 ab | (-2.55, -3.37) |
| Upper bole | -2.40 bc | (-2.15, -2.60) |
| Lower bole | -2.27 bc | (-1.99, -2.56) |
| Root | -1.68 d | (-1.48, -1.93) |

Table 3-3. Confidence ranges are 2.5 – 97.5%. Letters next to the $\Psi_{P50}$ represent categories of values that are not significantly different from each other.

### 3.3.5 Whole-tree conductance

For each day with $\Psi_{PD}$ and $\Psi_{MD}$ values water potentials recorded and sap flux installed, whole-tree conductance was calculated (Fig. 3-8). Mean flux values from 09:00 – 11:45 were used (to prevent confounding interactions such as limited PAR and low $\Psi_L$) and converted to flux per leaf area ($Q_L$), using a leaf area to sapwood area ratio ($A_L$:$A_S$) of 0.25 (Waring *et al.* 1982). The mean of those values was used to calculate whole-tree conductance ($k_H$, $cm^3$ $hour^{-1}$ $MPa^{-1}$) using a version of Darcy's Law (Ryan *et al.* 2000):

Equation 3-2:

$$k_H = \frac{Q_L}{(\Psi_{PD} - \Psi_{MD})}$$

Generally, $k_H$ declined across the season. T2, the largest tree, showed less reduction than the other two, both of which declined nearly to 100% loss of $k_H$.

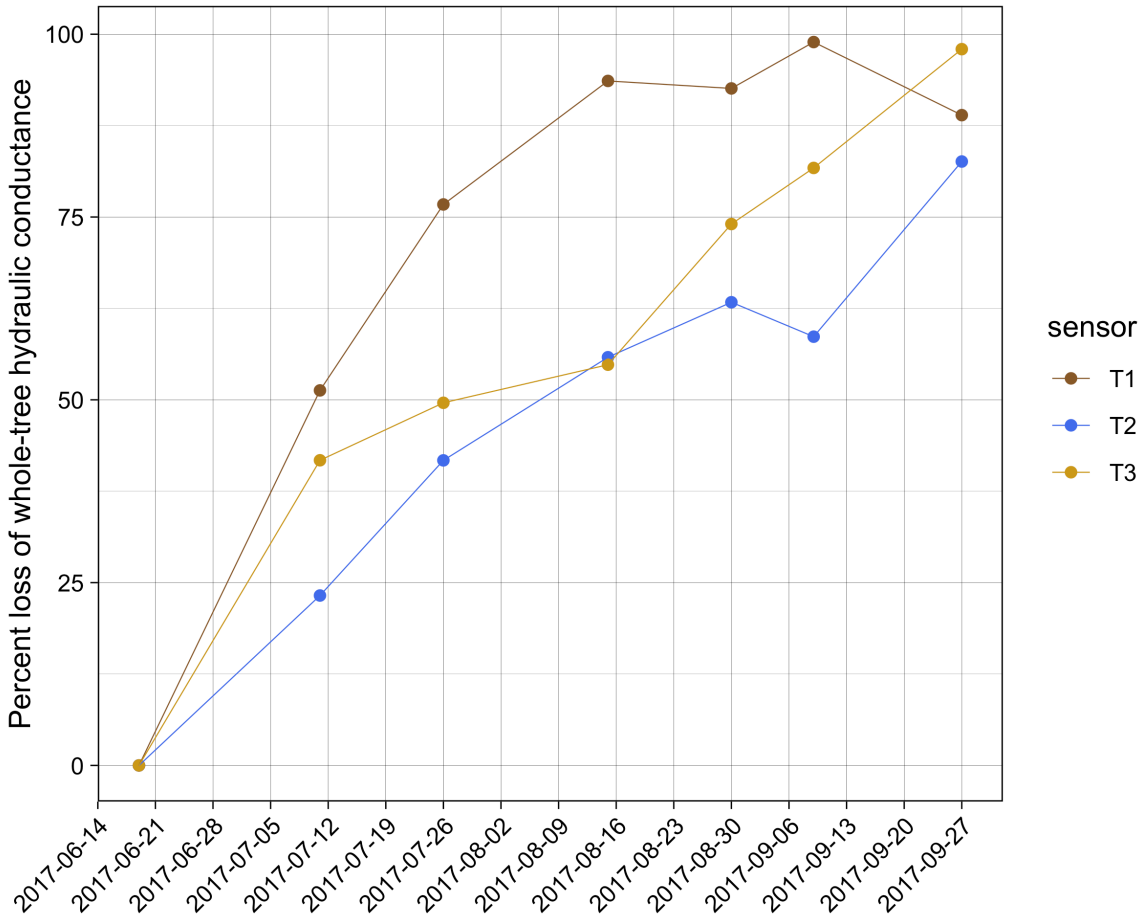


Figure 3-8. Percent loss of whole-tree hydraulic conductance across the season.

## 3.4.0 Discussion

### 3.4.1 Seasonal water stress

Across the season, the trees experienced a large and gradual decrease in their available water. The difference between $\Psi_{PD}$ and $\Psi_{MD}$ values, which were 1.4 MPa in June and July, became as low as 0.4 MPa in September. Using previously published water release curves on a similar *P. ponderosa* population (Eastern Cascades, OR USA), our hypothesis

that capacitively stored water would have a greater contribution to daily transpired water in the early season was supported (Fig. 3-9).

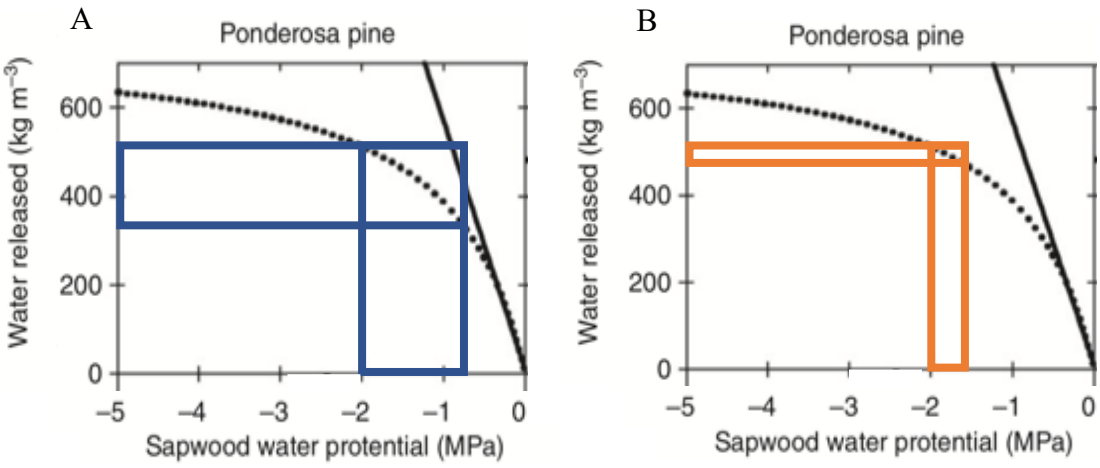


Figure 3-9. Top left panel from Fig. 1: the east side *P. ponderosa* samples, which had similar hydraulic vulnerability to embolism to our trees in this project. Colored boxes highlight the range of $\Psi_{leaf}$ experienced by our trees early in the study period (A, blue) and in September (B, orange).

The amount of water inside the sapwood decreases under tension during the day and increases while the tension is relieved overnight (Meinzer *et al.* 2004). The tree boles would not have experienced water potentials as low as the leaves, but they were likely similar. In lieu of an accurate estimate of the bole water potentials, we use the $\Psi_L$ values to approximate the relationship between the water potentials and their corresponding change in water content in the wood (Fig. 3-9). Earlier in the season, the water potential range represents a daily capacitive draw down of about 200 kg m$^{-3}$. By September, however, the daily change in water potential corresponds to only about 50 kg m$^{-3}$. So, the contribution of bole capacitively stored water was reduced by about 75% across the season. The daily sap flux, however, was

reduced by 93%, meaning that capacitance became a greater ratio of daily transpired water in the later season than it had been in the early season. Oaks in France (*Quercus ilex*) have behaved similarly, with the flux of capacitance decreasing in drought but becoming a relatively greater portion of total transpired water (Salomón *et al.* 2017).

### 3.4.2 Nighttime transpiration

The hypothesis that nighttime gas exchange would occur at about 33% of maximum gas exchange was not supported. At 2.8% of midmorning $g_S$, $g_{S\text{-}NOC}$ on the July night was much lower than a previous study had seen in similar trees in the region, which reported $g_{S\text{-}NOC}$ of 21-42% of the midmorning $g_S$ in July and August (Kavanagh *et al.* 2007). During the only significantly observed $g_{S\text{-}NOC}$, which occurred in July, $\Psi_{PD}$ was less negative (-0.83 MPa) than it was in September when gas exchange values were not significantly different from an empty chamber ($\Psi_{PD}$ = -1.59 MPa). A potential mechanism for this disparity is the similarity between the September $\Psi_{PD}$ and published water potentials at turgor loss point ($\Psi_{TLP}$) for *P. ponderosa* leaves (Johnson *et al.* 2009a and b, 2012). As discussed below, leaf conductance ($k_L$) is greatly reduced at $\Psi_{TLP}$. This could account for the lack of $g_{S\text{-}NOC}$ in September. Alternatively, the stomata may be more tightly regulated in at that lower $\Psi_L$.

### 3.4.3 Conductivity

Our hypothesis that hydraulic vulnerability to embolism would be greatest in the roots and decrease in downstream organs was supported by the results. The vulnerability curves for the root and small branches in this project were very similar to the *P. ponderosa* vulnerability

curves in Chapter 2. The curves are also similar to published *P. ponderosa* curves (roots: Domec *et al.* 2004; bole: Domec and Gartner 2003, Barnard *et al.* 2011; branch: Maherali & DeLucia 2000, Piñol & Sala 2000). Root conductivity likely decreased throughout the season by about half, based on the $\Psi_{PD}$ values and vulnerability curves.

### 3.4.4 Whole-tree conductance

Our hypothesis that whole-tree $k_H$ would be reduced to levels corresponding to the predicted degree of $K_S$ in the most vulnerable organ was not supported. While roots, as the most vulnerable measured organ, probably did experience a large decrease in conductivity, it was not as great a decrease as the observed decrease in $k_H$. That disparity, then, is due to a decrease in conductivity in something we did not measure: potentially in the leaves or soil (Johnson *et al.* 2018).

Some conifer species lose 98-100% of their leaf hydraulic conductance daily (Johnson *et al.* 2011, 2016), though many species can maintain some degree of $k_L$ at $\Psi_L$ corresponding to turgor loss (Brodribb and Holbrook 2006). *P. ponderosa*, however, can maintain $k_L$, around 20% of $k_{leaf\text{-}max}$ after their turgor loss point (Johnson *et al.* 2009a). In fact, $k_L$ does not appear to decline past 20% of $k_{L\text{-}MAX}$ at the water potentials studied, which are as low as -3.4 MPa and lower than the $\Psi_L$ values seen in the trees in this project (Johnson *et al.* 2009b, Johnson *et al.* 2012).

### 3.4.4 Conclusion

*P. ponderosa* is commonly more vulnerable to xylem embolism than other conifers (Piñol & Sala 2000, Domec & Gartner 2003), and trees tend not to overbuild their woody

xylem, potentially because there can be a trade-off between resistance to embolism and ease of water movement (Pockman & Sperry 2000). In this normal year, these three *P. ponderosa* trees operated remarkably close to catastrophic failure. These trees not only practically ran out of capacitively stored water, but they also reduced their $k_H$ nearly to zero by the end of the dry season. The fact that this was a normal year for temperature and precipitation, emphasizes the power of *P. ponderosa*'s ability to control their hydraulic strategies to prevent catastrophic failure.

### 3.5.0 References

Alder, N. N., W. Pockman, J. S. Sperry, and S. Nuismer. 1997. Use of centrifugal force in the study of xylem cavitation. Journal of Experimental Botany 48:665–674.

Anderegg, W. R. L., A. Wolf, A. Arango-Velez, B. Choat, D. J. Chmura, S. Jansen, T. Kolb, S. Li, F. C. Meinzer, P. Pita, V. Resco de Dios, J. S. Sperry, B. T. Wolfe, and S. Pacala. 2018. Woody plants optimise stomatal behaviour relative to hydraulic risk. Ecology Letters 21:968–977.

Barnard, D. M., and W. L. Bauerle. 2013. The implications of minimum stomatal conductance on modeling water flux in forest canopies. Journal of Geophysical Research: Biogeosciences 118:1322–1333.

Barnard, D. M., F. C. Meinzer, B. Lachenbruch, K. A. McCulloh, D. M. Johnson, and D. R. Woodruff. 2011. Climate-related trends in sapwood biophysical properties in two conifers: Avoidance of hydraulic dysfunction through coordinated adjustments in xylem efficiency, safety and capacitance. Plant, Cell and Environment 34:643–654.

Beikircher, B., T. Ameglio, H. Cochard, and S. Mayr. 2010. Limitation of the Cavitron technique by conifer pit aspiration. Journal of Experimental Botany 61:3385–3393.

Bell, D. M., E. J. Ward, A. C. Oishi, R. Oren, P. G. Flikkema, and J. S. Clark. 2015. A state-space modeling approach to estimating canopy conductance and associated uncertainties from sap flux density data. Tree Physiology 35:792–802.

Brodribb, T. J., and N. M. Holbrook. 2006. Declining hydraulic efficiency as transpiring leaves desiccate: Two types of response. Plant, Cell and Environment 29:2205–2215.

Brooks, J. R., F. C. Meinzer, J. M. Warren, J.-C. Domec, and R. Coulombe. 2006. Hydraulic redistribution in a Douglas-fir forest: lessons from system manipulations. Plant, Cell and Environment 29:138–150.

Burgess, S. S. O., M. A. Adams, N. C. Turner, C. R. Beverly, C. K. Ong, A. A. H. Khan, and T. M. Bleby. 2001. An improved heat pulse method to measure low and reverse rates of sap flow in woody plants. Tree Physiology 21:589–598.

Dawson, T. E., S. S. O. Burgess, K. P. Tu, R. S. Oliveira, L. S. Santiago, J. B. Fisher, K. A. Simonin, and A. R. Ambrose. 2007. Nighttime transpiration in woody plants from contrasting ecosystems. Tree physiology 27:561–75.

Domec, J. C., J. M. Warren, F. C. Meinzer, J. R. Brooks, and R. Coulombe. 2004. Native root xylem embolism and stomatal closure in stands of Douglas-fir and ponderosa pine: Mitigation by hydraulic redistribution. Oecologia 141:7–16.

Domec, J.-C., and B. L. Gartner. 2001. Cavitation and water storage capacity in bole xylem segments of mature and young Douglas-fir trees. Trees - Structure and Function 15:204–214.

Domec, J.-C., and B. L. Gartner. 2002. How do water transport and water storage differ in coniferous earlywood and latewood? Journal of Experimental Botany 53:2369–2379.

Domec, J.-C., and B. L. Gartner. 2003. Relationship between growth rates and xylem hydraulic characteristics in young, mature and old-growth ponderosa pine trees. Plant, cell & environment 26:471–483.

Domec, J. C., J. M. Warren, F. C. Meinzer, J. R. Brooks, and R. Coulombe. 2004. Native root xylem embolism and stomatal closure in stands of Douglas-fir and ponderosa pine: Mitigation by hydraulic redistribution. Oecologia 141:7–16.

Duursma, R.A., 2015. Plantecophys - An R Package for Analysing and Modelling Leaf Gas Exchange Data. PLoS ONE 10, e0143346.

Fisher, J. B., D. D. Baldocchi, L. Misson, T. E. Dawson, and A. H. Goldstein. 2007. What the towers don't see at night: nocturnal sap flow in trees and shrubs at two AmeriFlux sites in California. Tree physiology 27:597–610.

Goldstein, G., F. Meinzer, and M. Monasterio. 1984. The role of capacitance in the water balance of Andean giant rosette species. Plant, Cell & Environment 7:179–186.

Holbrook, N. M. 1995. Stem water storage. Pages 151–174 in B. L. Gartner, editor. Plant stems: Physiology and functional morphology. Academic Press, San Diego, CA, USA.

Hölttä, T., H. Cochard, E. Nikinmaa, and M. Mencuccini. 2009. Capacitive effect of cavitation in xylem conduits: Results from a dynamic model. Plant, Cell and Environment 32:10–21.

Howard, A. R., M. W. Van Iersel, J. H. Richards, and L. A. Donovan. 2009. Night-time transpiration can decrease hydraulic redistribution. Plant, Cell and Environment 32:1060–1070.

Hubbard, R. M., B. J. Bond, and M. G. Ryan. 1999. Evidence that hydraulic conductance limits photosynthesis in old Pinus ponderosa trees. Tree Physiology 19:165–172.

Hubbard, R. M., M. G. Ryan, V. Stiller, and J. S. Sperry. 2001. Stomatal conductance and photosynthesis vary linearly with plant hydraulic conductance in ponderosa pine. Plant, Cell and Environment 24:113–121.

Johnson, D. M., K. A. McCulloh, F. C. Meinzer, D. R. Woodruff, and D. M. Eissenstat. 2011. Hydraulic patterns and safety margins, from stem to stomata, in three eastern US tree species. Tree Physiology 31:659–668.

Johnson, D. M., K. A. McCulloh, D. R. Woodruff, and F. C. Meinzer. 2012. Evidence for xylem embolism as a primary factor in dehydration-induced declines in leaf hydraulic conductance. Plant, Cell and Environment 35:760–769.

Johnson, D. M., F. C. Meinzer, D. R. Woodruff, and K. A. McCulloh. 2009a. Leaf xylem embolism, detected acoustically and by cryo-SEM, corresponds to decreases in leaf hydraulic conductance in four evergreen species. Plant, Cell and Environment 32:828–836.

Johnson, D. M., D. R. Woodruff, K. A. McCulloh, and F. C. Meinzer. 2009b. Leaf hydraulic conductance, measured in situ, declines and recovers daily: Leaf hydraulics, water potential and stomatal conductance in four temperate and three tropical tree species. Tree Physiology 29:879–887.

Johnson, D. M., R. Wortemann, K. A. McCulloh, L. Jordan-Meille, E. Ward, J. M. Warren, S. Palmroth, and J.-C. Domec. 2016. A test of the hydraulic vulnerability segmentation hypothesis in angiosperm and conifer tree species. Tree Physiology 36:989–993.

Jupa, R., L. Plavcová, V. Gloser, and S. Jansen. 2016. Linking xylem water storage with anatomical parameters in five temperate tree species. Tree Physiology 36:756–769.

Johnson, D. M., J. C. Domec, Z. Carter Berry, A. M. Schwantes, K. A. McCulloh, D. R. Woodruff, H. Wayne Polley, R. Wortemann, J. J. Swenson, D. Scott Mackay, N. G. McDowell, and R. B. Jackson. 2018. Co-occurring woody species have diverse hydraulic strategies and mortality rates during an extreme drought. Plant Cell and Environment 41:576–588.

Kavanagh, K. L., R. Pangle, and A. D. Schotzko. 2007. Nocturnal transpiration causing disequilibrium between soil and stem predawn water potential in mixed conifer forests of Idaho. Tree physiology 27:621–629.

McCulloh, K. A., D. M. Johnson, F. C. Meinzer, and D. R. Woodruff. 2014. The dynamic pipeline: Hydraulic capacitance and xylem hydraulic safety in four tall conifer species. Plant, Cell and Environment 37:1171–1183.

Meinzer, F. C., D. R. Woodruff, J. C. Domec, G. Goldstein, P. I. Campanello, M. G. Gatti, and R. Villalobos-Vega. 2008. Coordination of leaf and stem water transport properties in tropical forest trees. Oecologia 156:31–41.

Meinzer, F. C., J. R. Brooks, J.-C. Domec, B. L. Gartner, J. M. Warren, D. R. Woodruff, K. Bible, and D. Shaw. 2006. Dynamics of water transport and storage in conifers studied. Plant Cell and Environment 29:105–114.

Meinzer, F. C., S. A. James, G. Goldstein, and D. Woodruff. 2003. Whole-tree water transport scales with sapwood capacitance in tropical forest canopy trees. Plant, Cell and Environment 26:1147–1155.

Meinzer, F. C., S. A. James, and G. Goldstein. 2004. Dynamics of transpiration, sap flow and use of stored water in tropical forest canopy trees. Tree Physiology 24:901–909.

Nardini, A., M. A. Lo Gullo, and S. Salleo. 2011. Refilling embolized xylem conduits: Is it a matter of phloem unloading? Plant Science 180:604–611.

Pfautsch, S., J. Renard, M. G. Tjoelker, and A. Salih. 2015. Phloem as Capacitor: Radial Transfer of Water into Xylem of Tree Stems Occurs via Symplastic Transport in Ray Parenchyma. Plant Physiology 167:963–971.

Phillips, N. G., M. G. Ryan, B. J. Bond, N. G. McDowell, T. M. Hinckley, and J. Čermák. 2003. Reliance on stored water increases with tree size in three species in the Pacific Northwest. Tree Physiology 23:237–245.

Piñol, J., and A. Sala. 2000. Ecological implications of xylem cavitation for several Pinaceae in the Pacific Northern USA. Functional Ecology 14:538–545.

Pockman, W. T., and J. S. Sperry. 2000. Vulnerability to Xylem Cavitation and the Distribution of Sonoran Desert Vegetation 87:1287–1299.

Richards, A. E., I. J. Wright, T. I. Lenz, and A. E. Zanne. 2014. Sapwood capacitance is greater in evergreen sclerophyll species growing in high compared to low-rainfall environments. Functional Ecology 28:734–744.

Ryan, M. G., B. J. Bond, B. E. Law, R. M. Hubbard, D. Woodruff, E. Cienciala, and J. Kucera. 2000. Transpiration and whole-tree conductance in ponderosa pine trees of different heights. Oecologia 124:553–560.

Salomón, R. L., J. M. Limousin, J. M. Ourcival, J. Rodríguez-Calcerrada, and K. Steppe. 2017. Stem hydraulic capacitance decreases with drought stress: implications for modelling tree hydraulics in the Mediterranean oak Quercus ilex. Plant Cell and Environment 40:1379–1391.

Scholander, P., H. Hammel, E. Bradstreet, and E. Hemmingsen. 1965. Sap Pressure in Vascular Plants. Science 148:339–346.

Scholz, F. G., N. G. Phillips, S. J. Bucci, F. C. Meinzer, and G. Goldstein. 2011. Hydraulic Capacitance: Biophysics and Functional Significance of Internal Water Sources in Relation to Tree Size. Pages 341–361 Size- and Age-Related Changes in Tree Structure and Function.

Sperry, J. S., J. R. Donnelly, and M. T. Tyree. 1988. A method for measuring hydraulic conductivity and embolism in xylem. Plant, Cell & Environment 11:35–40.

Sperry, J. S., and D. M. Love. 2015. What plant hydraulics can tell us about responses to climate-change droughts. New Phytologist 207:14–27.

Sperry, J. S. 2000. Hydraulic constraints on plant gas exchange. Agricultural and Forest Meteorology 104:13–23.

Tyree, M. T., and M. H. Zimmermann. 2002. Xylem Structure and the Ascent of Sap. Springer Berlin Heidelberg, Berlin, Heidelberg.

Tyree, M. T., and S. Yang. 1990. Water-storage capacity of Thuja, Tsuga and Acer stems measured by dehydration isotherms - The contribution of capillary water and cavitation. Planta 182:420–426.

Vergeynst, L. L., M. Dierick, J. A. N. Bogaerts, V. Cnudde, and K. Steppe. 2015. Cavitation: A blessing in disguise? New method to establish vulnerability curves and assess hydraulic capacitance of woody tissues. Tree Physiology 35:400–409.

Waring, R., P. Schroeder, and R. Oren. 1982. Application of the pipe model theory to predict canopy leaf area. Journal of Forest Research 12:556–560.

Warren, J. M., F. C. Meinzer, J. R. Brooks, J. C. Domec, and R. Coulombe. 2006. Hydraulic redistribution of soil water in two old-growth coniferous forests: Quantifying patterns and controls. New Phytologist 173:753–765.

Zimmerman, M., and C. Brown. 1971. Trees: Structure and function. Springer-Verlag, New York City, NY.

# Chapter 4: Effects of reducing stand density on seasonal water use in *Pinus ponderosa*

## 4.0.0 Abstract

Thinning a forest that is limited by water can reduce drought stress and improve drought resilience. We conducted an experiment on an even-aged stand of *Pinus ponderosa* trees in northern Idaho, reducing stand density in two treatments (mid-density and low density) with remaining high density control plots and monitored their water use through the second growing season after the treatment. Treated plots continued to draw down soil water at greater amounts longer into the growing season, where the control plots peaked in their water use early in the summer and then reduced their water fluxes. Predawn water potentials were sometimes less negative in the treated plots, with the effect being more pronounced in the mid-density treatment than the low density. Midday water potentials were more negative in the treated plots, potentially due to the increased temperature and turbulence within those plots. Whole-tree conductance was reduced to less than 10% of its maximum value by the end of September in control plots but was significantly greater in the mid-density treatment.

## 4.1.0 Introduction

Species and age class diversity improves resilience to drought and climate change in drought and is a common goal of land managers trying to cultivate resilient forests (Lasch *et al.* 2002, Brang *et al.* 2014). In stands that currently exist as monocultures, however, reducing the density of the forest can temporarily reduce the stand's vulnerability to drought and can also increase the diversity of plants, birds, bats, mammals, and reptiles (Lindner 2000, Lasch *et al.* 2002, Spittlehouse and Stewart 2003, Chmura *et al.* 2011, Gonsalves *et al.*

2018). Density reduction can also alter the energy and water budgets of stands and result in improved ecosystems services such as increased water output (Stednick 1996). For the remaining trees, decreased stand density improves their ability to survive, assimilate carbon, and grow through extended drought conditions (Navarro-Cerillo *et al.* 2019).

A simple framework under which tree mortality is often viewed offers two routes to mortality: 1) species that do less to reduce their stomatal conductance under high soil-canopy water deficits are susceptible to hydraulic failure as runaway cavitation depresses water conductivity, and 2) species that heavily regulate their stomata are prone to death from carbon imbalance, as their conservative hydraulic strategy also prevents photosynthesis (McDowell *et al.* 2008). In reality, these two processes cannot be uncoupled and both of these threats can be mitigated by thinning a stand. With fewer trees competing for available soil moisture, the remaining trees have access to more soil water. This delays the onset of a soil-canopy water deficit and resultant declines in hydraulic conductivity and depressed photosynthesis. Individuals in a thinned stand also have access to more sunlight and soil nutrients. High light conditions, in concert with sufficient nutrients to produce requisite enzymes, allow trees to assimilate carbon efficiently and at high flux densities. The duration of these effects are more complicated to predict and not addressed in this project, but reducing stand density is often effective in the short term at alleviating acute water stress and effective at increasing tree growth in the long term (Aussenac and Granier 1988, Bréda *et al.* 1995).

A meta-analysis on thinning as a drought mitigation strategy indicated that drought recovery of conifer trees is improved by decreasing stand density (Sohn *et al.* 2016). In thinning projects that reported leaf water potentials ($\Psi_L$) they commonly reported less

negative predawn water potentials ($\Psi_{PD}$), a strong indicator of tree-level water stress and available soil water (Aussenac and Granier 1988, Bréda *et al.* 1995, Feeney *et al.* 1998, Simonin *et al.* 2006). Many of the same projects and others also reported an increase of tree-level assimilation of carbon and/or radial growth (Cardill 2018, Park *et al.* 2018, del Campo *et al.* 2019). The effects that thinning had on the $\Psi_{PD}$ during dry periods were reduced through time after the treatment, largely disappearing after 4 years. The effect of thinning on growth, however, was generally sustained beyond the mediation of $\Psi_{PD}$. Thinning a forest before a drought has been shown to increase its ability to continue growing through drought and also is ability to recover after drought (Navarro-Cerillo *et al.* 2019).

While it is clear that thinning a forest can mediate drought effects in the short term and increase tree-level growth in the long term, the intensity of thinning that would be ideal for a stand is more complicated and unestablished. In this project, an 11-acre stand of *Pinus ponderosa* was partitioned into nine plots. Three plots were thinned to a mid-density treatment with a mean spacing of 16’; three other plots were thinned low-density treatment with a mean spacing of 20’, leaving three control plots with a mean spacing of 12’. The mid-density treatment is one commonly used in the region by forest managers, and the low-density treatment is more extreme than would usually be applied (personal communication with Dr. Rob Keefe).

Our guiding question was: how does thinning affect trees’ water use and status in the following year? We had a three-part hypothesis: thinning the stands will alleviate water stress, resulting in 1) less negative $\Psi_{PD}$ values and greater sap fluxes later into the season. 2) The effect will be most noticeable in the 20’ spacing with a more moderate result in the 16’ spacing. 3) The control plots will remove much of the soil water earlier in the season and

then reduce their flux, while the treatment plots will continue to draw down soil water at greater rates later into the season.

## 4.2.0 Methods

### 4.2.1 Site description and thinning treatment

This project occurred in an even-aged *Pinus ponderosa* stand on the University of Idaho Experimental Forest in 2018. The stand was twelve acres of 35-year-old *P. ponderosa* trees at 12’ spacing between adjacent trees and was separated into to three 1-acre-sized plots of 20’ pre-commercial thin (low density, PCT), three 16’ PCT (mid-density), and three 12’ control (high density) plots. The trees were felled in December of 2016 and removed in June of 2017. The treatments for the plots were assigned randomly for the 20’ and control treatments, and the 16’ plots, were installed based on where there was leftover 1-acre space within the stand.

### 4.2.2 Meteorological and soil data

A meteorological station was installed in 2016 in an adjacent stand of low-density, then ~12-year-old *Larix occidentalis*, *Pinus monticola*, and *P. ponderosa* trees. Trees within 20 m of the instruments were removed to simulate conditions above the canopy of the *P. ponderosa* study site, as is described in Chapter 3 (section 3.2.2). Decagon 5TE and 5TM (now Meter, Pullman, WA) soil volumetric water content (VWC) sensors were installed in each plot. The soil pits were placed equidistant between two trees that were the goal-distance apart (12’, 16’, and 20’). The upper sensors were installed at 35 – 45 cm, a depth with a high density of tree roots. The lower sensors were installed at 80 cm – 100 cm, at whatever

greatest depth could be accessed by digging with a shovel. Soil data was logged with Decagon EM50 dataloggers.

### 4.2.3 Sap flux, heat ratio method

Heat ratio method sap flux sensors were installed in 1-2 trees in each plot at breast height. After regular damage from animals on some trees in the 20' plots, there was uninterrupted sap flux data from two trees in low density plots, five trees in mid-density plots, and four trees in high density plots. The sensors recorded temperatures at three depths both above and below the heater probe before the heater probe sent a heat pulse. The six thermocouples would then record a second value, averaging the temperatures for 60-100 seconds after the heat pulse. The difference between the pre-heat-pulse and post-heat-pulse temperatures were used to calculate tree's sap flux velocity using the equations in Burgess *et al*. (2001). Temperature ratios were recorded on CR-1000 dataloggers connected AM 16/32B multiplexors (Campbell Scientific, Logan, UT) every 15-minutes from mid-to-late June to mid-October.

### 4.2.4 Water potential and calculation of whole-plant conductance

Ladders were installed in five plots to access the canopy with a 20' pole clipper. Two were installed in the low-density treatment with access to five trees, two in mid-density plots with access to five trees, and one in a control plot with access to four trees. Leaf water potentials from 2016 showed no difference between either $\Psi_{MD}$ or $\Psi_{PD}$ values in the pre-treatment plots, indicating that one control plot would be sufficient to represent un-thinned stands. Predawn and midday leaf water potentials were assessed using a Scholander-type

pressure chamber (Scholander *et al.* 1965; PMS, Corvallis, OR). Predawn samples were removed from trees in the hour before sunrise and sealed in plastic bags that had been breathed into to increase the humidity to prevent transpirational water loss. Predawn and midday water potentials along with sap flux, were used to calculate whole-tree conductance, as is described in section 3.3.5.

### 4.3.0 Results

#### 4.3.1 Meteorological data

Nighttime vapor pressure deficits were always greater than 0.12 kPa, suggesting that $\Psi_{PD}$ were likely not equal to the mean soil water potential of the active root area as this species has been shown to actively transpire at night when VPD are greater than 0.12 kPa (Kavanagh *et al.*, 1997). There was little precipitation over the study period (Fig. 4-1).

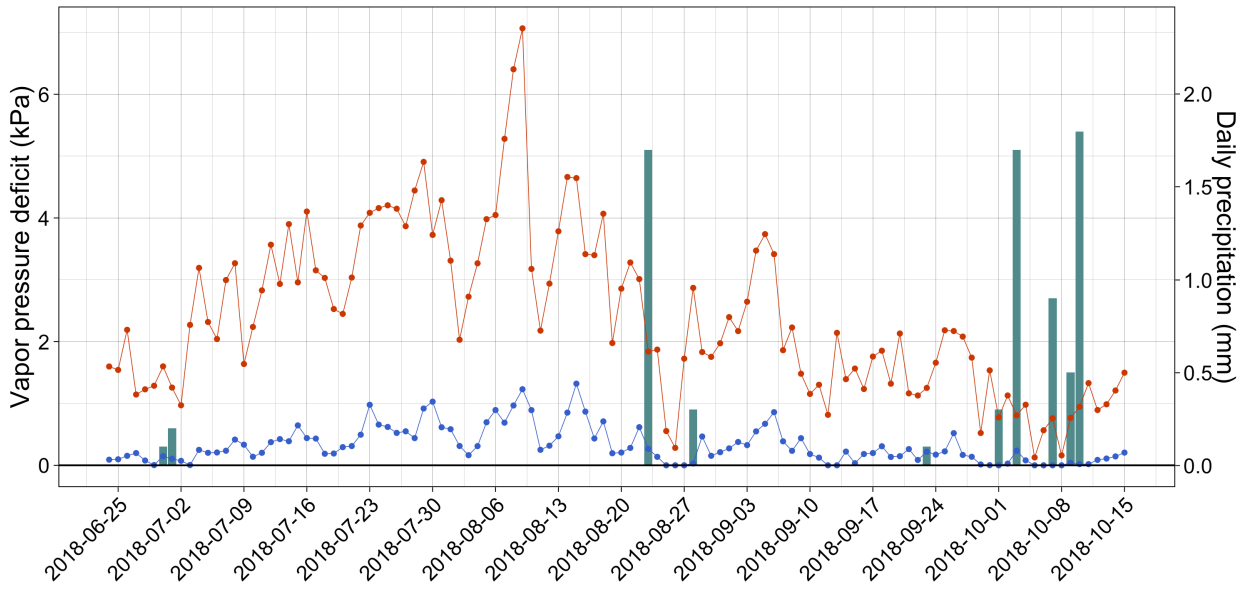


Figure 4-1. Daily minimum and maximum VPD and precipitation throughout the study period.

### 4.3.2 Water potential

Predawn leaf water potentials were not significantly different in either of the three treatments at the beginning of the study period. However, during August, the mid-density thinning treatment $\Psi_{PD}$ was significantly less negative than the low-density treatment or the control, which were not significantly different form each other over the majority of the study period (Fig. 4-2a). The $\Psi_{MD}$ for the control plots did not get more negative than -2.3 MPa, similar to pre-treatment years (Fig. 4-2b). The treated plots, however, had $\Psi_{MD}$ that were significantly more negative than the control plots for most of the study period.

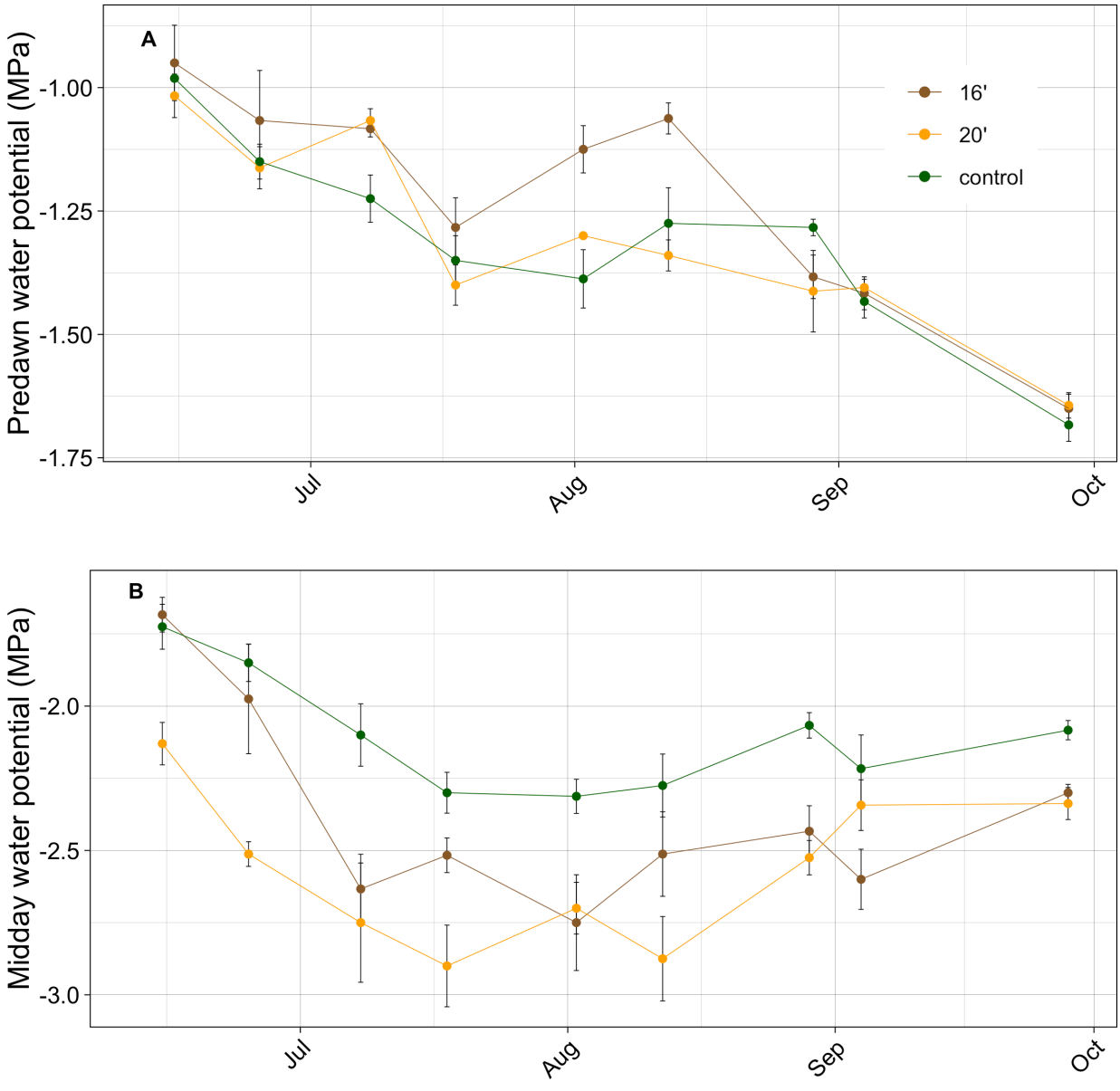


Figure 4-2. Predawn (A) and midday (B) water potentials for the treatments across the season. Error bars represent standard error. Sample size is between 3 and 7 for each point.

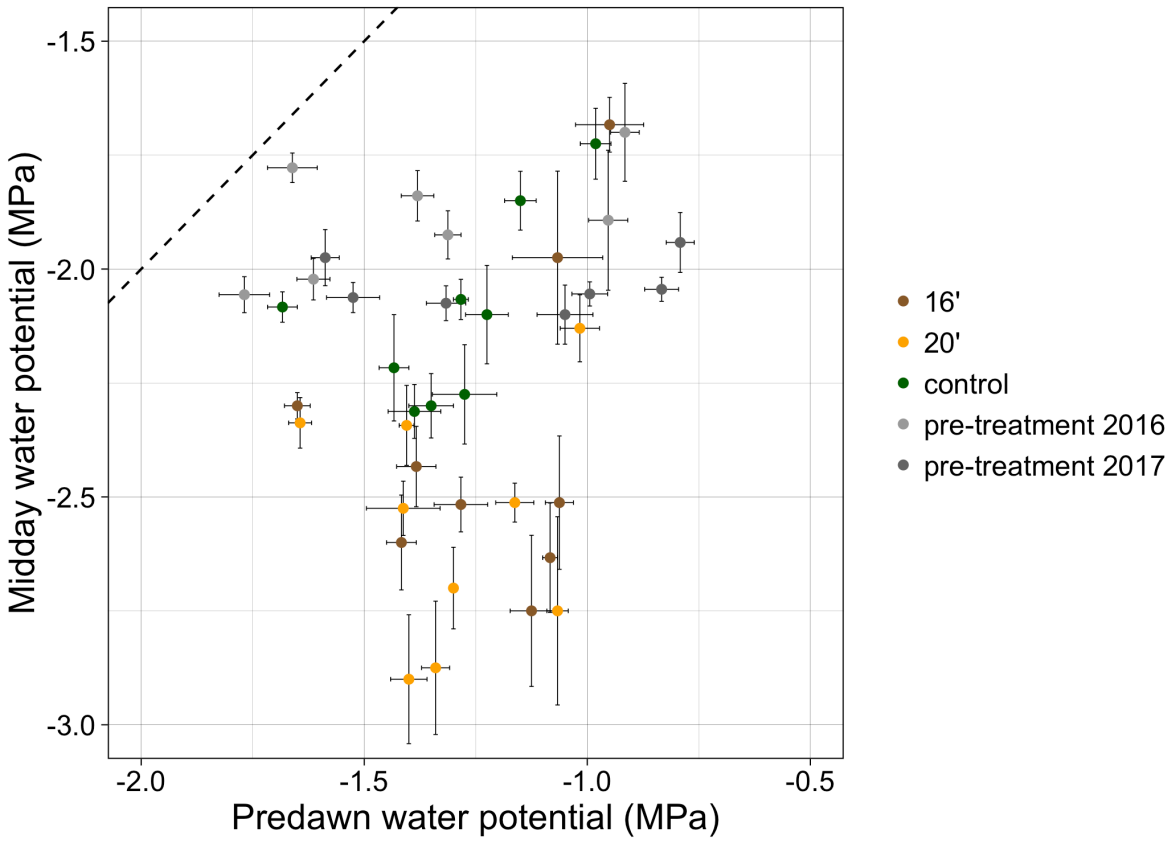


Figure 4-3. Daily means of predawn and midday water potentials. Error bars represent standard error.

### 4.3.3 Sap flux

There were only two trees in the low-density treatment that consistently recorded sap flux data through the season, so their means are not included. The mid-density treatment had six trees for which data was reliably recorded, and the control treatment had five. The control plots had significantly lower flux densities across the season (Fig. 4-4). The mid-density treatment not only had greater flux densities early in the season but also maintained greater flux densities through the later portion of the season, when the control values were close to zero.

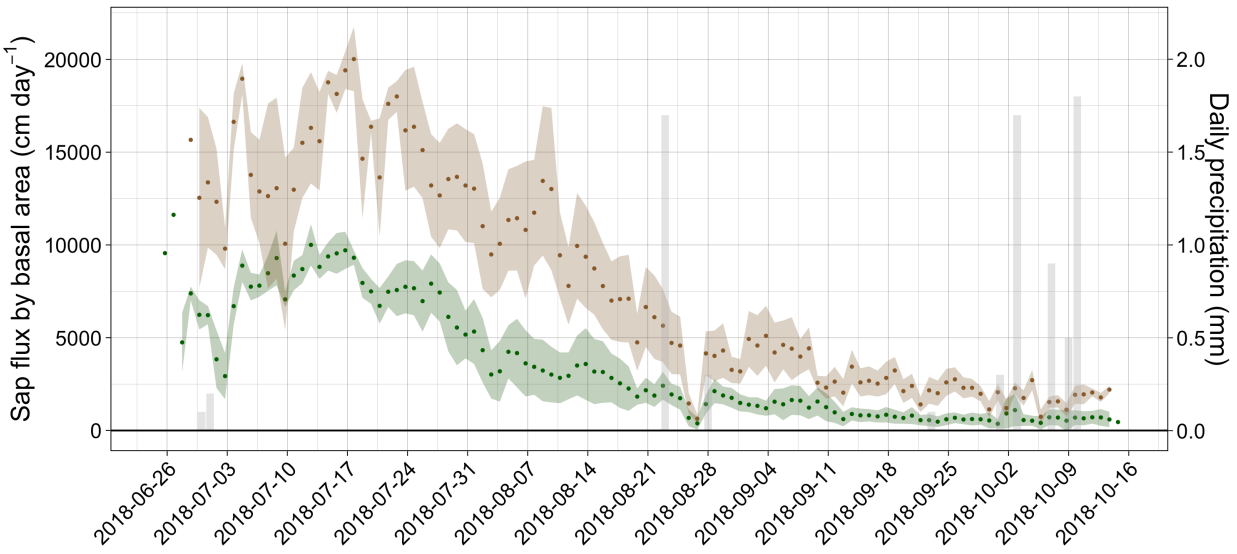


Figure 4-4. Mean sap flux density, normalized by basal area and, for trees in the control plots (green) and the mid-density plots (brown). Daily means are represented by circles, and the ribbons show the standard error for the means.

### 4.3.4 Whole-tree conductance

For the mid-density and control plots, which had sufficient sample sizes to compare, the early season conductances were not different (Fig. 4-5). Later in the season, however, the control trees' conductances were significantly reduced compared to the mid-density trees.

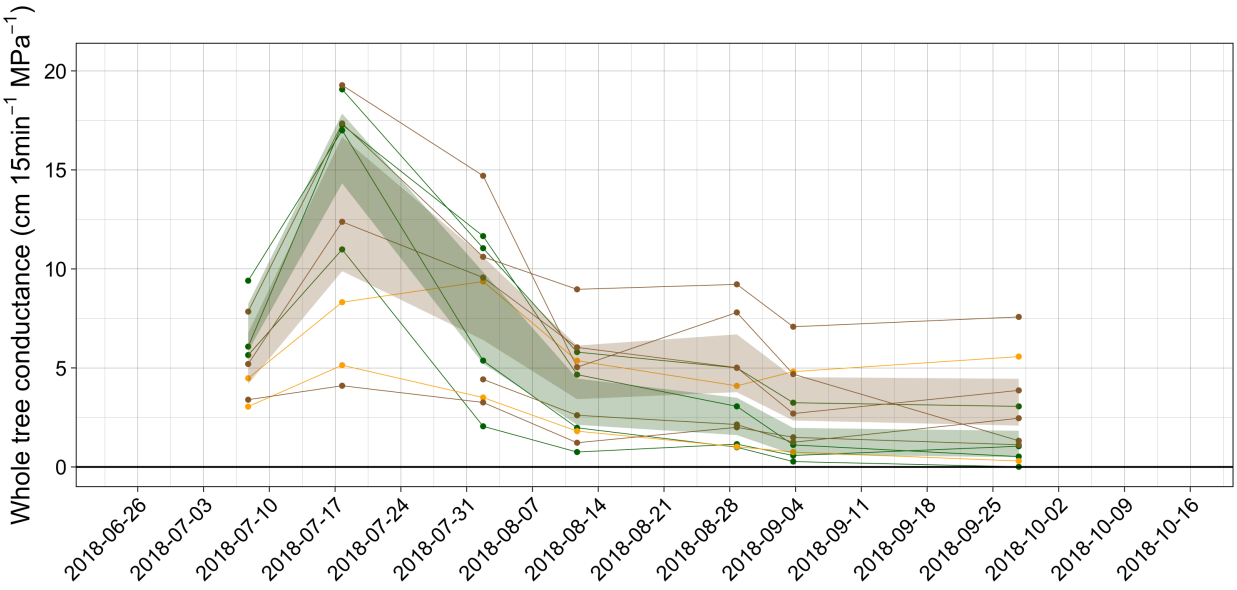


Figure 4-5. Points with lines represent each individual tree. Green represents control trees, brown is mid-density trees, and orange is low-density. Standard error for the mean whole-tree conductance values for the mid-density (brown) and control trees (green) are shown in the ribbons.

### 4.3.5 Soil water

The values of soil water content varied between sensors, with 0.10 to 0.17 as minima and 0.17 to 0.27 as maxima, based on soil and timing of logged data. To normalize the information, we looked at the difference between each day's VWC at midnight and the previous day's value. The value indicated for a day is the amount added or removed to the soil around the sensor between midnight at the beginning of that day and midnight at the end of that day. This indicates how much water was removed each day across the season, with means and standard error ranges shown in Figure 4-6. The timing of peak water extraction from the soil varied between the treatments. VWC in the control plots peaked and declined earliest in the season, and there was no difference between the two depths. The 20' treatment

also had parity between depths but with a peak extraction around two weeks later. Only the 16’ treatment showed a significant difference in VWC between the two depths, with the shallower water being extracted at a higher flux earlier in the season, then becoming similar to the deep-water extraction by the middle of August.

Peak water removal in the control plots occurred in mid-July for both sensor depths and declined to a relatively stable, low rate of removal by early August that continued for the rest of the season. The peak draw down for the low-density treatment occurred in late July with a slower rate of decrease, settling for low, steady by early September. The mid-density treatment, however, showed a disparity in the timing of peak draw down between the two sensor depths. The rate of water removal in the shallower depth was much greater and peaked in early-to-mid August. The greater depth had a more steady rate of draw down. The draw down at neither depth for the mid-density plots were reduced to the low rates seen in the controls and low-density treatment.

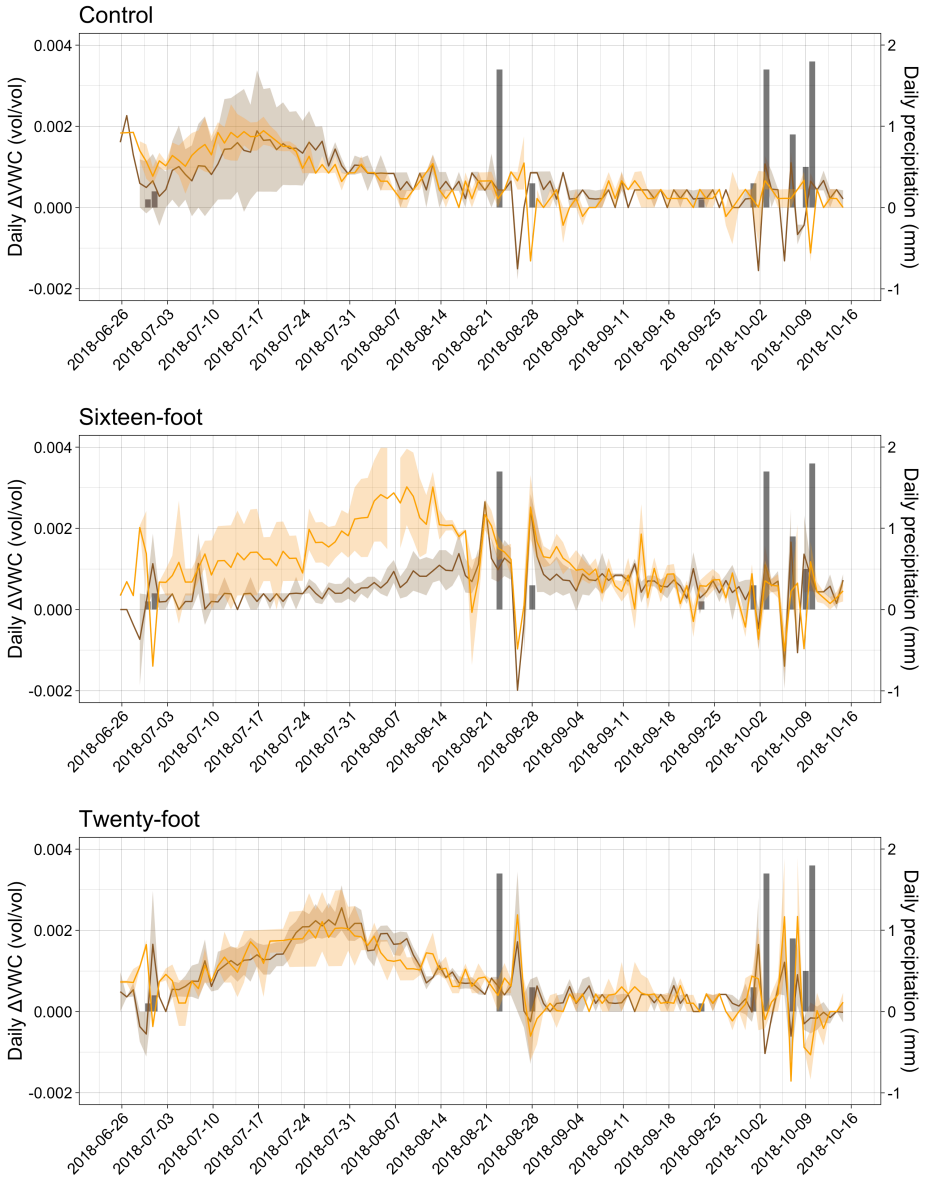


Figure 4-6. Water removed daily from the soil in volumetric water content (vol/vol) in the three treatments. Brown represents the deepest accessible soil (75 cm – 100 cm), and orange is the shallower layer (35 – 40 cm).

### 4.3.6 Diurnal sap flux

Sap flux was greater in in the thinned plots, especially later in the study period. On the July date, the control trees increase flux slowly through the morning, reaching 150

cm/15min, approximately the maximum flux that day, at about 11:30 and maintaining a similar flux until about 16:00. The treatment plots both increase their flux at greater rates through the morning, with an early peak at about 08:00. The treated plots show a periodic pulse of flux, increasing and then decreasing back down to around 150 cm/15min. For the September day, the control flux densities are very low, with two small peaks occurring in the early and mid-afternoon. The mid-density mean also shows a slower build-up to two peaks, with one occurring at about 10:30 and the second at 16:00. The low-density mean, which is a mean of two, increases more rapidly in the morning with a primary peak at about 10:00 and slowly declining through the rest of the day.

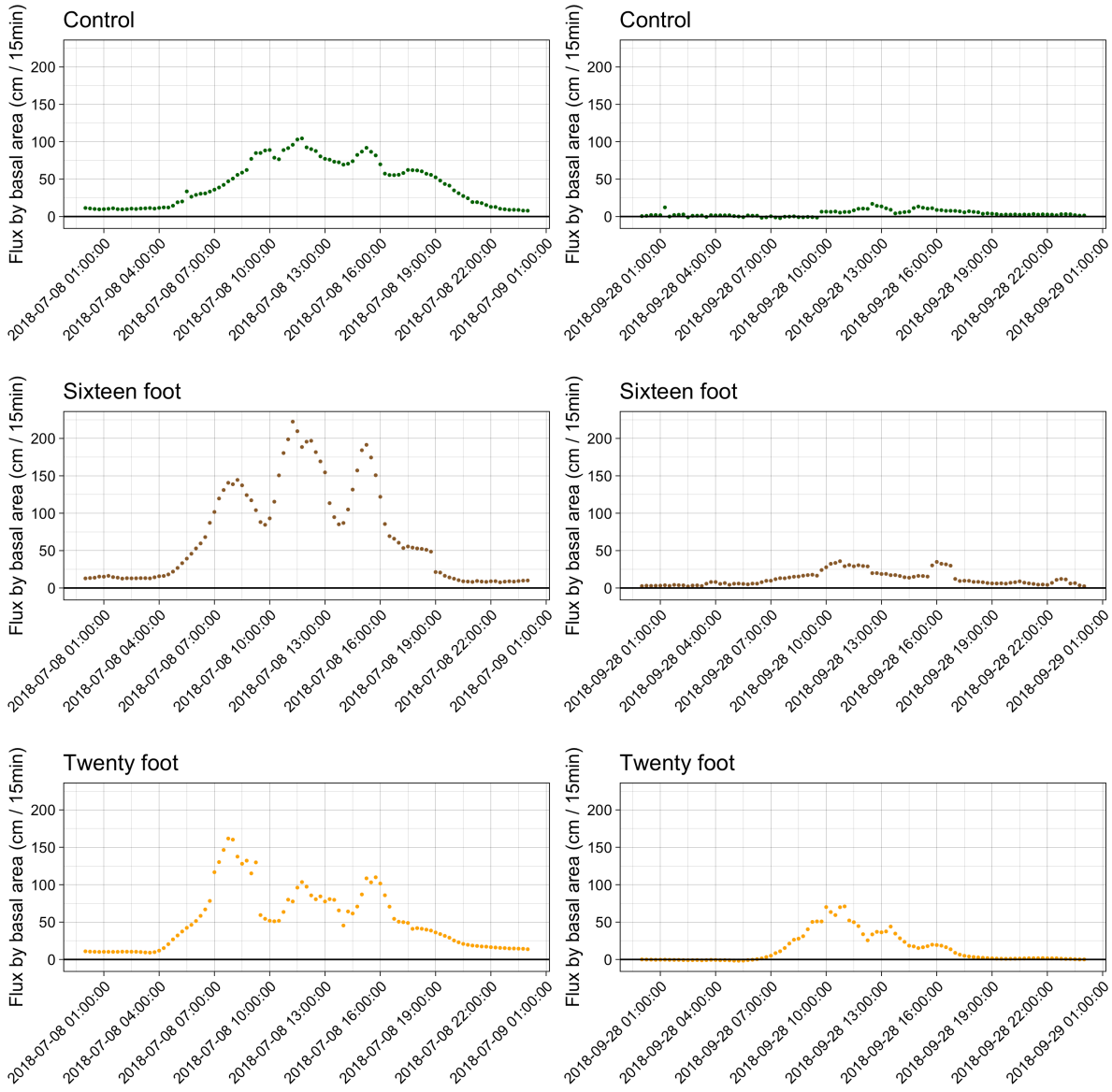


Figure 4-7. Means of flux for each treatment on a representative day in July.

## 4.4.0 Discussion

### 4.4.1 Sap flux and predawn water potentials

Our first hypothesis, that predicted that trees in thinned plots would have greater sap flux densities and less negative $\Psi_{PD}$ values was largely supported. The mid-density plots

maintained higher flux densities through the season. While $\Psi_{PD}$ values of all three densities converged by the end of the season, the treated plots, and especially the mid-density treatment, were often less negative. It is possible that because the control trees were more protected from turbulence that their $\Psi_{PD}$ values would be a better estimate of the soil water potential around their active roots than those of the treated plots. If that were the case, then the $\Psi_{PD}$ values from the treated plots would be more depressed, relative to the soil water potential near their roots.

### 4.4.2 Thinning effects on midday leaf water potential

Few of the previous forest thinning studies have reported leaf water potential values, and we are aware of only six that report $\Psi_{PD}$ values (Donner and Waring 1986, Rodriguez-Calcerrada *et al*. 2011, also see Table 1 in Sohn *et al.* 2016). Of those papers that did include $\Psi_{PD}$ values, most of the treated forests were angiosperm-dominated (Moreno and Cubera 2008, Stoneman *et al.* 1996). Other studies on gymnosperms did not see depressed $\Psi_{PD}$ values in thinned plots, potentially because the thinning had taken place 4 to 32 years decades prior to the study period (Schmid *et al.* 1991, Feeney *et al.* 1998, Kolb *et al.* 1998). Only Brix and Mitchell (1986) reported more negative $\Psi_{PD}$ values in treated plots of *Pseudotsuga menziesii*. They attributed those results to the increased solar radiation incident on the individual trees. The uniformity of our site, prior to treatments, may have made it easier to parse out differences in water potentials between treatments. Where other projects contend with various aspects, incident light, and other environmental conditions, ours had less variability other than the treatments.

It is possible that increased PAR incident on a tree's canopy may trigger a process that maintains higher stomatal conductance through more negative water potentials. A question this raises is whether the trees are isohydrodynamic, with the more negative $\Psi_{MD}$ being an adaptation facilitated by leaf osmotica, for instance (Franks *et al.* 2007)? Or, do the tree leaf hydraulic parameters remain the same, with the water potentials decreasing to a point that would severely affect the leaf hydraulic conductivity?

Another potential explanation is the effect that reducing canopy density has on the energy balance of stand. Erdoğan *et al.* (2018) saw an increase in both mean and maximum monthly air temperature in thinned plots of an oak-dominated forest. Qualitatively, we noticed higher temperatures and also much greater wind turbulence in the thinned plots and particularly the heavily thinned plots (Baker, unpublished data). A higher VPD and smaller boundary layer around each tree's canopy could drive higher fluxes. This is supported by the sap flux data, where the fluxes were greater in the thinned plots (Fig. 4-7).

### 4.4.3 Daily flux patterns

There were differences in daily sap flux patterns throughout the day in the three treatments (Fig. 4-7). The thinned plots had higher peak fluxes in the early season, with the "saddles" between peaks returning down to the standard control flux density on both dates pictured. The $\Psi_{PD}$ values, sampled at around 13:00, may have been coincident with a time of high flux that would require a high water potential gradient. The diurnal change in $\Psi_L$ ($\Psi_{PD} - \Psi_{MD}$) was between 1.5 and 1.7 MPa for the treated plots and 0.9 MPa for the control plots. On the second day shown, September 28$^{th}$, the diurnal change in $\Psi_L$ was 0.7 MPa for both treatments and 0.4 MPa for the control plot.

### 4.4.4 Soil moisture

Our third hypothesis, that a) control plots would draw down soil water earlier in the season and then reduce the rate of water removal and that b) the thinned plots would continue with a higher rate of draw down later into the season, was generally supported by the results. However, the mid-density thinning continued to draw down soil water later than the low-density thinning, which we did not expect. There may be an interaction effect in the mid-density treatment, where stand transpiration is reduced enough to maintain soil water later into the season but where the energy balance of the stand is not altered sufficiently to draw out the soil water earlier.

Another interesting aspect of the soil data is the recharge that occurs soon after the meager rainfall, particularly in August (1.77 mm). Considering how small the precipitation events were, it is unlikely for the water to have percolated through 35 – 45 cm of soil to the shallow sensors and certainly not 75 – 100 cm to the deeper sensors. Some projects have established the ability of conifer leaves to absorb rainfall into the tree, incorporating the water into the sap (Berry *et al.* 2014, 2018). It is possible, then, for the tree to move water down into the soil. Sap flux data from the previous chapter show two out of three trees with negative flow occurring in the upper bole during the first rainfall and high humidity events of 2017. This is not visible in the branch data, but they were, at the highest, halfway up the canopy and may not have been the site of absorption.

Another potential explanation for the recharge that occurs in late August is that the source water comes from a greater depth via hydraulic redistribution (HR). HR has been documented in *P. ponderosa* in Oregon (Brooks *et al*. 2002, Warren *et al.* 2011). The high VPDs that are common at this site during the growing season likely suppressed HR because

the water would move up through the tree via nighttime transpiration and/or capacitive recharge. However, the nighttime VPD August 26$^{th}$ – 28$^{th}$ was consistently 0 kPa, which had not occurred since mid-June. It is possible that, while the sap flux was suppressed by the low VPD's, water would move up from a depth beyond the 100 cm scope of our data. In the absence of a water potential gradient going up the tree, the deep soil water could recharge both the soil around the shallower roots via hydraulic redistribution.

An unexplored question about the underground dynamics is the potential for hydraulic redistribution to occur in the roots of trees that were harvested. It is commonly acknowledged that the trees require several years to expand their root system to access the soil previously occupied by their fallen neighbors. However, if the remaining roots are intact, could they move water passively and redistribute it before decomposing?

### 4.5.0 References

Aussenac, G., and A. Granier. 1988. Effects of thinning on water stress and growth in Douglas-fir. Canadian Journal of Forest Research 18:100–105.

Carter Berry, Z., and W. K. Smith. 2014. Experimental cloud immersion and foliar water uptake in saplings of Abies fraseri and Picea rubens. Trees - Structure and Function 28:115–123.

Berry, Z. C., N. C. Emery, S. G. Gotsch, and G. R. Goldsmith. 2019. Foliar water uptake: Processes, pathways, and integration into plant water budgets. Plant Cell and Environment 42:410–423.

Brang, P., P. Spathelf, J. B. Larsen, J. Bauhus, A. Bončína, C. Chauvin, L. Drössler, C. García-Güemes, C. Heiri, G. Kerr, M. J. Lexer, B. Mason, F. Mohren, U. Mühlethaler, S. Nocentini, and M. Svoboda. 2014. Suitability of close-to-nature silviculture for adapting temperate European forests to climate change. Forestry 87:492–503.

Bréda, N., G. Aussenac, and A. Granier. 1995. Effects of thinning on water stress and growth in Douglas-fir. Tree physiology 15:295–306.

Brix, H., and A. K. Mitchell. 1986. Thinning and nitrogen fertilization effects on soil and tree water stress in a Douglas-fir stand. Canadian Journal of Forest Research 16:1334–1338.

Brooks, J. R., F. C. Meinzer, R. O. B. Coulombe, and J. Gregg. 2002. Hydraulic redistribution of soil water during summer drought in two contrasting Pacific Northwest coniferous forests. Tree physiology 22:1107–1117.

Burgess, S. S. O., M. A. Adams, N. C. Turner, C. R. Beverly, C. K. Ong, A. A. H. Khan, and T. M. Bleby. 2001. An improved heat pulse method to measure low and reverse rates of sap flow in woody plants. Tree Physiology 21:589–598.

Cardil, A., J. B. Imbert, J. J. Camarero, I. Primicia, and F. Castillo. 2018. Temporal interactions among throughfall, type of canopy and thinning drive radial growth in an Iberian mixed pine-beech forest. Agricultural and Forest Meteorology 252:62–74.

Chmura, D. J., P. D. Anderson, G. T. Howe, C. A. Harrington, J. E. Halofsky, D. L. Peterson, D. C. Shaw, and J. Brad St.Clair. 2011. Forest responses to climate change in the northwestern United States: Ecophysiological foundations for adaptive management. Forest Ecology and Management 261:1121–1142.

del Campo, A. D., M. González-Sanchis, A. J. Molina, A. García-Prats, C. J. Ceacero, and I. Bautista. 2019. Effectiveness of water-oriented thinning in two semiarid forests: The

redistribution of increased net rainfall into soil water, drainage and runoff. Forest Ecology and Management 438:163–175.

Donner, B. L., and S. W. Running. 1986. Water stress response after thinning Pinus contorta stands in Montana. Forest Science 32:614–625.

Erdoğan, B. U., F. Gökbulak, Y. Serengil, İ. Yurtseven, and M. S. Özçelik. 2018. Changes in selected physical water quality characteristics after thinning in a forested watershed. Catena 166:220–228.

Feeney, S. R., T. E. Kolb, W. W. Covington, and M. R. Wagner. 1998. Influence of thinning and burning restoration treatments on presettlement ponderosa pines at the Gus Pearson Natural Area. Canadian Journal of Forest Research 28:1295–1306.

Franks, P. J., P. L. Drake, and R. H. Froend. 2007. Anisohydric but isohydrodynamic: Seasonally constant plant water potential gradient explained by a stomatal control mechanism incorporating variable plant hydraulic conductance. Plant, Cell and Environment 30:19–30.

Gonsalves, L., B. Law, T. Brassil, C. Waters, I. Toole, and P. Tap. 2018. Ecological outcomes for multiple taxa from silvicultural thinning of regrowth forest. Forest Ecology and Management 425:177–188.

Kavanagh, K. L., R. Pangle, and A. D. Schotzko. 2007. Nocturnal transpiration causing disequilibrium between soil and stem predawn water potential in mixed conifer forests of Idaho. Tree physiology 27:621–629.

Kolb, T. E., K. M. Holmberg, M. R. Wagner, and J. E. Stone. 1998. Regulation of ponderosa pine foliar physiology and insect resistance mechanisms by basal area treatments. Tree Physiology 18:375–381.

Lasch, P., M. Lindner, M. Erhard, F. Suckow, and A. Wenzel. 2002. Regional impact assessment on forest structure and functions under climate change - The Brandenburg case study. Forest Ecology and Management 162:73–86.

Lindner, M., P. Lasch, and M. Erhard. 2000. Alternative forest management strategies under climatic change - prospects for gap model applications in risk analyses. In: Special issue: Forestry scenario modelling in risk analysis and management. Selected papers from a meeting held in Joensuu, Finland. Silva Fennica 34:101–111.

McDowell, N., W. T. Pockman, C. D. Allen, D. D. Breshears, N. Cobb, T. Kolb, J. Plaut, J. Sperry, A. West, D. G. Williams, and E. A. Yepez. 2008. Mechanisms of plant survival and mortality during drought: Why do some plants survive while others succumb plants drought? New Phytologist 178:719–739.

Moreno, G., and E. Cubera. 2008. Impact of stand density on water status and leaf gas exchange in Quercus ilex. Forest Ecology and Management 254:74–84.

Navarro-Cerrillo, R. M., R. Sánchez-Salguero, C. Rodriguez, J. Duque Lazo, J. M. Moreno-Rojas, G. Palacios-Rodriguez, and J. J. Camarero. 2019. Is thinning an alternative when trees could die in response to drought? The case of planted Pinus nigra and P. Sylvestris stands in southern Spain. Forest Ecology and Management 433:313–324.

Park, J., T. Kim, M. Moon, S. Cho, D. Ryu, and H. Seok Kim. 2018. Effects of thinning intensities on tree water use, growth, and resultant water use efficiency of 50-year-old Pinus koraiensis forest over four years. Forest Ecology and Management 408:121–128.

Rodríguez-Calcerrada, J., I. M. Pérez-Ramos, J. M. Ourcival, J. M. Limousin, R. Joffre, and S. Rambal. 2011. Is selective thinning an adequate practice for adapting Quercus ilex coppices to climate change? Annals of Forest Science 68:575–585.

Schmid, J. M., S. A. Mata, R. K. Watkins, and M. R. Kaufmann. 1991. Water potential in ponderosa pine stands of different growing-stock levels. Canadian Journal of Forest Research 21:750–755.

Scholander, P., H. Hammel, E. Bradstreet, and E. Hemmingsen. 1965. Sap Pressure in Vascular Plants. Science 148:339–346.

Simonin, K., T. E. Kolb, M. Montes-Helu, and G. W. Koch. 2006. Restoration thinning and influence of tree size and leaf area to sapwood area ratio on water relations of Pinus ponderosa. Tree Physiology 26:493–503.

Sohn, J. A., S. Saha, and J. Bauhus. 2016. Potential of forest thinning to mitigate drought stress: A meta-analysis. Forest Ecology and Management 380:261–273.

Spittlehouse, D. L., and R. B. Stewart. 2003. Adaptation to climate change in forest management. Journal of Ecosystems and Management Adaptation 4:1–11.

Stednick, J. D. 1996. Monitoring the effects of timber harvest on water yield. Journal of Hydrology 176:79–95.

Stoneman, G. L., D. S. Crombie, K. Whitford, F. J. Hingston, R. Giles, C. C. Portlock, J. H. Galbraith, and G. M. Dimmock. 1997. Growth and water relations of Eucalyptus marginata (Jarrah) stands in response to thinning and fertilization. Tree Physiology 17:267–274.

Warren, J. M., J. R. Brooks, M. I. Dragila, and F. C. Meinzer. 2011. In situ separation of root hydraulic redistribution of soil water from liquid and vapor transport. Oecologia 166:899–911.

# Chapter 5: Conclusions

## 5.1.0 Conclusions

A living evergreen conifer tree changes very little on a scale that humans register aesthetically. With their subtle phenological changes and ubiquity in the West, conifers give the impression of a constancy of behavior as well as appearance. When an epidemic, fire or beetle, induces a visibly material shift, it can capture popular interest. At more stable times, the trees are relegated to a passively verdant backdrop. Such an illusion is exposed by more concentrated scrutiny. Indifferent to human attention, these forests operate with a dynamism that has allowed them to adapt and persist through nearly 400 million years of environmental disequilibrium. Some daily and certainly seasonal variations of conditions a tree experiences are as great as those that its progenitors experienced on a geological timescale, and the means by which they do so remain a relative mystery.

With water as the currency with which trees pay for carbon, forests in the West operate at the margins of solvency. The desperation of their status oscillates with the abundance of precipitation, the demand of the vapor pressure deficit, and the duration of both. While the change in access to vs. demand for water is changing at a greater-than-geological pace, we can see some species and communities struggle or fail to survive (e.g. Fig. 2 in Hartmann *et al.* 2018). Under drought and high temperatures, forests are not only more susceptible to pathogens, pests, and wildfire but can also succumb to water stress, independent of other disturbing protagonists (Hoffmann *et al.* 2011, McDowell *et al.* 2011). This necessitates our ability to predict how particular species will respond to varied conditions. Trees' responses to stressful or bounteous conditions differ in ways we do not

understand. For instance, in a matter of a month, the evident daily flux of water transpired through *P. ponderosa* trees was reduced to less than 10% of their previous flux. What triggers that regulation and how to predict those conditions remotely are questions we must continue to address.

While multitude questions are raised by the projects described in this dissertation, we have managed to address some previous gaps in our knowledge. The conifers we studied in Chapter 2, presumed to be representative of their species in similar soils, were able to continue photosynthesizing through high evaporative demand when soil water was abundant (less negative predawn water potentials). But they were then also able to reduce their stomatal conductance at times when predawn water potentials were less negative, despite similar midday water potentials through both sub-seasons. While the impetus for this shift may be a declining soil water potential, the mechanism by which the trees respond to it is elusive.

Our data in Chapter 3 echo the shift from great to lesser water use as drought continued in a more mature *P. ponderosa* stand only a mile away. Overall water flux was much less later in the season, and nighttime transpiration appeared to halt altogether. While currently outside the scope of that project, we suspect an aboveground culprit for that adjustment to be a decline of leaf hydraulic conductance at water potentials similar to the nighttime water potentials recorded during the absence of nighttime transpiration. Altogether, that project indicates that *P. ponderosa* operates remarkably near hydraulic failure. Well within the scope of the project, it appears that the vulnerable root xylem is largely responsible for the reduction in whole-tree hydraulic conductance. Combining root vulnerability with the phenomenon of the shallower, more densely-rooted, soil drying earlier,

belowground loss of conductance can easily account for the reduction of whole-tree hydraulic conductance.

If both of these perceptions are true, that there is hydraulic failure occurring at both the roots and the leaves, then these terminal organs could very well be preserving the integrity of the rest of the tree. The bole and branches are much more energetically expensive to replace and are safely resilient to embolisms at water potentials that seem to induce failure elsewhere (Zimmerman 1983, Tyree & Ewers 1991). As the conductivity of the roots is depressed by embolism, the leaf water potentials cannot recover to values less negative than their threshold for unhampered conductivity. With that lack of conductive leaf xylem, the whole-tree transpiration is reduced, preventing further decline in soil and tree water potential.

This brings to relevance the commonness of branch $P_{50}$ values being used as a proxy for whole-tree vulnerability to embolism in ecosystem models. The xylem of our trees' branches were consistently the least vulnerable organ measured. If instances such as these, where they are not the most likely organism to see its conductivity reduced, then branches are not a sufficient proxy for the wood of a plant. Across our species, there was not even a predictive relationship between branch and root vulnerability that could lend branch $P_{50}$ values post hoc utility. To assess a tree's vulnerability to embolism, both root vulnerability and soil composition and depth must be taken into account.

Even with the intricate strategies they have to avoid drought stress, it can be useful to thin a forest to open up resources such as light and soil water, thereby encouraging survival and growth. From our results, it appeared that the 16' density thinning treatment was the most effective at enabling the trees to have greater access to water, one year after the stands were thinned. They then moved more water, by basal area, than either the controls or the 20'

spacing, which may have experienced a “thinning shock” due to the intense shift in light, water, and wind conditions. Whether a 16’ treatment is the best way to manage *P. ponderosa* in this region is not fully answerable by our data. Hydraulically speaking, the intermediate thin appeared to have assuaged stress while still providing room for tree growth.

The most encouraging impression that our data gives is that of the resilience of trees to continue functioning through high evaporative demand when a hydraulic buffer is available to them. For these trees, the buffer was a deep soil with the capacity to hold huge amounts of water. For some systems, that buffer is a snowpack, consistent afternoon rainfall, morning dewfall, or a monsoon season. Compared to other systems’ buffers, the deep ash-capped loams in the Inland Northwest are likely to persist as a water source for these forests, allowing them to be resilient to climate change.

### 5.2.0 References

Hartmann, H., C. F. Moura, W. R. L. Anderegg, N. K. Ruehr, Y. Salmon, C. D. Allen, S. K. Arndt, D. D. Breshears, H. Davi, D. Galbraith, K. X. Ruthrof, J. Wunder, H. D. Adams, J. Bloemen, M. Cailleret, R. Cobb, A. Gessler, T. E. E. Grams, S. Jansen, M. Kautz, F. Lloret, and M. O'Brien. 2018. Research frontiers for improving our understanding of drought-induced tree and forest mortality. New Phytologist 218:15–28.

Hoffmann, W. A., R. M. Marchin, P. Abit, and O. L. Lau. 2011. Hydraulic failure and tree dieback are associated with high wood density in a temperate forest under extreme drought. Global Change Biology 17:2731–2742.

McDowell, N. G., D. J. Beerling, D. D. Breshears, R. A. Fisher, K. F. Raffa, and M. Stitt. 2011. The interdependence of mechanisms underlying climate-driven vegetation mortality. Trends in Ecology and Evolution 26:523–532.

Tyree, M. T., and F. W. Ewers. 1991. The hydraulic architecture of trees and other woody plants. New Phytologist 119:345–360.

Zimmerman, M. 1983. Xylem Structure and the Ascent of Sap. Page (T. E. Timell, Ed.). 1st edition. Springer, Berlin Heidelberg.

# Appendix A: Supplemental Figures for Chapter 2

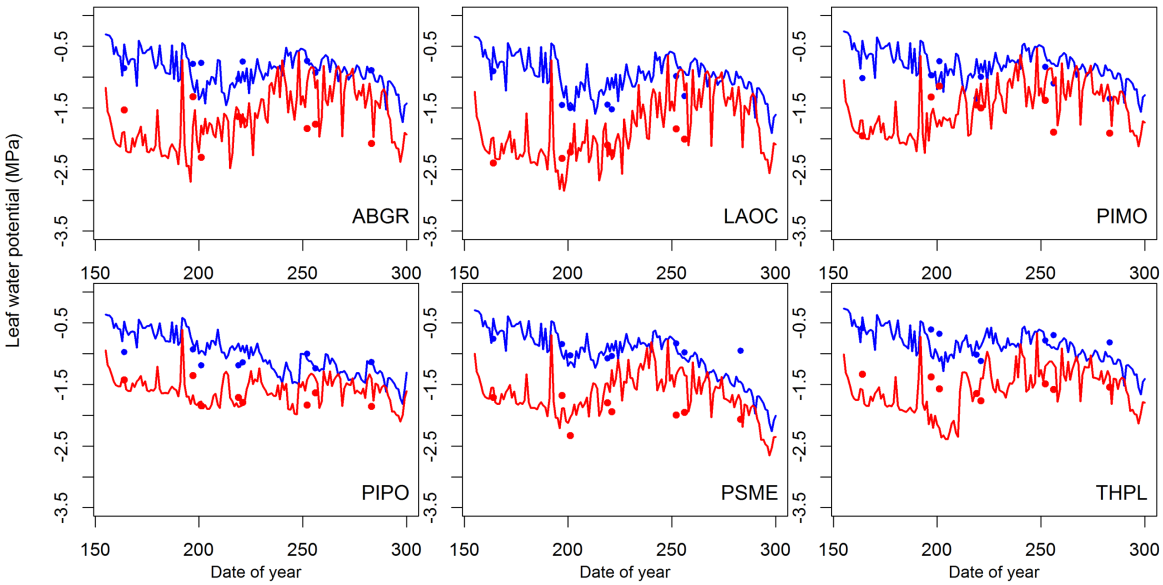


Supplemental Figure 2-1. Predicted (lines) and observed (dots) $\Psi_{PD}$ and $\Psi_{MD}$ over the course of growing season in year 2015. Red colors represent midday (12:00-14:00), and blue colors represent predawn (4:00-6:00).

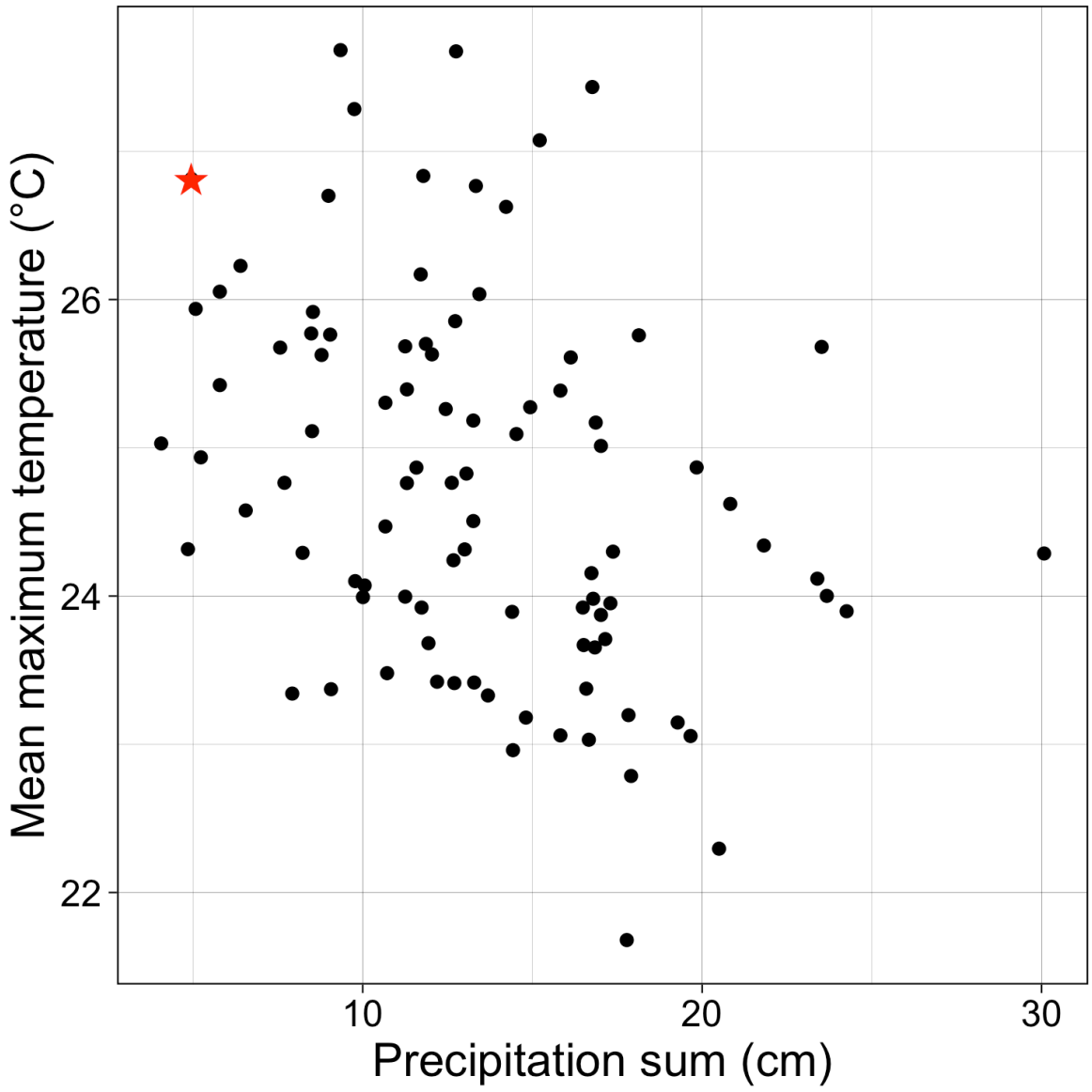


Supplemental Figure 2-2. Weather data from a long-term NOAA meteorological station in Potlatch, ID. The red star represents the year of 2015. Data is from the Julian days of the study period in 2015 for each year.

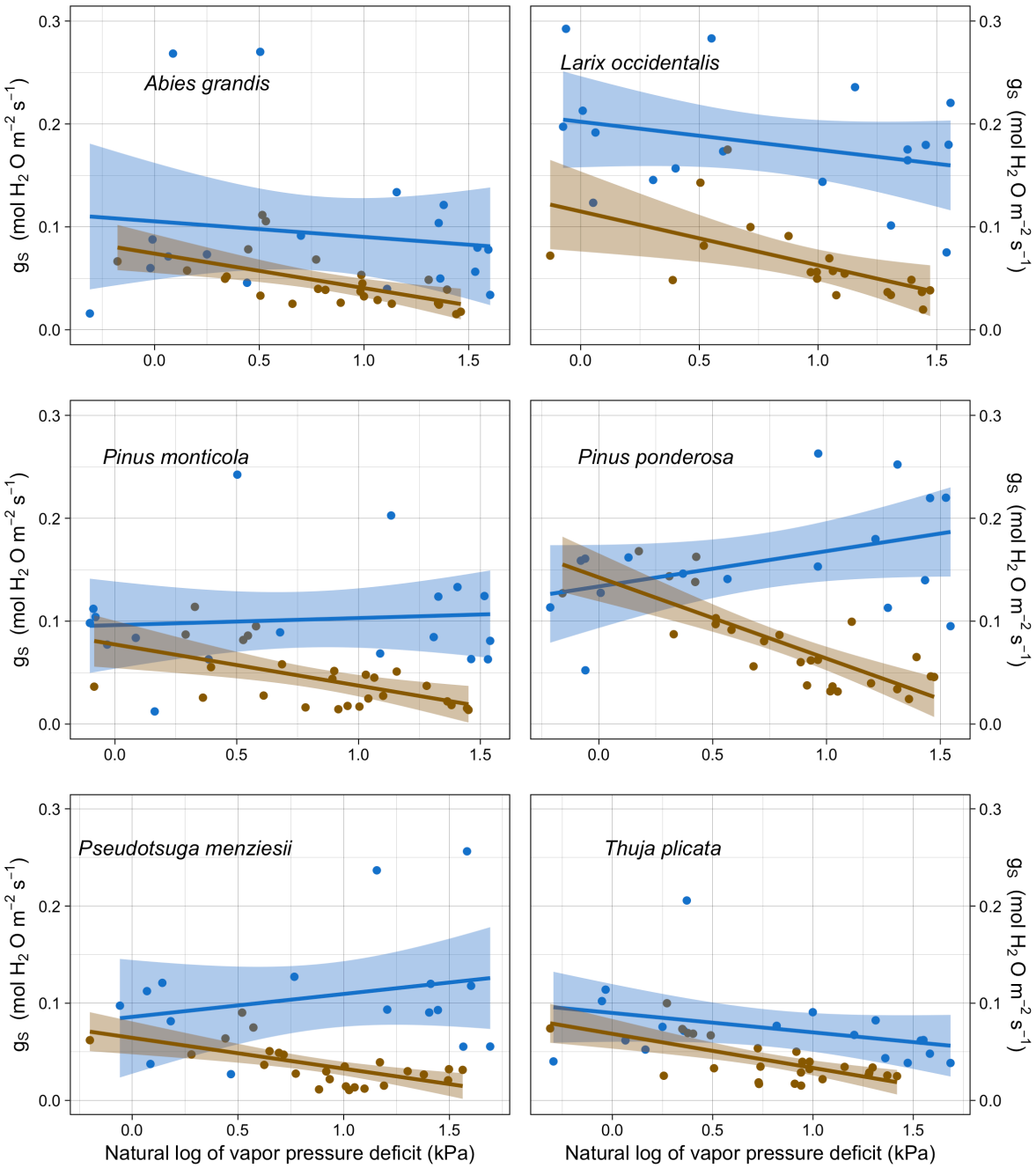


Supplemental Figure 2-3. Blue dots and lines represent wet sub-season data, and brown dots and lines are dry sub-season data. Each data point represents the mean values of 3-4 trees on the same day.

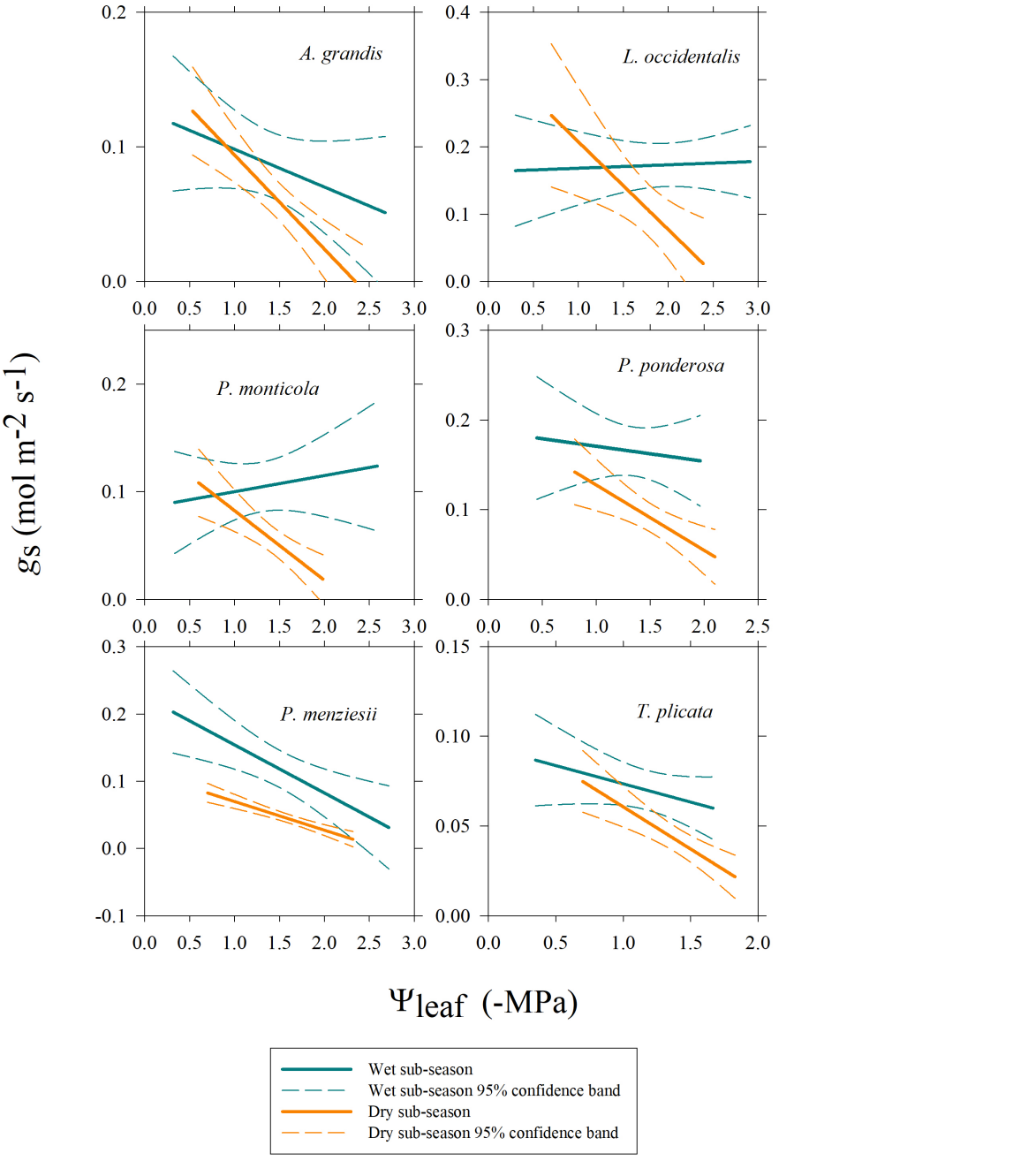


Supplemental Figure 2-4. Blue lines represent wet sub-season data, and orange lines are dry sub-season data. *L. occidentalis* and *P. monticola* have significantly different slopes between the dry and wet seasons ($\alpha = 0.05$). *A. grandis*, *P. ponderosa*, *P. menziesii*, and *T. plicata* have slopes that are not significantly different from each other. Data points represent hourly means of 3-4 trees.

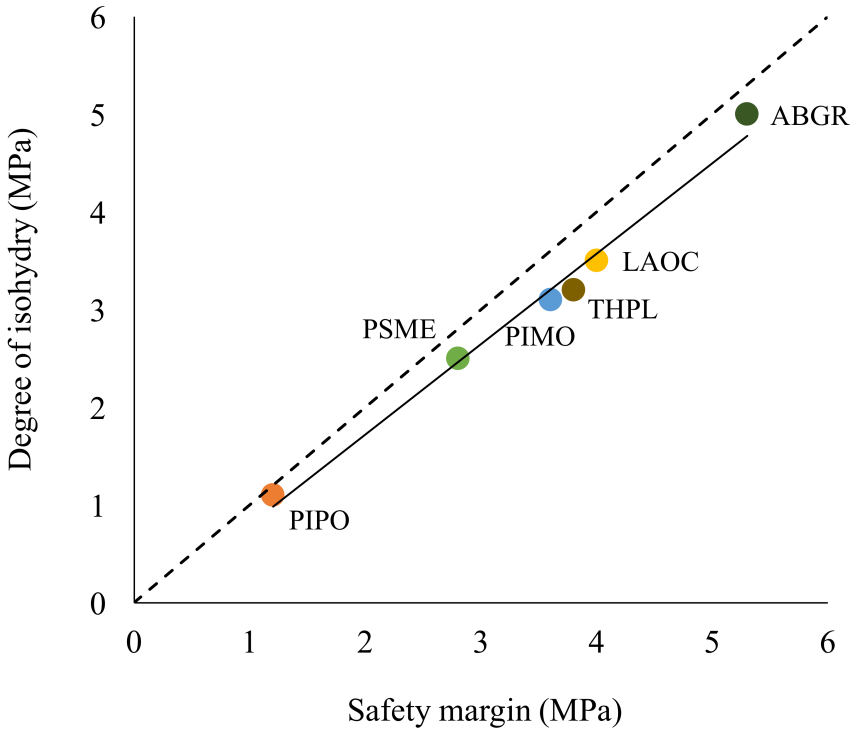


Supplemental Figure 2-5. Y-axis is degree of isohydry, defined as $P_{g12} - P_{50}$; x-axis is safety margin, $\Psi_{MIN} - P_{50}$, as described in Skelton *et al*. (2015). $P_{g12}$ is the $\Psi_L$ at which the $g_S$ is 12% of $g_{S\text{-}MAX}$. $\Psi_{MIN}$ is the most negative $\Psi_L$ observed. $R^2$=0.986. Dashed line is 1:1.

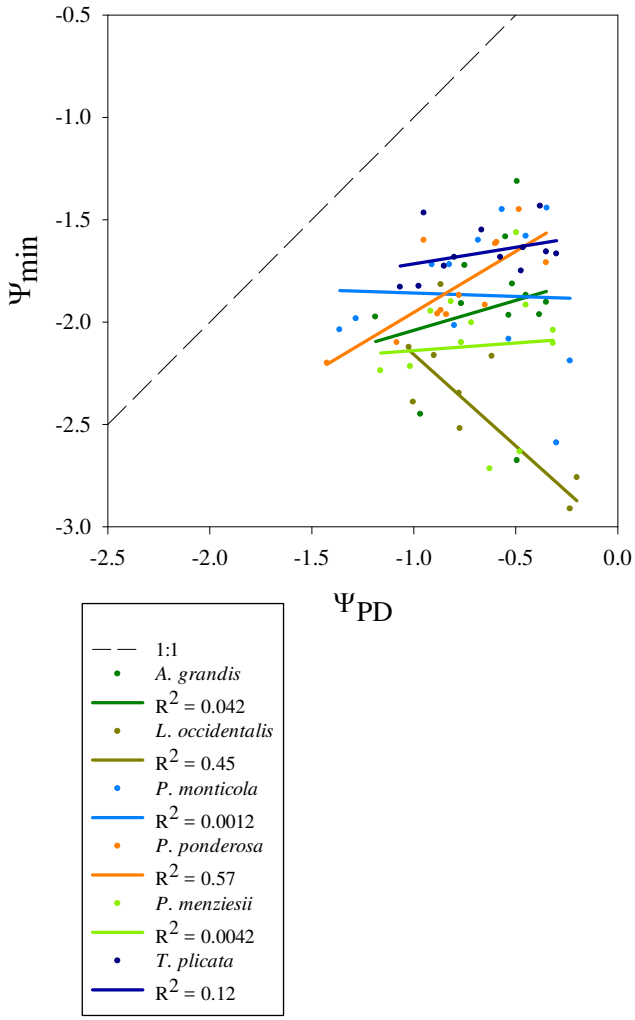


Supplemental Figure 2-6. Each data point represents the mean values of 3-4 trees on the same day. $R^2$ values are listed in legend.

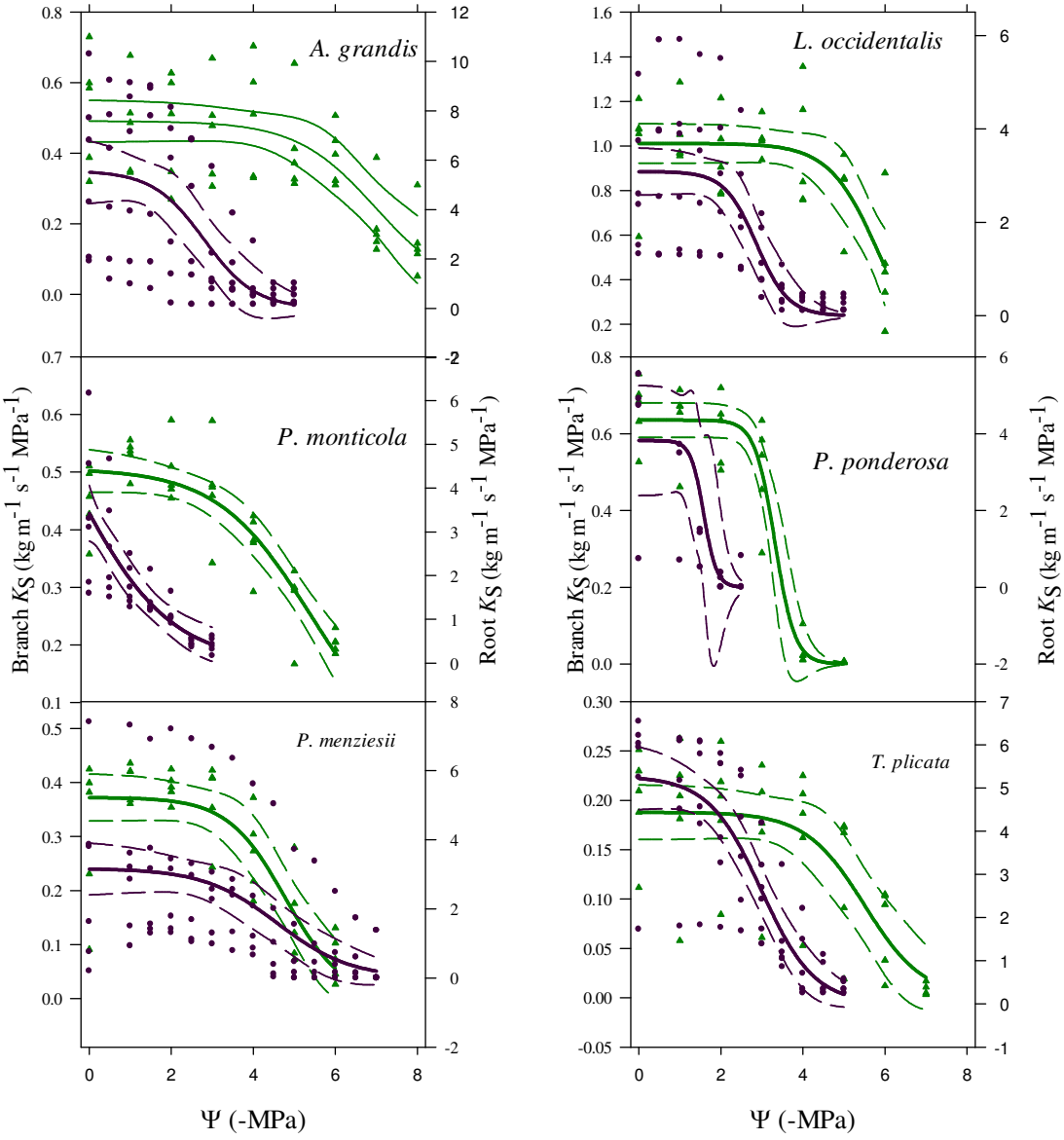


Supplemental Figure 2-7. Data points represent the $K_S$ of a single branch (green triangle) or root (purple circle).

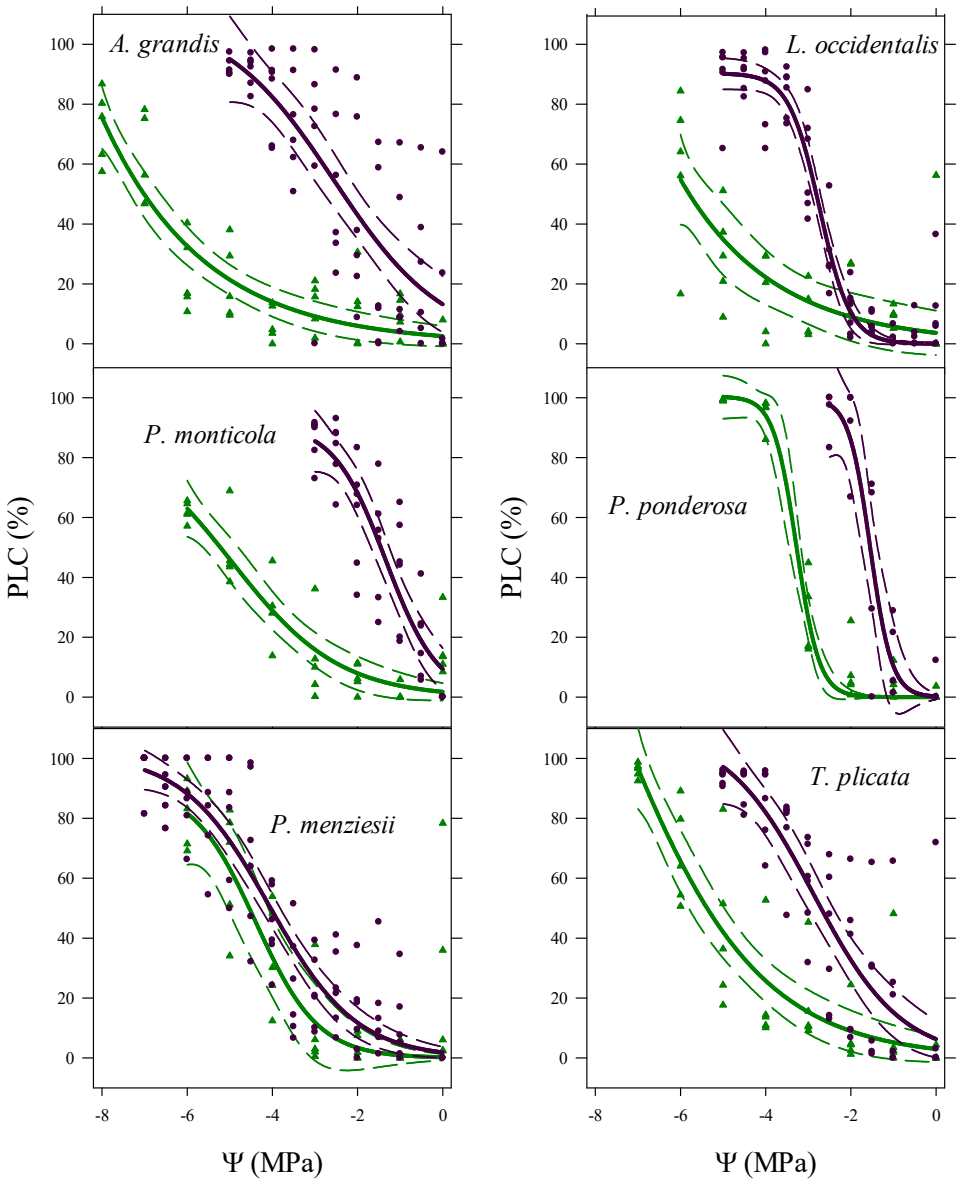


Supplemental Figure 2-8. Data points represent percent loss of conductivity of a single branch (green triangle) or root (purple circle).

# Appendix B: Supplemental Table for Chapter 2

| | model | ln(gs)=a+b*ln(VPD) | | ln(gs)=a+b*$\|\Psi_{leaf}\|$ | | ln(gs) =a+b*$\|\Psi_{leaf}\|$+c*ln(VPD)+d*($\|\Psi_{leaf}\|$:ln(VPD) | | | | ln(gs) =a+b*$\|\Psi_{PD}\|$+c*ln(VPD)+d*($\|\Psi_{PD}\|$:ln(VPD)) | | | |
|---|---|---|---|---|---|---|---|---|---|---|---|---|---|
| | species | b | adjusted $R^2$ | b | adjusted $R^2$ | b | c | d | adjusted $R^2$ | b | c | d | adjusted $R^2$ |
| Wet and dry sub-seasons, averaged within days | ABGR | -0.499 | 0.161 | -0.687 | 0.284 | -0.673 | | | 0.266 | | | | 0.472 |
| | LAOC | -0.688 | 0.240 | | 0.036 | | | | 0.220 | -2.413 | -0.984 | | 0.736 |
| | PIMO | -0.417 | 0.065 | -0.609 | 0.095 | -1.100 | -1.387 | | 0.156 | | | -1.910 | 0.512 |
| | PIPO | -0.440 | 0.117 | -0.861 | 0.197 | | | | 0.194 | | 1.032 | -2.067 | 0.465 |
| | PSME | | -0.012 | -0.767 | 0.175 | -1.349 | | | 0.204 | | 1.710 | -3.026 | 0.272 |
| | THPL | -0.374 | 0.106 | -0.891 | 0.340 | -0.646 | | | 0.332 | | | | 0.282 |
| Wet sub-season, averaged within days | ABGR | | -0.049 | | 0.169 | | | | 0.197 | -16.897 | -4.018 | | 0.563 |
| | LAOC | | 0.044 | | 0.020 | | | | -0.023 | | | | 0.448 |
| | PIMO | | -0.041 | | -0.060 | | | | -0.132 | -6.344 | | | 0.395 |
| | PIPO | | 0.019 | | -0.016 | | 1.494 | | 0.334 | | | | 0.327 |
| | PSME | | -0.002 | | 0.014 | | | | 0.216 | | | | -0.044 |
| | THPL | | 0.123 | | 0.149 | | | 0.038 | 0.326 | | | | 0.197 |
| Dry sub-season, not averaged | ABGR | -0.895 | 0.171 | -1.012 | 0.215 | -1.448 | -2.416 | 1.273 | 0.280 | | | | 0.208 |
| | LAOC | -1.469 | 0.265 | -0.912 | 0.079 | | | | 0.249 | -2.900 | | | 0.325 |
| | PIMO | -1.187 | 0.387 | -0.876 | 0.158 | -0.834 | -1.661 | | 0.445 | | | | 0.433 |
| | PIPO | -1.058 | 0.338 | -0.845 | 0.129 | | -1.553 | | 0.350 | | | | 0.369 |
| | PSME | -1.266 | 0.131 | -1.261 | 0.153 | | | | 0.180 | | | -2.741 | 0.251 |
| | THPL | -0.648 | 0.151 | -1.109 | 0.299 | -1.170 | | | 0.289 | | | | 0.274 |
| Dry sub-season, averaged within days | ABGR | -1.094 | 0.643 | -0.933 | 0.394 | -0.779 | | | 0.603 | | -2.008 | | 0.218 |
| | LAOC | -1.277 | 0.625 | -1.049 | 0.283 | | | | 0.598 | | | | 0.250 |
| | PIMO | -1.104 | 0.449 | -0.954 | 0.201 | | | | 0.514 | | | | 0.167 |
| | PIPO | -1.100 | 0.698 | -0.945 | 0.226 | | | | 0.684 | | | | 0.157 |
| | PSME | -0.930 | 0.455 | -0.950 | 0.490 | | | | 0.594 | | | -2.933 | 0.282 |
| | THPL | -0.642 | 0.267 | -0.987 | 0.349 | -1.336 | | | 0.361 | | | | 0.312 |

| | model | ln(gs)=a+b*$\|\Psi_{PD}\|$+c*$\|\Psi_{leaf}\|$+d*($\|\Psi_{PD}\|$:$\|\Psi_{leaf}\|$) | | | | ln(gs)=a+b*$\|\Psi$PD$\|$+c*$\|\Psi$leaf$\|$+d*ln(VPD)+e*($\|\Psi_{PD}\|$:$\|\Psi_{leaf}\|$)+f*($\|\Psi_{PD}\|$:$\|$ln(VPD))+g*($\|\Psi_{leaf}\|$:ln(VPD))+h*$\|\Psi_{PD}\|$:$\|\Psi_{leaf}\|$:ln(VPD) | | | | | | | |
|---|---|---|---|---|---|---|---|---|---|---|---|---|---|---|---|---|
| | species | b | c | d | adjusted $R^2$ | b | c | d | e | f | g | h | adjusted $R^2$ |
| Wet and dry sub-seasons, averaged within days | ABGR | | | -1.044 | 0.390 | | | | | | | | 0.496 |
| | LAOC | | | | 0.454 | | | | | | | | 0.722 |
| | PIMO | | | | 0.288 | | | | | | | | 0.499 |
| | PIPO | | | | 0.330 | | | | | -8.868 | | | 0.512 |
| | PSME | | | | 0.261 | | | | | | | | 0.689 |
| | THPL | | | | 0.370 | | | | 3.161 | -5.995 | -2.282 | 4.064 | 0.392 |
| Wet sub-season, averaged within days | ABGR | -10.600 | | | 0.452 | | | | | | | | 0.427 |
| | LAOC | | | | 0.070 | | | | | | | | 0.381 |
| | PIMO | | | | 0.192 | | | | | | | | 0.195 |
| | PIPO | | | | 0.310 | | | | | | | | 0.239 |
| | PSME | | | | -0.019 | | | | | | | | 0.037 |
| | THPL | | | | 0.236 | | | | | | | | 0.381 |
| Dry sub-season, not averaged | ABGR | -0.235 | -0.149 | 0.129 | 0.328 | | -3.628 | | | | | | 0.276 |
| | LAOC | -0.748 | | | 0.487 | | | | | | | | 0.290 |
| | PIMO | | -0.127 | | 0.270 | | -3.192 | -7.312 | | | | | 0.464 |
| | PIPO | | -0.146 | | 0.221 | | | | | | | | 0.368 |
| | PSME | | | | 0.348 | | | | | | | | 0.273 |
| | THPL | | | | 0.312 | | | | | | | | 0.370 |
| Dry sub-season, averaged within days | ABGR | -4.011 | -2.433 | 2.232 | 0.462 | -6.184 | -2.708 | | | | | | 0.748 |
| | LAOC | | | | 0.711 | | | | | | | | 0.724 |
| | PIMO | | | | 0.149 | -9.173 | -5.642 | -16.055 | | 17.085 | 10.089 | -11.346 | 0.569 |
| | PIPO | | -3.357 | | 0.259 | | | | | | | | 0.670 |
| | PSME | | -1.797 | | 0.476 | | | | | | | | 0.646 |
| | THPL | | | | 0.388 | | | | | | | | 0.313 |

Supplemental Table 2-1. Coefficients of simple and multiple linear regressions shown are significant at $p<0.05$. The datasets used are listed on the left. Data "averaged within days" consists of means of 3-4 trees' parameters within species each hour. "Not averaged" data occurs only in dry sub-season and relates each individual tree's vapor pressure deficit (VPD), leaf water potential ($\Psi_L$), and/or predawn water potential (ΨPD). VPDs were in KPa; $\Psi_L$ and $\Psi_{PD}$ values were in bars; and gS were in mol $m^{-2}$ $s^{-1}$.

# Appendix C: Supplemental Text for Chapter 2

Samples that included mature shoots were consistently around 0.6 MPa more negative than samples comprised entirely of new growth, a pattern that was not seen in the other species current vs. previous year growth. We speculate that there may be greater resistance to water going to the more mature *L. occidentalis* foliage, effectively shunting water to the developing leaves and xylem in the distal portion of the branch and necessitating more negative water potentials in the mature sections to maintain transpiration. The relatively little new growth in June of 2015, compared to the following months, could account for why similarly sized samples would contain more mature shoots. If more mature shoots depressed $\Psi_{leaf}$, the later water potential measurements that did not include mature shoots in the sample overestimated the water potentials in *L. occidentalis.* Another potential explanation could be the immaturity of the needles on the *L. occidentalis* samples. For the other species, second year needles were sampled when current year needles were not yet hardened. For the deciduous *L. occidentalis*, however, first year samples were used because they were the only needles present.